THE UNIVERSITY OF CHICAGO

MOLECULAR AND ENVIRONMENTAL CONTROLS ON AEROBIC ANOXYGENIC PHOTOTROPHY

A DISSERTATION SUBMITTED TO
THE FACULTY OF THE DIVISION OF THE PHYSICAL SCIENCES
IN CANDIDACY FOR THE DEGREE OF
DOCTOR OF PHILOSOPHY

DEPARTMENT OF THE GEOPHYSICAL SCIENCES

BY
JUAN GABRIEL VARGAS ASENSIO

CHICAGO, ILLINOIS
AUGUST 2020

This work is dedicated to my life partner Carol and my family for their infinite love and support.

TABLE OF CONTENTS

LIST OF FIGURES

LIST OF TABLES

ACKNOWLEDGEMENTS

To Maureen Coleman for her support over the years. Committee members Jake Waldbauer, Sean Crosson and Howard Shuman.

Current and old lab members of the Coleman and Waldbauer labs. Aretha Fiebig, David Hershey and Lydia Varesio.

Thank you all.

ABSTRACT

Aerobic anoxygenic phototrophy (AAP) is a metabolic process found in diverse aerobic proteobacteria across aquatic environments. Unlike classical anoxygenic photosynthetic bacteria, the bacteria that perform AAP are often obligate aerobes and are thought to use this pathway to supplement their primarily heterotrophic metabolism. The environmental and molecular factors that control AAP, however, are poorly understood. Using the model marine organism *Erythrobacter longus*, and the recently isolated freshwater strain *Porphyrobacter* LM6, we investigated the metabolic pathways and regulatory mechanisms that interact with AAP.

First, we constructed deletion mutants of *E. longus* for several genes involved in light harvesting and the glyoxylate shunt pathway. By comparing the growth of wild type and mutants we demonstrate that light enhanced the growth of wild-type *E. longus* on pyruvate, glucose and butyrate minimal medium, but not in rich medium; and that the enhanced growth was product of the absorption of energy from light. We discarded that the glyoxylate shunt as the metabolic pathway responsible for light enhanced growth in *E. longus*, yet we confirmed that the shunt is the only for acetate metabolism in this strain and possibly other AAP strains from the order Sphingomonadales.

Next, we used global transposon mutagenesis to assess gene fitness under varying nutritional conditions in *Porphyrobacter* LM6. The mutant libraries were grown on two different carbon sources (glucose and butyrate) in two different light regimes: 24h dark, and 14h:10h light:dark cycles. As expected, genes in central carbon metabolism had differential fitness effects in butyrate vs. glucose. Notably, the glyoxylate shunt genes isocitrate lyase and malate synthase, along with the anaplerotic carbon assimilation gene malic enzyme, appear to be important on butyrate but not glucose. We next examined the role of phototrophy. Light provided a growth

advantage to wild-type cells grown in glucose but had no effect in butyrate. Consistent with this, genes encoding pigment biosynthesis and photosystem machinery were not important for fitness in butyrate, but had strong fitness effects in cells grown in the light with glucose. We determined that the anapleortic reactions performed by phosphoenolpyruvate carboxylase and phosphoenolpyruvate carboxykinase facilitate the light enhanced growth observed in glucose. Catalase/peroxidase and the oxidative stress response regulator *oxyR* had strong fitness effects in both butyrate and glucose, implying that ROS are a strong selective pressure for this organism. We also demonstrated that *ppsR* is a key regulator of phototrophy using a targeted gene knockout. These results suggest that the regulation of carbon metabolism and phototrophy are intertwined, and that, surprisingly, phototrophy is advantageous on glucose but not butyrate. Further, ROS detoxification appears to be a key pathway for survival of AAP bacteria.

To further explore the impact of ROS in the physiology of AAP, we used another transposon library in *E. longus.* The production of bacteriochlorophyll-a (Bchla) in the presence of oxygen produces reactive oxygen species (ROS) that are detrimental for their survival in the environment. Yet, the mechanisms used by these bacteria to regulate phototrophic metabolism and overcome the effects of oxidative stress are not fully understood. As expected, we found that superoxide dismutase and catalase are important enzymes against reactive oxygen species (ROS). Mutants deficient in carotenoid biosynthesis also had low fitness under increased oxidative stress, confirming their photoprotective role in AAP bacteria. Glutathione-based systems for repairing ROS damage are vital for the survival of *E. longus*, as the enzymes glutathione synthase and glutathione peroxidase are required for growth. Mutants of the transcriptional regulator *oxyR* presented some of the lowest fitness suggesting its role as major regulator in response to oxidative stress. The mutants of catalase and glutathione reductases showed similar fitness patterns to *oxyR*

regulon suggesting that these could be part of its regulon in *E. longus*. Taken together, our results demonstrate that *E. longus*, and likely other AAP strains, use a combination of enzymatic mechanisms and photoprotective carotenoids against reactive oxygen species (ROS).

Together, our genetics and physiology results shed new light on a widespread and ecologically important metabolic strategy in aquatic systems.

CHAPTER 1

Introduction

Microorganisms play a key role in the global biogeochemical cycles. They possess great metabolic capacity and diversity allowing them to perform chemical transformations on most of Earth substrates in order to produce energy. While doing so, microorganisms have shaped every environmental niche we know. Therefore, it is fundamental to study the roles and metabolism of microorganisms in the environment to further understand the complex processes that drive this planet.

Microorganisms drive the global carbon cycle, a process that controls climate in the planet mitigating global warming (Riebesell et al., 2007). The most dynamic part of the carbon cycle is known as the microbial loop. In this process, photosynthetic organisms fix atmospheric CO2 in the surface ocean, and provide the rest of the community with organic matter (Jiao & Zheng, 2011). Grazing and viral infection facilitate the flux of organic carbon releasing these molecules into the water where the labile carbon compounds are rapidly consumed, and the recalcitrant molecules sink to the sediments as particulate organic carbon (Fuhrman, 1999; Jiao et al., 2010; Jiao & Zheng, 2011; Zimmerman et al., 2020). Light provides energy for carbon fixation in photosynthetic organisms, however, light is also used by photoheterotrophic bacteria to complement their metabolism. It has been hypothesized that photoheterotrophs use light for ATP production, to facilitate active transport and for flagellar motility (Kirchman & Hanson, 2013). Both proteorhodopsin and bacteriochlorophyll based photoheterotrophic bacteria are abundant and widespread in aquatic systems (Koblížek, 2015; Kolber et al., 2000; Martinez-Garcia et al., 2012; Zubkov, 2009). These bacteria include some of most active members of microbial communities in surface waters such as SAR11, Roseobacters, among others (Shi et al., 2010). Hence, the

contribution of photoheterotrophs to the carbon cycle has been subject of study in the last two decades (Kolber et al., 2001).

Understanding the mechanisms used in photoheterotrophs to take advantage of the extra energy from light to increase their organic carbon assimilatory efficiency is vital to comprehend the role they play in the global carbon cycle, and the extent of their contribution to the carbon budget in aquatic ecosystems.

1.1. Aerobic anoxygenic phototrophy

Aerobic anoxygenic phototrophic bacteria (AAPB) are predominantly heterotrophic, and obligate aerobes that produce bacteriochlorophyll-*a* (Bchl*a*) (Koblížek, 2015; V. Yurkov & Csotonyi, 2009). AAPB lack the enzyme RuBisCO, hence they are incapable of photoautotrophy (V. Yurkov & Csotonyi, 2009). The genomes of AAPB contain a genomic region of about 40Kb called the photosynthetic gene cluster that includes the genes necessary for a complete photosystem type II, the biosynthesis of Bchl*a*, and other genes involved in carotenoid biosynthesis and regulation (Zheng et al., 2011, 2016).

AAPB produce Bchl*a* under aerobic conditions unlike closely related anoxygenic photosynthetic bacteria, which downregulates Bchl*a* biosynthesis in the presence of oxygen. Most of the known strains of AAPB produce Bchl*a* in the dark, and down regulate its biosynthesis during light periods when this pigment is most needed (V. V. Yurkov & van Gemerden, 1993). This is an unusual pattern that has not been reported in other Bchl*a* producing phototrophs, and has been subject to different hypotheses. The regulation of pigment biosynthesis in AAPB is driven by light, however the genetic details of this regulation are yet not fully understood (Rathgeber et al., 2004; T. Shiba, 1987; V. V. Yurkov & van Gemerden, 1993). AAPB also produce diverse carotenoid

pigments that accumulate in the cytoplasm of many strains given their polarity. For this reason, it is considered that carotenoids main function in AAPB is photoprotective instead of light harvesting (V. Yurkov et al., 1993; V. Yurkov & Csotonyi, 2009; V. Yurkov & Hughes, 2017). Many questions remain unanswered about AAPB such as: what are the environmental drivers of the expression of phototrophy? What metabolic pathways are used by AAPB to take advantage of phototrophy? And how is AAP regulated? The approach used in this work to address these questions is to combine physiological measurements with genetics to disentangle the molecular details that govern aerobic anoxygenic phototrophy.

1.2. Ecology and distribution of AAPB

AAPB were first reported in the late 1970s when a Japanese group isolated aerobic strains that produced Bchl*a* (Harashima et al., 1978; Tsuneo Shiba et al., 1979). Since, AAPB strains have been isolated from a myriad of aquatic systems (Koblížek, 2015; V. Yurkov & Csotonyi, 2009). Furthermore, AAPB have being detected using molecular or biochemical techniques in ocean and freshwater environments worldwide (Auladell et al., 2019; Koblížek, 2015; Kolber et al., 2000; Martinez-Garcia et al., 2012; Shi et al., 2010; Yutin et al., 2005, 2007). The abundance of AAPB has also been debated in recent years. It was first hypothesized that AAPB were abundant in oligotrophic waters where phototrophy could be essential to survive under nutrient limitation (Kolber et al., 2000). However, others demonstrated that AAPB are more abundant in coastal ecosystems and environments with higher availability of organic carbon (Jiao et al., 2007; Lamy et al., 2011; Sieracki et al., 2006). Recent findings using different molecular techniques and infrared epifluorescence measurements of Bchl*a*, showed that the abundance of AAPB corresponds to about 10% of the community in the ocean (Rathgeber et al., 2004; Schwalbach &

Fuhrman, 2005; V. Yurkov & Hughes, 2013, 2017). In freshwater systems their abundance ranges from 2% up to 29% of the microbial community (Čuperová et al., 2013; V. Yurkov & Hughes, 2017). In both cases, the abundance of AAPB is subject to seasonal and temperature variations (V. Yurkov & Hughes, 2017).

1.3. Physiology of AAPB: What we know so far

The photosynthetic capacity of the AAPB photosystem has been demonstrated in the model strains *Erythrobacter* NAP1 and *Roseobacter denitrificans* (Hauruseu & Koblížek, 2012; Kai Tang et al., 2010). Hence, AAPB are able to harvest light energy and generate a proton motive force gradient that facilitates the synthesis of ATP and the regeneration of reducing equivalents. Light exposure increases ATP levels and inhibits respiration in AAPB cultures (Harashima & Kawazoe, 1987; Koblížek et al., 2010; Okamura et al., 1986). It has been shown that the strain *Erythrobacter* NAP1 inhibits respiration in the light by switching electron transfer from the respiratory chain to cyclic photophosphorylation (Hauruseu & Koblížek, 2012). Light-enhanced growth has been demonstrated in AAPB strains growing on several carbon substrates presenting differential bacterial growth efficiency in the light vs dark (Biebl & Wagner-Dobler, 2006; Hauruseu & Koblížek, 2012; Spring et al., 2009; V. Yurkov et al., 1993). However, the pathways and mechanisms used by AAPB to use light to enhance its growth are still not completely understood. One way AAPB can take advantage of light is by using ATP and reducing equivalents derived from light for inorganic carbon fixation via anaplerotic reactions (Palovaara et al., 2014). This has been demonstrated in *Erythrobacter* NAP1 and *Dinoroseobacter shibae*, which increase their carboxylation activity and growth in the light (Bill et al., 2017; Hauruseu & Koblížek, 2012).

The Rhodobacterales strains *R. denitrificans* and *D. shibae* use the ethylmalonyl CoA pathway (EMC) to enhance their growth in the light (Bill et al., 2017; Tomasch et al., 2011). The EMC pathway includes inorganic carbon incorporation as TCA cycle intermediaries using ATP and reduced cofactors derived from light (Kuo-hsiang Tang et al., 2011). But, is this the mechanism used by all AAPB for light enhancement growth? A genomic comparison of alphaproteobacteria genomes showed that this pathway is not evenly distributed in AAPB, thus there must be other strategies used by AAPB that lack the EMC.

So far, most of the research done in AAPB has been focused on their physiological response to light and carbon. However, there are fewer efforts being done to elucidate the molecular details behind AAPB metabolism. Here we aim to fill this knowledge gap by combining physiological measurements and genetics to probe the influence of phototrophy in the physiology of these bacteria. We developed a genetic system in the model organism *Erythrobacter longus*, one of the first isolated strains of AAPB. Furthermore, we applied the same approach to study *Porphyrobacter* LM6, a freshwater strain recently isolated from Lake Michigan. **The main goal of this thesis is to disentangle the molecular mechanisms for carbon utilization and light enhanced growth of AAPB, as well as the mechanisms of genetic regulation related to these processes**. By comparing the findings obtained from both marine and freshwater strains, we also aim to test the universality of our findings across AAPB in different habitats.

We study the importance of light and the type of carbon substrate as ecological drivers of aerobic anoxygenic photosynthesis. Also, we investigated the conditions in which light is advantageous for the growth of *Erythrobacter longus* (Chapter 2) and *Porphyrobacter* LM6 (Chapter 3). Furthermore, we generate a Bchl*a* deficient strain and tested the consequences of this genotype for

the physiology of *Erythrobacter longus*. To our knowledge, this is the first report of the use of a non-phototrophic mutant strain of AAPB to study the impact of light in their physiology and their ability to use carbon substrates. In addition, we generate a mutant incapable of using the glyoxylate shunt, a pathway that we hypothesized could be used by AAPB for light-enhanced growth.

Although useful and informative, the minimalist single gene deletion mutant approach is laborious and time consuming. Thus, we took advantage of recently developed barcoded transposon libraries to produce a collection of mutants of the majority of the genes on our strains. This technology allowed us to test the effect of the mutation on thousands of genes under multiple growing conditions. The experiments performed in this thesis were designed to interrogate the relevance of carbon metabolisms pathways, and to identify other mechanisms that AAPB use in combination with phototrophy to efficiently grow on carbon substrates (Chapter 3). One of the most important findings generated by this work was the confirmation of *ppsR* as the major transcriptional repressor of phototrophy in AAPB, and the uncovering of other transcriptional regulators that play vital roles in *Porphyrobacter* LM6 and likely other strains of AAPB.

In the final chapter of this thesis we challenged our collection of mutants of *Erythrobacter longus* to increased levels of oxidative stress (Chapter 4). The use of Bchl*a* to harvest light under aerobic conditions by AAPB generates singlet oxygen and hydrogen peroxide. In addition, AAPB live in the surface ocean where reactive oxygen species (ROS) accumulate as a byproduct of the aerobic metabolism of the microbial community. Therefore, we hypothesized that ROS represents one of the biggest threats to AAPB survival and ecological success. The aim of these experiments is to identify the molecular mechanisms used by AAPB to counteract the toxic effect of light-

derived and exogenous ROS, and the regulatory functions involved (Chapter 4). We found evidence of the genes used by *E. longus* in response to ROS and confirmed the photoprotective role of carotenoids for this strain. We identified *oxyR* as the most important regulator of ROS detoxification in *E. longus,* rather than the *ecf-phyR* system described for other related phototrophs.

Together, our genetic and physiology results shed new light on a widespread and ecologically important metabolic strategy in aquatic systems.

1.4. References

Auladell, A., Sánchez, P., Sánchez, O., Gasol, J. M., & Ferrera, I. (2019). Long-term seasonal and interannual variability of marine aerobic anoxygenic photoheterotrophic bacteria. *The ISME Journal*, *13*(8), 1975–1987.

Biebl, H., & Wagner-Dobler, I. (2006). Growth and bacteriochlorophyll a formation in taxonomically diverse aerobic anoxygenic phototrophic bacteria in chemostat culture: Influence of light regimen and starvation. *Process Biochemistry*, *41*, 2153–2159.

Bill, N., Tomasch, J., Riemer, A., Muller, K., Kleist, S., Schmidt-Hohagen, K., Wagner-Döbler, I., & Schomburg, D. (2017). Fixation of CO2 using the ethylmalonyl-CoA pathway in the photoheterotrophic marine bacterium Dinoroseobacter shibae. *Environmental Microbiology*, 2645–2669.

Čuperová, Z., Holzer, E., Salka, I., Sommarug, R., & Koblížek, M. (2013). Temporal changes and altitudinal distribution of aerobic anoxygenic phototrophs in mountain lakes. *Applied and Environmental Microbiology*, *79*(20), 6439–6446.

Fuhrman, J. a. (1999). Marine viruses and their biogeochemical and ecological effects. *Nature*, *399*, 541–548.

Harashima, K., & Kawazoe, K. (1987). Light-Stimultated Aerobic Growth of Erythrobacter Species OCh114. *Plant & Cell Physiology*, *28*(2), 365–374.

Harashima, K., Shiba, T., Totsuka, T., Shimizu, U., & Taga, N. (1978). Occurence of bacteriochlorophyll a in a strain of an aerobic heterotrophic bacterium. *Agricultural and Biological Chemistry*, *42*(8), 1627–1628.

Hauruseu, D., & Koblížek, M. (2012). Influence of Light on Carbon Utilization in Aerobic

Anoxygenic Phototrophs. *Applied and Environmental Microbiology*, *78*(20), 7414–7419.

Jiao, N., Herndl, G. J., Hansell, D. A., Benner, R., Kattner, G., Wilhelm, S. W., Kirchman, D. L., Weinbauer, M. G., Luo, T., Chen, F., & Azam, F. (2010). Microbial production of recalcitrant dissolved organic matter: Long-term carbon storage in the global ocean. *Nature Reviews Microbiology*, *8*(8), 593–599.

Jiao, N., Zhang, Y., Zeng, Y., Hong, N., Liu, R., Chen, F., & Wang, P. (2007). *Distinct distribution pattern of abundance and diversity of aerobic anoxygenic phototrophic bacteria in the global ocean*. *9*, 3091–3099.

Jiao, N., & Zheng, Q. (2011). The Microbial Carbon Pump: From Genes to Ecosystems. *Applied and Environmental Microbiology*, *77*(21), 7439–7444.

Kirchman, D. L., & Hanson, T. E. (2013). *Bioenergetics of photoheterotrophic bacteria in the oceans*. *5*, 188–199.

Koblížek, M. (2015). Ecology of aerobic anoxygenic phototrophs in aquatic environments. *FEMS Microbiology Reviews*, *January*, 854–870.

Koblížek, M., Mlcouskova, J., Kolber, Z. S., & Kopecky, J. (2010). On the photosynthetic properties of marine bacterium COL2P belonging to Roseobacter clade. *Archives of Microbiology*, *192*, 41–49.

Kolber, Z. S., Plumley, F. G., Lang, a S., Beatty, J. T., Blankenship, R. E., VanDover, C. L., Vetriani, C., Koblizek, M., Rathgeber, C., & Falkowski, P. G. (2001). Contribution of aerobic photoheterotrophic bacteria to the carbon cycle in the ocean. *Science*, *292*(5526), 2492–2495.

Kolber, Z. S., Van Dover, C. L., Niederman, R. a, & Falkowski, P. G. (2000). Bacterial photosynthesis in surface waters of the open ocean. *Nature*, *407*(1993), 177–179.

Lamy, D., Jeanthon, C., Cottrell, M. T., Kirchman, D. L., Wambeke, F. V., Ras, J., Dahan, O., & Oc, O. (2011). *Ecology of aerobic anoxygenic phototrophic bacteria along an oligotrophic gradient in the Mediterranean Sea*. 973–985.

Martinez-Garcia, M., Swan, B. K., Poulton, N. J., Gomez, M. L., Masland, D., Sieracki, M. E., & Stepanauskas, R. (2012). High-throughput single-cell sequencing identifies photoheterotrophs and chemoautotrophs in freshwater bacterioplankton. *The ISME Journal*, *6*(1), 113–123.

Okamura, K., Mitsumori, F., Ito, O., Takamiya, K.-I., & Nishimura, M. (1986). Photophosphorylation and Oxidative Phosphorylation in Intact Cells and Chromatophores of an Aerobic Photosynthetic Bacterium, Erythrobacter sp. Strain OChll4. *Journal of Bacteriology*, *168*(3), 1142–1146.

Palovaara, J., Akram, N., Baltar, F., Bunse, C., Forsberg, J., & Pedrós-alió, C. (2014). Stimulation of growth by proteorhodopsin phototrophy involves regulation of central metabolic pathways in marine planktonic bacteria. *PNAS*, E3650–E3658.

Rathgeber, C., Beatty, J. T., & Yurkov, V. (2004). Aerobic phototrophic bacteria: New evidence for the diversity , ecological importance and applied potential of this previously overlooked group. *Photosynthesis Research*, 113–128.

Riebesell, U., Schulz, K. G., Bellerby, R. G. J., Botros, M., Fritsche, P., Meyerhöfer, M., Neill, C., Nondal, G., Oschlies, A., Wohlers, J., & Zöllner, E. (2007). Enhanced biological carbon consumption in a high CO2 ocean. *Nature*, *450*(7169), 545–548.

Schwalbach, M. S., & Fuhrman, J. A. (2005). Wide-ranging abundances of aerobic anoxygenic phototrophic bacteria in the world ocean revealed by epifluorescence microscopy and quantitative PCR. *Limnology and Oceanography*, *50*(2), 620–628.

Shi, Y., Tyson, G. W., Eppley, J. M., & Delong, E. F. (2010). Integrated metatranscriptomic and metagenomic analyses of stratified microbial assemblages in the open ocean. *The ISME Journal*, *5*(6), 999–1013.

Shiba, T. (1987). O2 regulation of bacteriochlorophyll synthesis in the aerobic bacterium Erythrobacter. *Plant Cell Physiol.*, *28*(7), 1313–1320.

Shiba, Tsuneo, Simidu, U., & Taga, N. (1979). Distribution of Aerobic Bacteria Which Contain Bacteriochlorophyll a. *Applied and Environmental Microbiology*, *38*(1), 43–45.

Sieracki, M. E., Gilg, I. C., Thier, E. C., Poulton, N. J., & Goericke, R. (2006). Distribution of planktonic aerobic anoxygenic photoheterotrophic bacteria in the northwest Atlantic. *Limnology and Oceanography*, *51*(1), 38–46.

Spring, S., Lunsdorf, H., Fuchs, B. M., & Tindall, B. J. (2009). The Photosynthetic Apparatus and Its Regulation in the Aerobic Gammaproteobacterium Congregibacter litoralis gen. Nov ., sp. Nov . *PLoS ONE*, *4*(3).

Tang, Kai, Zong, R., & Zhang, F. (2010). Characterization of the Photosynthetic Apparatus and Proteome of Roseobacter denitrificans. *Current Microbiology*, *60*, 124–133.

Tang, Kuo-hsiang, Tang, Y. J., & Blankenship, R. E. (2011). Carbon metabolic pathways in phototrophic bacteria and their broader evolutionary implications. *Frontiers in Microbiology*, *2*(August), 1–23.

Tomasch, J., Gohl, R., Bunk, B., Diez, M. S., & Wagner Dobler, I. (2011). Transcriptional response of the photoheterotrophic marine bacterium Dinoroseobacter shibae to changing light regimes. *Isme J*, 1957–1968.

Yurkov, V., & Csotonyi, J. T. (2009). *The Purple Phototrophic Bacteria. Chapter 3. New Light*

on Aerobic Anoxygenic Phototrophs. (p. 55).

Yurkov, V., Gad'on, N., & Drews, G. (1993). The major part of polar carotenoids of the aerobic bacteria Roseococcus thiosulfatophilus RB3 and Erythromicrobium ramosum E5 is not bound to the bacteriochlorophyll a-complexes of the photosynthetic apparatus. *Archives of Microbiology*, *160*(5), 372–376.

Yurkov, V., & Hughes, E. (2013). Genes Associated with the Peculiar Phenotypes of the Aerobic Anoxygenic Phototrophs. In *Advances in Botanical Research* (Vol. 66, p. 358). Elsevier.

Yurkov, V., & Hughes, E. (2017). Aerobic Anoxygenic Phototrophs: Four Decades of Mystery. In P. C. Hallenbeck (Ed.), *Modern Topics in the Phototrophic Prokaryotes: Environmental and Applied Aspects* (pp. 193–214). Springer International Publishing.

Yurkov, V. V., & van Gemerden, H. (1993). Impact of light/dark regimen on growth rate, biomass formation and bacteriochlorophyll synthesis in Erythromicrobium hydrolyticum. *Archives of Microbiology*, 84–89.

Yutin, N., Suzuki, M. T., & Beja, O. (2005). Novel Primers Reveal Wider Diversity among Marine Aerobic Anoxygenic Phototrophs †. *Applied and Environmental Microbiology*, *71*(12), 8958–8962.

Yutin, N., Suzuki, M. T., Teeling, H., Weber, M., Venter, J. C., Rusch, D. B., & Béjà, O. (2007). Assessing diversity and biogeography of aerobic anoxygenic phototrophic bacteria in surface waters of the Atlantic and Pacific Oceans using the Global Ocean Sampling expedition metagenomes. *Environmental Microbiology*, *9*, 1464–1475.

Zheng, Q., Lin, W., Liu, Y., Chen, C., & Jiao, N. (2016). A comparison of 14 Erythrobacter genomes provides insights into the genomic divergence and scattered distribution of phototrophs. *Frontiers in Microbiology*, *7*(JUN).

Zheng, Q., Zhang, R., Koblížek, M., Boldareva, E. N., Yurkov, V., Yan, S., & Jiao, N. (2011). Diverse arrangement of photosynthetic gene clusters in aerobic anoxygenic phototrophic bacteria. *PLoS ONE*, *6*(9), 1–7.

Zimmerman, A. E., Howard-Varona, C., Needham, D. M., John, S. G., Worden, A. Z., Sullivan, M. B., Waldbauer, J. R., & Coleman, M. L. (2020). Metabolic and biogeochemical consequences of viral infection in aquatic ecosystems. *Nature Reviews Microbiology*, *18*(1), 21–34.

Zubkov, M. V. (2009). Photoheterotrophy in marine prokaryotes. *Journal of Plankton Research*, *31*(9), 933–938.

CHAPTER 2

Molecular and environmental controls on aerobic anoxygenic phototrophy in *Erythrobacter longus*

2.1. Abstract

Aerobic anoxygenic phototrophy is a metabolic process found in diverse proteobacteria and is widespread across aquatic environments. Aerobic anoxygenic phototrophic bacteria (AAPB) are typically obligate aerobes and are thought to use sunlight to supplement their heterotrophic metabolism. To identify the environmental and molecular factors that control AAP, we characterized the physiology of the model organism *Erythrobacter longus* under a range of conditions and generated deletion mutants in key genes for phototrophy and carbon metabolism. We found that light enhanced the growth of *E. longus* when pyruvate, butyrate or glucose was provided as the sole carbon source, but this effect was not observed in complex medium. Light-enhanced growth was more pronounced as carbon supply was reduced. To explore the molecular basis of this phenotype, we constructed a deletion mutant strain unable to synthesize the light harvesting pigment bacteriochlorophyll-*a*. Light-enhanced growth was diminished in the mutant strain compared to wild type in pyruvate, demonstrating that bacteriochlorophyll-based phototrophy underlies this phenotype. However, the effect of the Δ*bchID* strain was dependent on the carbon substrate. The glyoxylate shunt is one of the carbon metabolism pathways that are differentially encoded by Sphingomonadales APPB. A mutant strain lacking the gene isocitrate lyase (Δ*icl*), a key enzyme of the glyoxylate shunt, was unable to grow on acetate and butyrate, but *icl* was not required for growth on pyruvate, glucose or complex media in light or dark conditions. We did not observe a relationship between AAPB and the glyoxylate shunt in these

conditions. Phototrophy and the glyoxylate shunt pathways are vital for the ecological success of AAPB in the environment.

2.2. Introduction

Aerobic anoxygenic phototrophic bacteria (AAPB) are widespread in aquatic environments (Koblížek, 2015a; Kolber et al., 2000, 2001). These Proteobacteria are typically strict aerobes and heterotrophic; however, they are also capable of light harvesting and photophosphorylation (Beatty, 2002; Koblížek et al., 2003; Koblížek, 2015b; Rathgeber et al., 2004; Tsuneo Shiba et al., 1979). AAPB use bacteriochlorophyll-*a* (Bchl*a*) and a Type II photosystem to harness photons to produce a proton motive force that can then be used for motility, active transport of nutrients and ATP production (Kirchman & Hanson, 2013). The activity of the photosystem of AAPB has been confirmed in several strains using fluorometric measurements (Hauruseu & Koblížek, 2012; Rathgeber et al., 2012; Kai Tang et al., 2010). Furthermore, *Erythrobacter* NAP1 has been shown to switch electron transport and ATP production from oxidative phosphorylation to cyclic photophosphorylation over light periods in cultures growing on light:dark cycles, demonstrating the ability of AAP to transition from heterotrophic to photoheterotrophic metabolism in response to light availability (Hauruseu & Koblížek, 2012). AAPB also showed decreased respiration rates (Harashima & Kawazoe, 1987; Koblížek et al., 2010) and increased ATP concentration (Candela et al., 2001; Okamura et al., 1986) in light conditions.

The environmental signals that control AAPB activity are not fully understood. Studies have shown that illumination (Rathgeber et al., 2004; V. V. Yurkov & Beatty, 1998; V. V. Yurkov & van Gemerden, 1993), oxygen tension (T. Shiba, 1987), nutritional state, or pH (Hiraishi &

Shimada, 2001) influence the production of Bchl*a* in AAPB. However, little is known about the molecular networks used by AAPB to respond to environmental signals, or whether specific energetic demands (e.g. active transport, motility) necessitate phototrophy. In related classical anoxygenic photosynthetic bacteria (e.g. *Rhodobacter*, *Rhodopseudomonas*), expression of photosynthesis-related genes is repressed by oxygen (Bauer et al., 2003; Ponnampalam et al., 1995); by contrast, in AAPB, bacteriochlorophyll-*a* is synthesized in the presence of oxygen and most AAPB require oxygen for growth (Fuchs et al., 2007; Harashima & Kawazoe, 1987; Nishimura et al., 1996, 1999; Tsuneo Shiba et al., 1979; Suyama et al., 2002; V. V. Yurkov & van Gemerden, 1993). Hence AAPB have evolved distinct regulatory mechanisms controlling the expression of the photosynthetic gene cluster that have not been elucidated.

The ability to use light allows a more efficient carbon utilization in AAPB (Koblížek, 2011). Light inhibits respiration of AAPB and enhances ATP production via photophosphorylation; moreover, light also stimulates carboxylation activity for inorganic carbon assimilation (Hauruseu & Koblížek, 2012). It has been demonstrated in AAPB strains that light enables carbon accumulation as biomass that would otherwise be respired to produce energy (Koblížek, 2011; V. V. Yurkov & van Gemerden, 1993). These findings indicate that AAPB might play a unique and important role in the carbon cycle. However, it is possible that the contribution of AAPB to the carbon cycle has been underestimated (Kolber et al., 2001). It has been shown that anaplerotic carbon fixation plays a role in the light-enhanced growth observed in some AAP strains (Bill et al., 2017; Hauruseu & Koblížek, 2012). Anaplerotic reactions can contribute between 0.6% - 11% of the cellular carbon in *Erythrobacter* NAP1 as shown in isotopically labeled carbon uptake experiments, but the specific pathways used by this strain to incorporate inorganic carbon are not well understood (Hauruseu & Koblížek, 2012; Koblížek et al., 2003). In the AAPB

Dinoroseobacter shibae (*Rhodobacteraceae*), ethylmalonyl-CoA pathway (EMC), a carbon metabolism pathway that includes the incorporation of inorganic carbon to produce biosynthetic intermediaries of the TCA cycle, is upregulated when grown in the light (Bill et al., 2017; Tomasch et al., 2011). However, the EMC pathway is not evenly distributed in AAP (Kuo-hsiang Tang et al., 2011), and is absent in strains of *Erythrobacter,* suggesting that other mechanisms may take advantage of the extra energy from light and anaplerotic carbon fixation. *Erythrobacter longus* genomes encode the glyoxylate shunt pathway which reduces the loss of carbon as CO2 by shortcutting the TCA cycle, producing glyoxylate as an intermediary (Petushkova & Tsygankov, 2017; Kuo-hsiang Tang et al., 2011). This carbon savings comes at a cost of 2 NADH and 1 ATP molecules per cycle, which could be augmented by photosynthetic electron transport. It is not known if there is a molecular link between the glyoxylate shunt and phototrophic metabolism.

We investigated the carbon and illumination conditions in which light enhances the growth of AAP strain *E. longus*. We generated a non-phototrophic strain by the deletion of two genes involved in the biosynthesis of Bchl*a*, and monitored the growth of *E. longus* on different carbon substrates to further understand the contribution of light to biomass production by *E. longus*. Additionally, we generated a mutant strain lacking the isocitrate lyase gene in order to probe the involvement of the glyoxylate shunt in AAP and central carbon metabolism. The results from this study shed light on the physiological conditions in which AAP is expressed and benefits the growth of *E. longus,* and the pathways contributing to the light enhanced growth.

2.3. Results

2.3.1. Carbon substrate and light interactively impact the growth of *E. longus*

We examined the effect of light on growth of *E. longus* using an artificial seawater (ASW) base medium supplemented with pyruvate, glucose, butyrate, or peptone plus yeast extract. Highest growth rate and maximum growth were observed in rich peptone medium (Fig. 2.1). Regardless of the light treatment, among the defined media, the highest growth rates were observed in butyrate (0.12 doublings/day, stdev=0.02), followed by glucose (0.039 doublings/h, stdev=0.006) and pyruvate (0.006 doublings/h, stdev=0.004) (Fig. S2.1). No significant differences were observed in the duration of the lag phase among the carbon conditions.

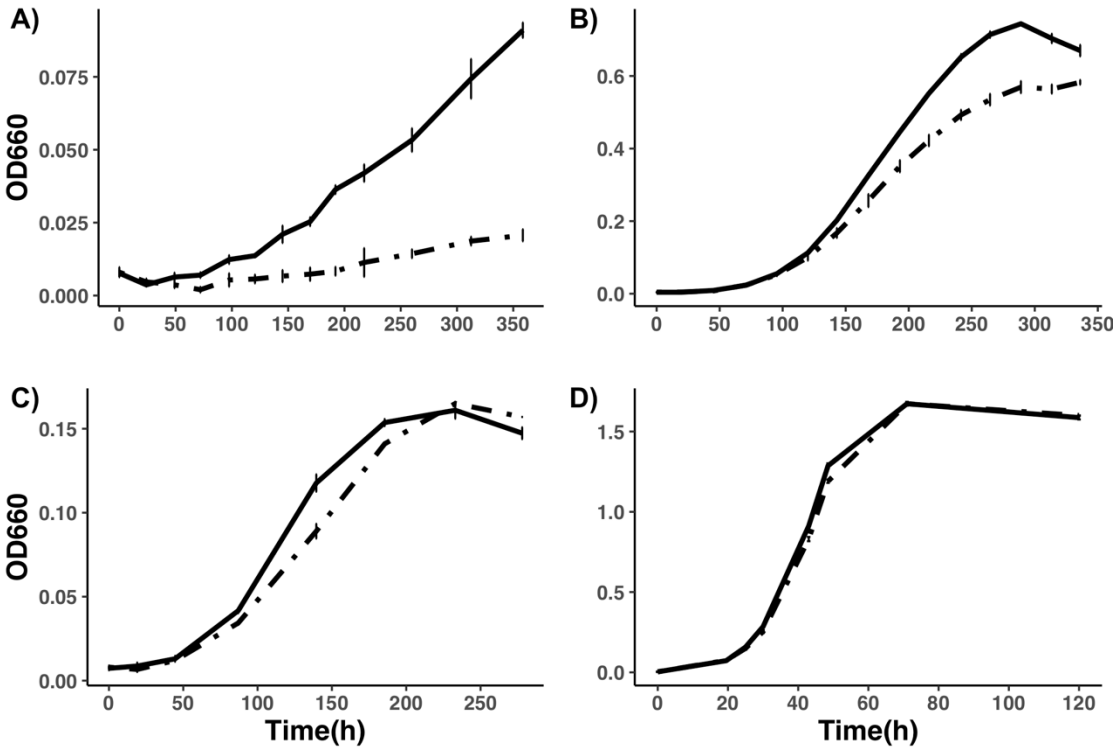

Figure 2.1. *Erythrobacter longus* growth on different carbon sources in L-D cycles and continuous darkness. A) ASW + Pyruvate, B) ASW + Butyrate, C) ASW + Glucose, D) ASW + Peptone + YE. Solid lines, 14:10h (light: dark) cycles; dashed lines, 24h dark. Error bars show standard deviation of three replicates.

Light enhanced the growth of *E. longus* on pyruvate, butyrate and glucose, demonstrating the ability of the strain to utilize extra energy from light. Light did not enhance growth of cultures

in a complex medium containing peptone and yeast extract (Fig. 2.1). The largest light-enhanced growth effect was observed in pyruvate, where cultures grew 4X faster and reached a 4X higher OD in L-D cycles than in continuous darkness (Fig. 2.1d, Fig. S2.2). Light also increased growth rates of glucose (1.3X faster) and butyrate (1.4X faster) cultures (Fig. S2.2). Pyruvate and butyrate cultures also reached higher maximum OD in L-D cycles compared with continuous darkness, but this effect was not observed in glucose cultures (Fig. S2.3).

2.3.2. Light-enhanced growth is more pronounced under carbon limitation

It has been hypothesized that light is more beneficial when carbon is limiting (low concentration) (Palovaara et al., 2014). To test this hypothesis, we grew *E. longus* in ASW minimal medium amended with different concentrations of pyruvate. Of the substrates we tested, pyruvate cultures showed the largest enhancement of growth in L-D cycles relative to continuous darkness. Light-enhanced growth was observed at all pyruvate concentrations tested in this experiment (Fig. 2.2 and Fig. S2.4). However, the contribution of light to growth increased as pyruvate concentration decreased. The fold-change improvement in growth rate conferred by light (i.e., growth rate in L-D cycles / growth rate in continuous darkness) was significantly higher in the 30mM and 60mM pyruvate conditions than in 120mM pyruvate (Fig. 2.2d). Likewise, the fold-change increase in maximum OD (i.e., maximum OD in L-D cycles / maximum OD in continuous darkness) was significantly higher in both 30mM and 60mM pyruvate conditions than in 120mM pyruvate (Fig. 2.2e).

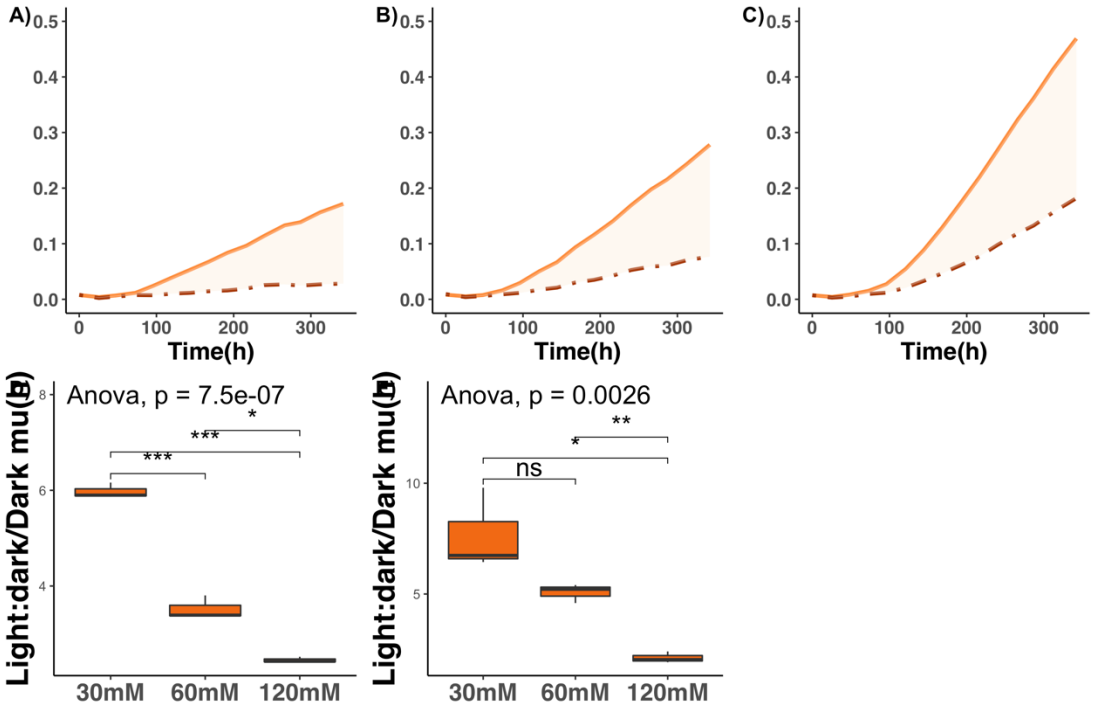

Figure 2.2. *E. longus* growth under increasing concentrations of pyruvate. A) Growth with 30mM pyruvate, B) 60mM pyruvate, C) 120mM pyruvate. Light orange= 14h:10 light: dark cultures, dark orange= 24h dark. D) Enhancement of growth rates by light, at three pyruvate concentrations. Values show fold change in growth rate (light: dark / continuous darkness). E) Ratio of maximum OD660 between light: dark cultures vs full darkness cultures. The maximum growth (OD) was estimated by fitting a model using grofit. For D) and E) the global p value was calculated using an anova test. The pairwise comparison of the treatments was performed using t-test. ns= non-significant. *= p<0.05. **=p<0.005. ***=p<0.0005.

2.3.3. Bchl*a*-deficient mutant of *E. longus* shows decreased light-enhanced growth

To further study the contribution of light to the physiology of AAPB, we created a non-phototrophic mutant strain of *E. longus* incapable of light harvesting. The mutant strain lacks the genes *bchI* and *bchD* (Δ*bchID*). Together with *bchH*, the proteins encoded by these genes form an enzymatic complex that performs the first step in the bacteriochlorophyll-*a* biosynthetic pathway (Fig. 2.3a). Colonies of the mutant non-phototrophic strain showed a brighter orange color compared with wild type colonies of *E. longus*. The mutant phenotype was tested first using

spectrophotometry. The Bchl*a* peak typically observed in *E. longus* cells at 865nm was absent in the Δ*bchID* mutant grown on ASW media supplemented with peptone and yeast extract regardless of the light regime (Fig. 2.3c). This result was further confirmed over L-D cycles: the Δ*bchID* strain did not exhibit the diel periodicity of Bchl*a* synthesis observed in the wild type strain (Fig. 2.3b). The wild type pigment phenotype was restored by complementation of the mutant with plasmid-borne copies of intact *bchID* and its native promoter region (Fig. 2.3c and Fig. 2.3d).

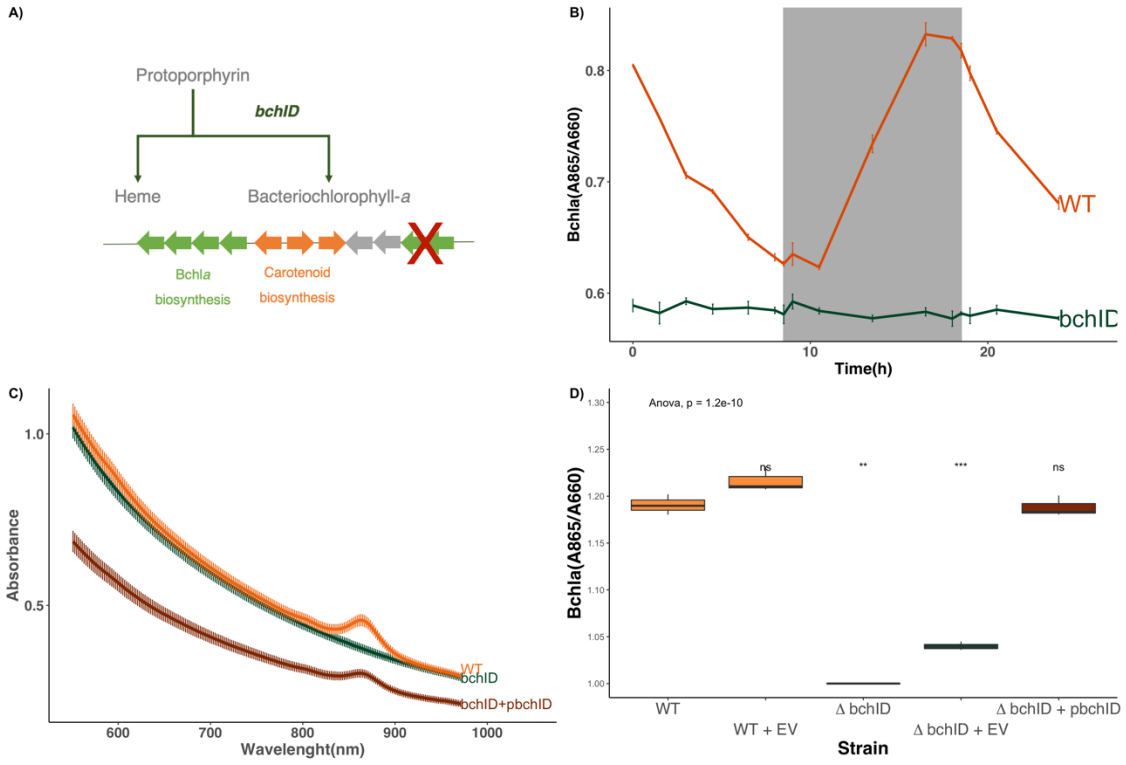

Figure 2.3. Bacteriochlorophyll-*a* production on *E. longus* wild type and Δ*bchID*. A) Schematic of the diverging pathway for Bchl*a* and the genomic map of *E. longus* photosynthetic gene cluster. The X marks the deleted genes *bchI* and *bchD* in the Δ*bchID* strain. B) Bchl*a* production of wild type and Δ*bchID* over a 14h:10h light: dark cycle. Gray area= 10h dark period. C) Absorbance spectra of cells of wild type (WT), Δ*bchID* (*bchID*) and the complemented strain Δ*bchID* + *pbchID* (*bchID*+p*bchID*). D) Bchl*a* production (estimated by the absorbance ratio A865/A660) in wild type, Δ*bchID* mutant and complemented strains. EV, empty vector. Values are normalized to the Δ*bchID* strain. The global p-value was calculated using an ANOVA test; pairwise comparisons were performed for each treatment relative to the wild type using Student's t-test. ns, non-significant; *, p<0.05; **, p<0.005; *** p<0.0005.

The growth of the Δ*bchID* mutant was impaired in some, but not all, carbon and light conditions. In rich peptone/yeast extract medium, the Δ*bchID* mutant grew almost identically to the wild-type strain in both L-D and dark conditions (Fig 2.4). This result is consistent with our observation that light, presumably harnessed by Bchl*a,* conferred no growth advantage in wild-type *E. longus* in rich medium (Fig. 2.1d). By contrast, the Δ*bchID* strain showed dramatic growth differences in pyruvate and butyrate cultures compared to the wild type (Fig. 2.4). With pyruvate as carbon source, the Δ*bchID* mutant showed a 50% reduction in growth rate and lower maximum OD compared to the wild-type strain in the L-D condition; in continuous darkness, the mutant and wild-type grew similarly (Fig. 2.4, S2.5, S2.6). Despite deletion of *bchID,* the mutant still showed enhanced growth in L-D relative to continuous darkness. With butyrate as a carbon source, the Δ*bchID* strain showed severe growth defects in both L-D and continuous darkness conditions (Fig. 2.4), suggesting that Bchl*a* is somehow required for normal growth on butyrate. With glucose as the carbon source, the Δ*bchID* strain showed reduced growth rates in both L-D and dark conditions, and light still enhanced growth even in the mutant. These results suggest that light may play other regulatory and physiological roles that are carbon type dependent on *E. longus*. Together, these findings demonstrate that light, Bchl*a*-based phototrophy, and carbon metabolism are intertwined in complex ways in *E. longus*.

The complementation of the genes *bchD* and *bchI* partially recovered the wild type maximum growth phenotype as light: dark/dark ratios of the complemented strain were significantly higher than the Δ*bchID* strain (Fig. S2.7).

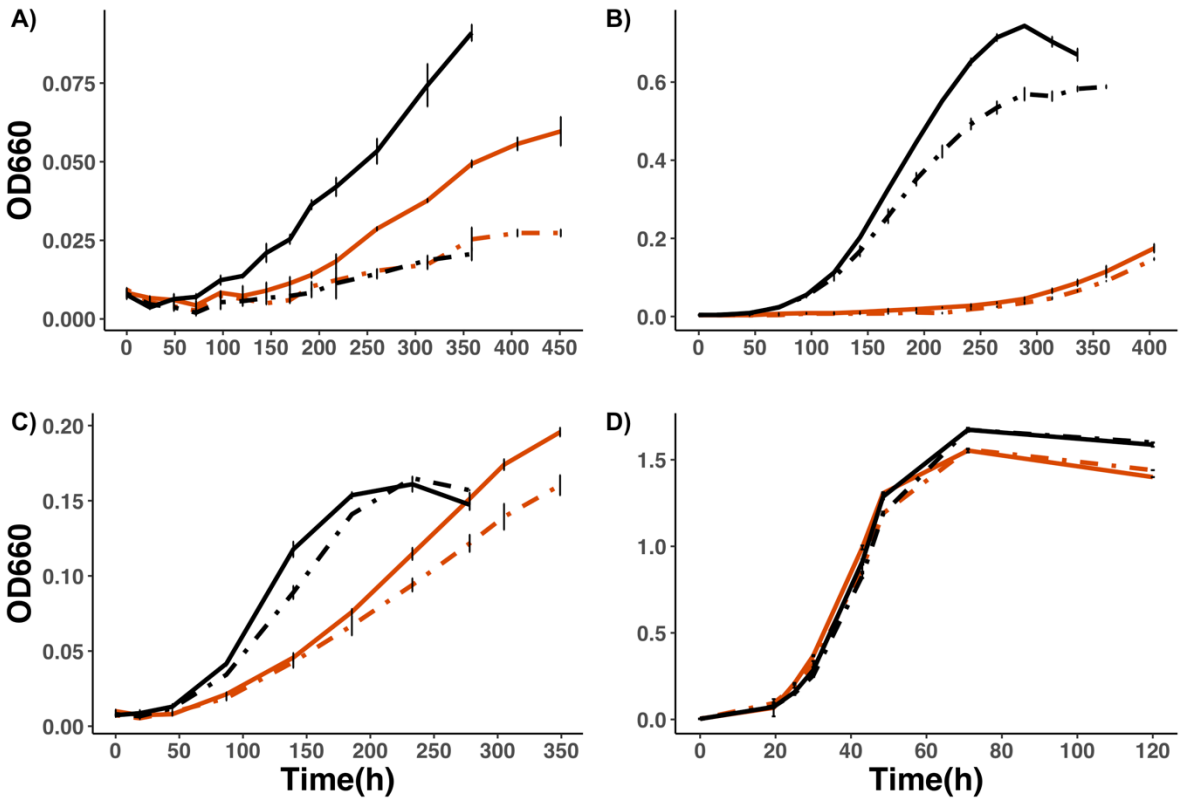

Figure 2.4. Growth of *E. longus* wild type (black) and *ΔbchID* (red) in carbon sources. a) ASW + Pyruvate, b) ASW + Butyrate, c) ASW + Glucose, d) ASW + Peptone + YE. Solid lines= 14h:10h light: dark cycles. Dashed lines= 24h dark. Error bars= standard deviation of three replicates.

2.3.4. The glyoxylate shunt is required for acetate assimilation in *E. longus*

To explore the pathways linking carbon metabolism and light-enhanced growth in *E. longus,* we compared the genomes of 1268 Alphaproteobacteria strains in the orders *Rhodobacterales* and *Sphingomonadales* (Table 2.1). These two orders include most of the known strains of AAPB, including *E. longus* (*Sphingomonadales*). We mined these genomes for photosynthesis marker genes, including Bchl*a* biosynthesis genes (*bchXYZ*) and photosystem genes (*pufLM*) (full list of functions in Table S2.6). We found 18.7% of *Sphingomonadales* genomes have the capacity for light harvesting, compared to 27.1% of *Rhodobacterales*. All the *Sphingomonadales* genomes with light harvesting capacity also encoded the genes isocitrate lyase

(*icl*) and malate synthase, the two genes that constitute the glyoxylate shunt pathway. In contrast, only 11% of *Rhodobacterales* genomes with photosynthesis markers also encode genes for the glyoxylate shunt. We then examined the distribution of the ethylmalonyl CoA pathway (EMC), which is another acetate assimilation pathway that unlike the glyoxylate shunt, involves inorganic carbon incorporation to the TCA cycle. This pathway shows the opposite pattern: the majority of Sphingomonadales genomes (99.8%) lack key genes for the EMC pathway, while in Rhodobacterales the EMC pathway is prevalent (86.8%) and only 9.1% of the Rhodobacterales genomes with photosynthetic markers encode the glyoxylate shunt.

Table 2.1. Genomic comparison of *Alphaproteobacteria* from the orders Sphingomonadales and Rhodobacterales.

	Sphingomonadales	Rhodobacterales
Total genomes*	501	767
Genomes with photosynthesis markers** (%)	18.7	27.1
Genomes with glyoxylate shunt (%)	87.8	9.1
Genomes with photosynthetic markers that also have glyoxylate shunt (%)	100	11
Genomes with EMC pathway (%)	0.2	86.8

*Genomes available at the Integrated Microbial Genomes and Microbiomes database (May 2019), img.jgi.doe.gov
**Photosynthesis markers and genes in the glyoxylate shunt and EMC pathways are listed in Table S6.

To investigate the role of the glyoxylate shunt in *E. longus* metabolism, we generated a mutant strain carrying a deletion of isocitrate lyase (Δ*icl*), the first step of the glyoxylate shunt pathway. There was no difference in growth between wild-type and Δ*icl* strains growing in

complex medium, and no effect of light was observed in these cultures (Fig. 2.5a). However, the Δ*icl* strain was incapable of growing in butyrate (Fig. 2.5b) and acetate (data not shown), demonstrating that this pathway is required for the assimilation of acetate and other carbon substrates that enter the TCA cycle as two-carbon molecules in *E. longus*. Complementation of the mutant with the wild-type copy of *icl* recovered the ability to grow in acetate (not shown) and butyrate (Figure 2.5c).

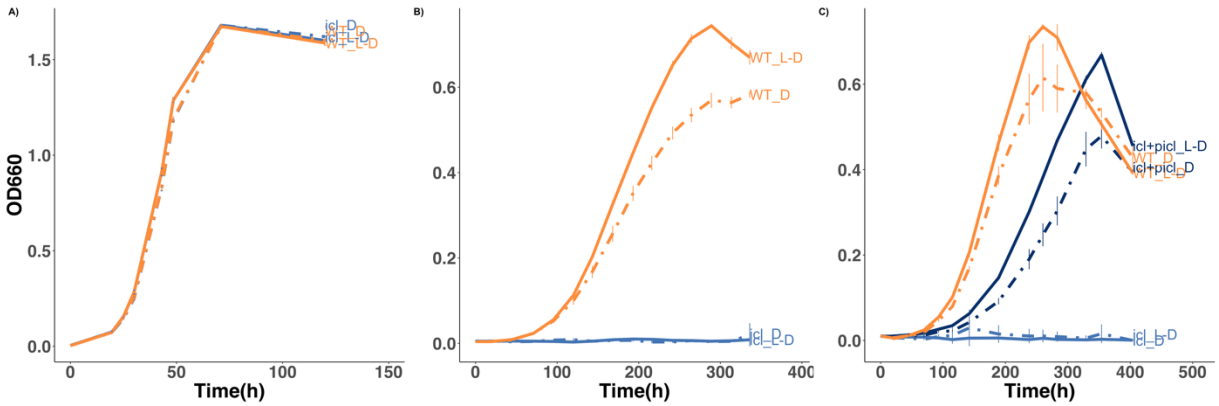

Figure 2.5. Effect of *icl* mutation on *E. longus* growth. A) wild-type (WT) vs *Δicl* (icl) growth in complex medium (ASW + peptone and yeast extract) in L-D and dark conditions. B) WT vs *Δicl* growth on ASW + 30mM butyrate. C) WT, *Δicl,* and complemented strain (*Δicl* + p*icl*) grown on ASW + 30mM butyrate. L-D, 14:10h light:dark cycles; D, 24h continuous darkness. Error bars= standard deviation of three replicates.

2.4. Discussion

Aerobic anoxygenic phototrophs are widespread in the euphotic zone of marine and freshwater aquatic systems (Koblížek, 2015a; Kolber et al., 2001). Despite their ubiquity, there remain many unanswered questions about their physiology and ecology, and the selective pressures that favor photoheterotrophy in some taxa and environments remain unknown. To better understand the fitness benefits and costs conferred by phototrophy, we used genetics to delete key genes in the

Bchl*a* biosynthetic pathway. Additionally, to disentangle the relationship between carbon metabolism and phototrophy, we also deleted a key gene in the glyoxylate shunt.

AAPB harvest sunlight using Bchl*a*, like related classical anoxygenic photosynthetic bacteria, but are distinguished from their cousins by producing pigments and photosystems under aerobic conditions. It has been proposed that AAPB benefit from phototrophy by growing faster and reaching larger cell size (increased biomass), likely contributing to the carbon cycle more than other heterotrophic bacteria of what is estimated based on cell counts (Kirchman & Hanson, 2013; Ritchie & Johnson, 2012; Stegman et al., 2014; Zheng et al., 2016). The ability to complement their metabolism with light energy seems largely beneficial for these bacteria, especially in oligotrophic waters (Kolber et al., 2001). However, AAPB are not the dominant members of aquatic microbial communities. Hence, it is important to better understand the conditions in which phototrophy is beneficial for growth, how this process is regulated, and the potential cellular costs of this metabolism, to understand the constraints on AAPB distribution and activity in natural environments.

Our experiments demonstrate that the effect of light on growth depends on the carbon substrate. No difference was observed between light-exposed cultures and dark cultures grown on a carbon-replete medium containing amino acids, vitamins and other trace nutrients. By contrast, light was advantageous for growth in all three individual carbon substrates used in this experiment. These results suggest that ATP, and the reducing equivalents generated by phototrophy contribute to *E. longus* growth on certain carbon substrates. Among the substrates we tested, pyruvate produced the least biomass, yet it was the substrate in which light was most beneficial. Furthermore, our results confirm that light is advantageous for *E. longus* under carbon limitation. AAPB are frequently reported in microbial surveys in oligotrophic waters, however they are more

abundant in coastal waters where there is more carbon available (Kirchman & Hanson, 2013; Lami et al., 2007; V. Yurkov & Hughes, 2017). Previous results on the closely related *Erythrobacter* sp. NAP1 showed that this strain switches from respiration to photosynthetic electron transfer, and combines phototrophy with anaplerotic carbon fixation to accumulate organic carbon to supply biosynthetic intermediaries allowing the strain to grow more efficiently on single carbon substrates in the light (Hauruseu & Koblížek, 2012). Our results in *E. longus* are consistent with these findings from NAP1.

The biology of AAPB has been largely studied using biochemistry and physiological measurements. Recently, sequencing surveys in marine and freshwater systems have improved our understanding of the abundance and distribution of AAPB (Cepáková et al., 2016; Čuperová et al., 2013; Salka et al., 2008; Yutin et al., 2007). However, there are few reports using genetics to test hypotheses about AAPB. We generated a genetically modified strain incapable of phototrophy with the goal of testing if light contributes to light enhanced growth in *E. longus.* The genomes of AAPB encode myriad protein domains that are capable of sensing light, redox state and small molecules (Fiebig et al., 2019; Henry & Crosson, 2011; Takala et al., 2015; Taylor & Zhulin, 1999). One possible explanation for light-enhanced growth is that proteins containing such domains (LOV, GAF and PAS domains) and/or bacteriophytochromes sense light and trigger a regulatory response in order to switch metabolic pathways or modify rates of catabolism and anabolism, thereby inducing differential growth in the light. We created the Bchl*a* deficient strain incapable of harvesting light energy, and demonstrated that the light harvested is used by *E. longus* to enhance its growth.

The metabolic pathways that directly benefit from light derived energy have been recently studied in other AAPB. *Dinoroseobacter shibae*, an AAPB in the *Rhodobacteraceae* family, has

been shown to use the EMC pathway for light-enhanced growth (Bill et al., 2017). *D. shibae* takes advantage of reducing equivalents and ATP produced by prototrophy to fix inorganic carbon via anaplerotic reactions and produce metabolic intermediates via the TCA cycle. However, this pathway is not present in the genome of *E. longus*. We compared genomes from two orders of *Alphaproteobacteria* that contain most of the known AAPB. The *Rhodobacterales* includes the model organisms *D. shibae* and *Roseobacter denitrificans*, along with other strains in the *Roseobacter* group known for being metabolically diverse and active members of marine microbial communities (Luo & Moran, 2015; Newton et al., 2010; Piwosz et al., 2018; Wagner-Döbler & Biebl, 2006). The *Sphingomonadales* includes the genera *Erythrobacter* and *Porphyrobacter,* and other phototrophic and non-phototrophic taxa from marine and freshwater environments. We found that members of these two orders use distinct strategies for acetate assimilation. The *Rhodobacterales* use the EMC pathway, which involves fixation of CO_2 and HCO_3^- to form malate (Laguna et al., 2011; Kuo-hsiang Tang et al., 2011). This pathway increases carbon-use efficiency by these AAPB, allowing biomass production with less respiration of organic carbon (Bill et al., 2017). The *Sphingomadales* instead use the glyoxylate shunt. This pathway bypasses reactions of the TCA cycle in which carbon is lost as CO_2. Although the shunt is favorable for the carbon economy of the cell, it does not directly involve inorganic carbon fixation nor does it use ATP or reducing equivalents. Nevertheless, we demonstrated that the glyoxylate shunt is the only pathway for acetate assimilation as mutants of isocitrate lyase are unable to grow on acetate and butyrate. Acetate assimilation is required to grow on fatty acids, lipids and other substrates that enter the TCA cycle as acetyl-CoA (Kuo-hsiang Tang et al., 2011). Our findings suggest that *Sphingomonadales* depend on the shunt to metabolize these substrates. Similarly, RuBisCO deletion mutants of the anoxygenic phototroph *Rhodopseudomonas palustris,* which also encodes

the glyoxylate shunt, failed to grow on acetate compared to *Rhodobacter sphaeroides* which uses EMC and was able to grow photoheterotrophically in acetate (Laguna et al., 2011).

Here we investigated the physiology of the AAPB model organism *Erythrobacter longus* under light:dark and dark regimes. This work contributes to the understanding of the ecophysiology of AAP by demonstrating that light-enhanced growth depends on the type and concentration of the carbon available. *E. longus* grows faster and to higher biomass on complex media with a variety of carbon substrates possibly explaining why AAPB are more abundant in eutrophic coastal waters. In this condition *E. longus* did not require extra energy from light however, light becomes advantageous to growth under energy limitation. These results suggest that phototrophy aids AAPB to thrive in oligotrophic environments where carbon available does not favor their rapid growth. Also, we showed that *E. longu*s, and possibly all AAP from the order Sphingomonadales, require the glyoxylate shunt as their only pathway for the assimilation of important organic substrates.

2.5. Methods

2.5.1. Bacterial strains

These experiments were conducted on *Erythrobacter longus* DSM6997^{T} (GenBank assembly accession: GCA_000715015.1) (Wang et al., 2014). The *E. coli* strains used for genetics experiments were maintained and propagated in Luria Broth (LB). Antibiotics kanamycin and chloramphenicol were added as needed. The summary of all bacterial strains used and generated in this study can be found in Table S2.5.

2.5.2. Growth media and conditions

Erythrobacter longus was maintained and propagated in 0.5X Marine Broth Difco 2216 BD (MBh= liquid cultures, MAh= agar plates) at 28°C, and preserved in 10% glycerol stocks. Solid media was achieved by the addition of 15g/L of agar (Fisher Scientific).

Carbon utilization comparisons were performed in modified Artificial Seawater (ASW) base media (Wyman et al., 1985), supplemented with 2mM of NH_4Cl (Fisher Scientific), 0.13mM of $K_2HPO_4 * 3H_2O$ (Fisher Scientific), trace metal mix(Waterbury & Willey, 1988), and vitamin mix (Guillard & Ryther, 1962). Complex rich medium was made from 5g/L of peptone (Difco) and 1g/L of yeast extract (Difco) added to the ASW base media. Three single carbon media were made adding 30 mM sodium pyruvate (Fisher Scientific), 30mM sodium butyrate (Fisher Scientific), and 30mM dextrose (Fisher Scientific).

All experiments were performed on a Percival incubator under fluorescent light 180uE and grown on 14h:10h light:dark cycles or 24h dark cycles at 24°C and shaking at 250rpm. The 24h dark was achieved by covering the tubes with aluminum foil.

2.5.3. Growth curve experiments

A starting culture of *E. longus* was initiated by the inoculation of a single colony from a MAh plate in 8mL of MBh media and incubated under the conditions detailed above until late exponential phase (determined by OD660). The cells were then washed twice in ASW base (no carbon added), and resuspended in an equal volume of ASW base. Triplicate 15ml tubes containing 8mL ASW base supplemented with specific carbon sources were inoculated with the washed cell suspension of *E. longus* and incubated under the conditions previously described. The optical density of the tubes was directly measured on a Spec 20 spectrophotometer (Thermo) at 600nm or 660nm.

2.5.4. Bacteriochlorophyll-*a* determinations

The Bchl*a* determinations were done using *E. longus* cells washed twice in NaCl 3% solution and resuspended in NaCl 3% + 4mg/ml sucrose (Harashima et al., 1980)). Absorbance spectra (450nm - 1000nm) of triplicate cultures were measured on a Spec 20 spectrophotometer (Thermo). The absorbance spectra were then examined to determine the Bchl*a* peak and normalized by the absorbance of the suspension at 660nm (proxy for cell density) to estimate the amount of pigment.

2.5.5. Allele deletions and complementation

Deletions of the adjacent genes *bchI* and *bchD* (Δ*bchID*), and isocitrate lyase (Δ*icl*) were performed by double recombination as previously described (Hmelo et al., 2015). Briefly, 500bp from the upstream and downstream regions of the target genes were PCR amplified using the primers ST5. The PCR was performed using Phusion High-Fidelity DNA Polymerase (Thermo Scientific) and the following amplification program: initial denaturation of 98°C for 30s, 25 cycles of 98°C for 10s, 62°C for 30, 72°C for 30s, and a final extension of 72°C for 5 minutes. The upstream and downstream regions were fused using overlap extension PCR, using the above amplification program without the addition of the primers until after 20 cycles of self-amplification. The resulting product was digested and ligated using T4 ligase (Thermo Scientific) into the plasmid pNPTS138-cat carrying a chloramphenicol resistance marker and the gene *sacB* (ST5). The plasmids carrying the recombinant alleles were then chemically transformed into *E. coli* TOP10 cells. The genetic sequence of alleles was confirmed by Sanger sequencing. The plasmid containing the alleles was conjugated into exponentially grown cells of *E. longus* by mixing a cell suspension of the wild type strain with *E. coli* TOP10 containing the plasmid and an

E. coli Fc3 helper strain. The conjugation mix was spotted in a Poretics 0.2um filter (GVS Life Sciences) on top of a MAh plate and incubated overnight at room temperature in the dark. After the incubation, the mixture was plated in MAh + 4ug/ml of chloramphenicol. Single antibiotic resistant colonies were then streaked in MAh + 5% of sucrose plates for a second selection by *sacB*. Candidate colonies were screened by PCR using Promega GoTaq 2X green master mix (Promega) using the following program: initial denaturation of 95°C for 2 min, 35 cycles of 95°C for 30s, 62°C for 30, 72°C for 60s, and a final extension of 72°C for 10 minutes. The products were confirmed by sequencing using primers that anneal outside the recombinant regions (Table S2.5).

The complementation of the mutant strains was performed by the amplification of the wild type allele of the genes *bchID* and *icl* including 150bp of the upstream region using Phusion High-Fidelity DNA Polymerase (Thermo Scientific) as described above. The products were cloned into the plasmid pBXMCS-6 (Table S2.5) using Gibson assembly (New England Biolabs). The plasmids carrying the wild type alleles were transferred to *E. longus* by conjugation as described above, and plated in MBh + 4ug/ml of kanamycin. The presence of the plasmid was confirmed by PCR and the sequences were confirmed by Sanger sequencing using the primers Pxyl and M13F (Table S2.5).

The growth of wild type, deletion mutants and the complemented strains was compared using the growth experiment protocol detailed above.

2.5.6. Statistical analysis and plotting

All statistical analysis and plotting was done in Rv3.5.3 using the packages ggpubr (https://cran.r-project.org/web/packages/ggpubr/index.html) and ggplot2 (https://cloud.r-

project.org/web/packages/ggplot2/index.html). The statistical comparison of treatment effects on multiple groups was performed using an ANOVA test. The pairwise comparisons between groups were calculated using a parametric t-test, both analyses were done using the package ggpubr. The growth curves were fitted using the grofit v.1.1.1 R package (Kahm et al., 2010). The fit of each growth curve to the model was examined independently.

2.6. References

Bauer, C., Elsen, S., Swem, L. R., Swem, D. L., & Masuda, S. (2003). Redox and light regulation of gene expression in photosynthetic prokaryotes. *Phil. Trans. R. Soc. Lond.*, 147–154.

Beatty, J. T. (2002). On the natural selection and evolution of the aerobic phototrophic bacteria. *Photosynthesis Research*, 109–114.

Bill, N., Tomasch, J., Riemer, A., Muller, K., Kleist, S., Schmidt-Hohagen, K., Wagner-Döbler, I., & Schomburg, D. (2017). Fixation of CO2 using the ethylmalonyl-CoA pathway in the photoheterotrophic marine bacterium *Dinoroseobacter shibae. Environmental Microbiology*, 2645–2669.

Candela, M., Zaccherini, E., & Zannoni, D. (2001). Respiratory electron transport and light-induced energy transduction in membranes from the aerobic photosynthetic bacterium Roseobacter denitrificans. *Archives of Microbiology*, 168–177.

Cepáková, Z., Hrouzek, P., Žišková, E., Nuyanzina-Boldareva, E., Šorf, M., Kozlíková-Zapomělová, E., Salka, I., Grossart, H.-P., & Koblížek, M. (2016). High turnover rates of aerobic anoxygenic phototrophs in European freshwater lakes. *Environmental Microbiology*, *18*(12), 5063–5071.

Čuperová, Z., Holzer, E., Salka, I., Sommarug, R., & Koblížek, M. (2013). Temporal changes and altitudinal distribution of aerobic anoxygenic phototrophs in mountain lakes. *Applied and Environmental Microbiology*, *79*(20), 6439–6446.

Fiebig, A., Varesio, L. M., Navarreto, X. A., & Crosson, S. (2019). Regulation of the *Erythrobacter litoralis* DSM 8509 general stress response by visible light. *Molecular Microbiology*, *112*(2), 442–460.

Fuchs, B. M., Spring, S., Teeling, H., Quast, C., Amann, R., Ferriera, S., Johnson, J., Glockner, F. O., & Amann, R. (2007). Characterization of a marine gammaproteobacterium capable of aerobic anoxygenic photosynthesis. *PNAS*, *104*(8), 2891–2896.

Guillard, R. R. L., & Ryther, J. H. (1962). Studies of Marine Planktonic Diatoms: I. Cyclotella Nana Hustedt, and Detonula Confervacea (cleve) Gran. *Canadian Journal of Microbiology*, *8*(2), 229–239.

Harashima, K., Hayasaki, J., Ikari, T., & Shiba, T. (1980). O2-stimulated synthesis of bacteriochlorophyll and carotenoids in marine bacteria. *Plant and Cell Physiology*, *21*(7), 1283–1294.

Harashima, K., & Kawazoe, K. (1987). Light-Stimultated Aerobic Growth of *Erythrobacter* Species OCh 114. *Plant & Cell Physiology*, *28*(2), 365–374.

Hauruseu, D., & Koblížek, M. (2012). Influence of Light on Carbon Utilization in Aerobic Anoxygenic Phototrophs. *Applied and Environmental Microbiology*, *78*(20), 7414–7419.

Henry, J. T., & Crosson, S. (2011). Ligand binding PAS domains in a genomic, cellular, and structural context. *Annual Review of Microbiology*, *65*, 261–286.

Hiraishi, A., & Shimada, K. (2001). Aerobic anoxygenic photosynthetic bacteria with zinc-bacteriochlorophyll. *J. Gen. Appl. Microbiol*, *180*, 161–180.

Kahm, M., Hasenbrink, G., Lichtenberg-Fraté, H., Ludwig, J., & Kschiho, M. (2010). grofit: Fitting Biological Growth Curves with R. *Journal of Statistical Software*, *33*(7).

Kirchman, D. L., & Hanson, T. E. (2013). Bioenergetics of photoheterotrophic bacteria in the oceans. *Environmental Microbiology Reports*. *5*, 188–199.

Koblížek, M. (2011). Role of photoheterotrophic bacteria in the marine carbon cycle. In: Microbial Carbon Pump in the Ocean (N. Jiao, F. Azam, & S. Sanders, Eds.). Science/AAAS.

Koblížek, M. (2015a). Ecology of aerobic anoxygenic phototrophs in aquatic environments. *FEMS Microbiology Reviews*, *January*, 854–870.

Koblížek, M. (2015b). Ecology of aerobic anoxygenic phototrophs in aquatic environments. *FEMS Microbiology Reviews*, *39*(6), 854–870.

Koblížek, M., Béjà, O., Bidigare, R. R., Christensen, S., Benitez-Nelson, B., Vetriani, C., Kolber, M. K., Falkowski, P. G., & Kolber, Z. S. (2003). Isolation and characterization of *Erythrobacter* sp. Strains from the upper ocean. *Archives of Microbiology*, *180*(5), 327–338.

Koblížek, M., Mlcouskova, J., Kolber, Z. S., & Kopecky, J. (2010). On the photosynthetic properties of marine bacterium COL2P belonging to Roseobacter clade. *Archives of Microbiology*, *192*, 41–49.

Kolber, Z. S., Plumley, F. G., Lang, a S., Beatty, J. T., Blankenship, R. E., VanDover, C. L., Vetriani, C., Koblizek, M., Rathgeber, C., & Falkowski, P. G. (2001). Contribution of

aerobic photoheterotrophic bacteria to the carbon cycle in the ocean. *Science*, *292*(5526), 2492–2495.

Kolber, Z. S., Van Dover, C. L., Niederman, R. a, & Falkowski, P. G. (2000). Bacterial photosynthesis in surface waters of the open ocean. *Nature*, *407*(1993), 177–179.

Laguna, R., Tabita, F. R., & Alber, B. E. (2011). Acetate-dependent photoheterotrophic growth and the differential requirement for the Calvin–Benson–Bassham reductive pentose phosphate cycle in Rhodobacter sphaeroides and Rhodopseudomonas palustris. *Archives of Microbiology*, *193*(2), 151–154.

Lami, R., Cottrell, M. T., Ras, J., Ulloa, O., Obernosterer, I., Claustre, H., Kirchman, D. L., & Lebaron, P. (2007). High Abundances of Aerobic Anoxygenic Photosynthetic Bacteria in the South Pacific Ocean. *Applied and Environmental Microbiology*, *73*(13), 4198–4205.

Luo, H., & Moran, M. A. (2015). How do divergent ecological strategies emerge among marine bacterioplankton lineages ? *Trends in Microbiology*, 1–8.

Newton, R. J., Griffin, L. E., Bowles, K. M., Meile, C., Gifford, S., Givens, C. E., Howard, E. C., King, E., Oakley, C. a, Reisch, C. R., Rinta-Kanto, J. M., Sharma, S., Sun, S., Varaljay, V., Vila-Costa, M., Westrich, J. R., & Moran, M. A. (2010). Genome characteristics of a generalist marine bacterial lineage. *The ISME Journal*, *4*(6), 784–798.

Nishimura, K., Shimada, H., Ohta, H., Masuda, T., Shioi, Y., & Takamiya, K. (1996). Expression of the puf Operon in an Aerobic Photosynthetic Bacterium, *Roseobacter denitrificans*. *Plant Cell Physiology*, *37*(2), 153–159.

Nishimura, K., Shinmen, T., Obayashi, T., Masuda, T., Ohta, H., & Takamiya, K.-I. (1999). Photosynthetic regulatory gene cluster in an aerobic photosynthetic bacterium, *Roseobacter denitrificans*. *The Journal of General and Applied Microbiology*, *45*(3), 129–134.

Okamura, K., Mitsumori, F., Ito, O., Takamiya, K.-I., & Nishimura, M. (1986). Photophosphorylation and Oxidative Phosphorylation in Intact Cells and Chromatophores of an Aerobic Photosynthetic Bacterium, *Erythrobacter* sp. Strain OChll4. *Journal of Bacteriology*, *168*(3), 1142–1146.

Palovaara, J., Akram, N., Baltar, F., Bunse, C., Forsberg, J., & Pedrós-alió, C. (2014). Stimulation of growth by proteorhodopsin phototrophy involves regulation of central metabolic pathways in marine planktonic bacteria. *PNAS*, E3650–E3658.

Petushkova, E. P., & Tsygankov, A. A. (2017). Acetate Metabolism in the Purple Non sulfur Bacterium *Rhodobacter capsulatus*. *Biochemistry*. *82*(5).

Piwosz, K., Kaftan, D., Dean, J., Šetlík, J., & Koblížek, M. (2018). Nonlinear effect of irradiance on photoheterotrophic activity and growth of the aerobic anoxygenic phototrophic

bacterium *Dinoroseobacter shibae*. *Environmental Microbiology*, *20*(2), 724–733.

Ponnampalam, S. N., Buggy, J. J., & Bauer, C. E. (1995). Characterization of an aerobic repressor that coordinately regulates bacteriochlorophyll, carotenoid, and light harvesting-II expression in *Rhodobacter capsulatus*. *Journal of Bacteriology*, *177*(11), 2990–2997.

Rathgeber, C., Alric, J., Andre, E. H., & Yurkov, V. (2012). The photosynthetic apparatus and photoinduced electron transfer in the aerobic phototrophic bacteria *Roseicyclus mahoneyensis* and *Porphyrobacter meromictius*. *Photosynthesis Research*, *110*, 193–203.

Rathgeber, C., Beatty, J. T., & Yurkov, V. (2004). Aerobic phototrophic bacteria: New evidence for the diversity, ecological importance and applied potential of this previously overlooked group. *Photosynthesis Research*, 113–128.

Ritchie, A. E., & Johnson, Z. I. (2012). Abundance and Genetic Diversity of Aerobic Anoxygenic Phototrophic. *Applied and Environmental Microbiology*. 2858–2866.

Salka, I., Moulisová, V., Koblížek, M., Jost, G., Jürgens, K., & Labrenz, M. (2008). Abundance, depth distribution, and composition of aerobic bacteriochlorophyll a-producing bacteria in four basins of the central Baltic Sea. *Applied and Environmental Microbiology*, *74*(14), 4398–4404.

Shiba, T. (1987). O2 regulation of bacteriochlorophyll synthesis in the aerobic bacterium *Erythrobacter*. *Plant Cell Physiol.*, *28*(7), 1313–1320.

Shiba, Tsuneo, Simidu, U., & Taga, N. (1979). Distribution of Aerobic Bacteria Which Contain Bacteriochlorophyll a. *Applied and Environmental Microbiology*, *38*(1), 43–45.

Stegman, M. R., Cottrell, M. T., & Kirchman, D. L. (2014). Leucine incorporation by aerobic anoxygenic phototrophic bacteria in the Delaware estuary. *ISME*, *8*(11), 2339–2348.

Suyama, T., Shigematsu, T., Suzuki, T., Tokiwa, Y., Kanagawa, T., Nagashima, K. V. P., & Hanada, S. (2002). Photosynthetic Apparatus in *Roseateles depolymerans* 61A Is Transcriptionally Induced by Carbon Limitation. *Applied and Environmental Microbiology*. *68*(4), 1665–1673.

Takala, H., Björling, A., Linna, M., Westenhoff, S., & Ihalainen, J. A. (2015). Light-induced Changes in the Dimerization Interface of Bacteriophytochromes. *Journal of Biological Chemistry*, *290*(26), 16383–16392.

Tang, Kai, Zong, R., & Zhang, F. (2010). Characterization of the Photosynthetic Apparatus and Proteome of *Roseobacter denitrificans*. *Current Microbiology*, *60*, 124–133.

Tang, Kuo-hsiang, Tang, Y. J., & Blankenship, R. E. (2011). Carbon metabolic pathways in phototrophic bacteria and their broader evolutionary implications. *Frontiers in Microbiology*, *2*(August), 1–23.

Taylor, B. L., & Zhulin, I. B. (1999). PAS domains: Internal sensors of oxygen, redox potential, and light. *Microbiology and Molecular Biology Reviews : MMBR*, *63*(2), 479–506.

Tomasch, J., Gohl, R., Bunk, B., Diez, M. S., & Wagner Dobler, I. (2011). Transcriptional response of the photoheterotrophic marine bacterium *Dinoroseobacter shibae* to changing light regimes. *Isme J*, 1957–1968.

Wagner-Döbler, I., & Biebl, H. (2006). Environmental Biology of the Marine Roseobacter Lineage. *Annual Review of Microbiology*, *60*(1), 255–280.

Wang, Y., Zhang, R., Zheng, Q., & Jiao, N. (2014). Draft Genome Sequences of Two Marine Phototrophic Bacteria, *Erythrobacter longus* Strain DSM 6997 and *Erythrobacter litoralis* Strain DSM 8509. *Genome Announcements*, *2*(4), 1–2.

Waterbury, J. B., & Willey, J. M. (1988). Isolation and growth of marine planktonic cyanobacteria. In *Methods in Enzymology* (Vol. 167, pp. 100–105). Academic Press.

Wyman, M., Gregory, R. P. F., & Carr, N. G. (1985). Novel Role for Phycoerythrin in a Marine Cyanobacterium, *Synechococcus* Strain DC2. *Science*, *230*(4727), 818–820.

Yurkov, V., & Hughes, E. (2017). Aerobic Anoxygenic Phototrophs: Four Decades of Mystery. In P. C. Hallenbeck (Ed.), *Modern Topics in the Phototrophic Prokaryotes: Environmental and Applied Aspects* (pp. 193–214). Springer International Publishing.

Yurkov, V. V., & Beatty, J. T. (1998). Aerobic Anoxygenic Phototrophic Bacteria. *Microbiology and Molecular Biology Reviews*. *62*(3), 695–724.

Yurkov, V. V., & van Gemerden, H. (1993). Impact of light/dark regimen on growth rate, biomass formation and bacteriochlorophyll synthesis in *Erythromicrobium hydrolyticum*. *Archives of Microbiology*, 84–89.

Yutin, N., Suzuki, M. T., Teeling, H., Weber, M., Venter, J. C., Rusch, D. B., & Béjà, O. (2007). Assessing diversity and biogeography of aerobic anoxygenic phototrophic bacteria in surface waters of the Atlantic and Pacific Oceans using the Global Ocean Sampling expedition metagenomes. *Environmental Microbiology*, *9*, 1464–1475.

Zheng, Q., Lin, W., Liu, Y., Chen, C., & Jiao, N. (2016). A comparison of 14 *Erythrobacter* genomes provides insights into the genomic divergence and scattered distribution of phototrophs. *Frontiers in Microbiology*, *7*.

2.7. Supporting Figures

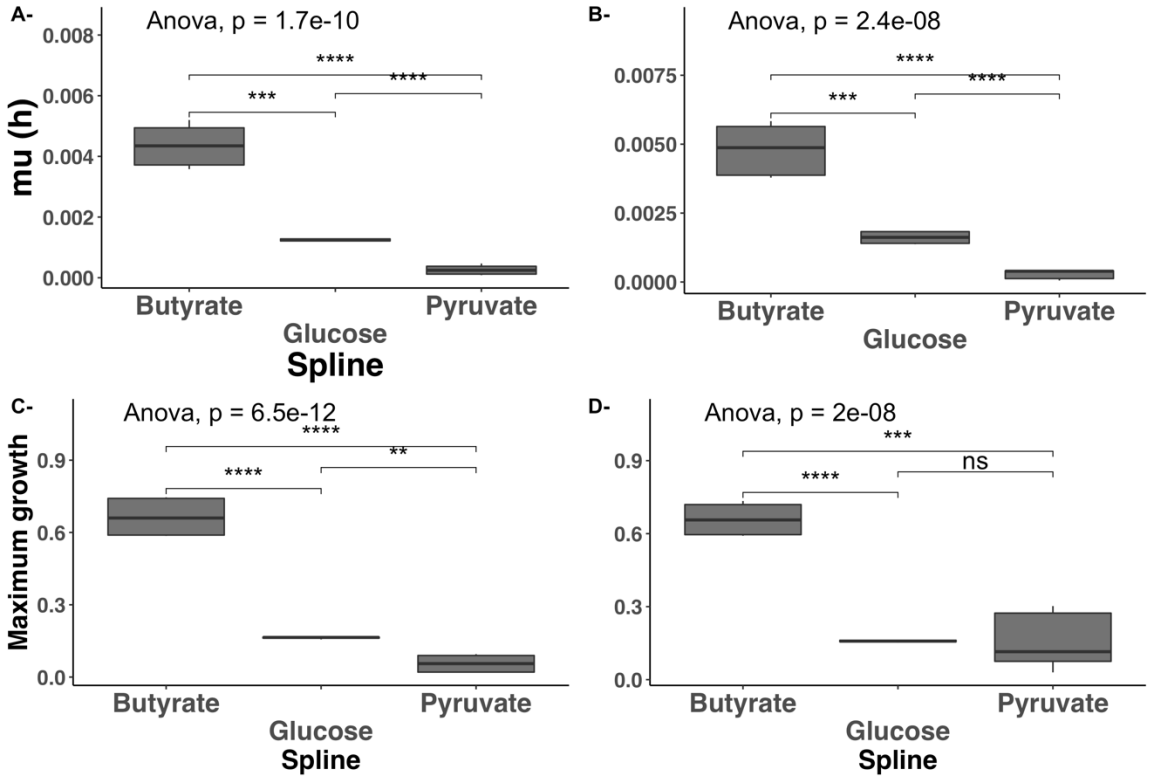

Figure S2.1. Analysis of growth curves of *E. longus* on single carbon substrates, with the data for both light treatments averaged together. A) and B) growth rate in hours calculated based on spline or model fit respectively. C) and D) maximum growth calculated based on spline or model fit respectively. The global p value was calculated using an anova test. The pairwise comparison of the treatments was performed using t-test. ns= non-significant. *= $p<0.05$. **=$p<0.005$. ***=$p<0.0005$.

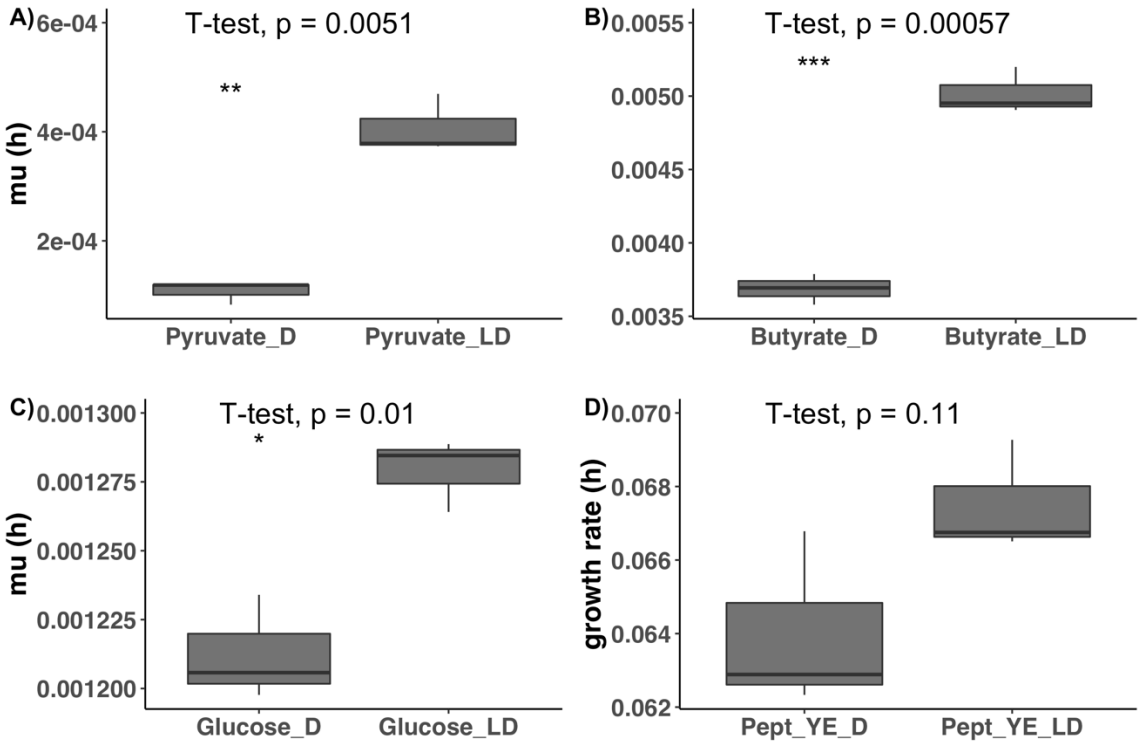

Figure S2.2. Growth rates comparison of *E. longus* wild type growing in light/dark cycles vs continuous darkness on carbon substrates. A- ASW + Pyruvate. B- ASW + Butyrate. C- ASW + Glucose. D- ASW + Peptones + yeast extract. LD= 14h:10h light: dark cycles. D= 24h dark. Pept_YE= Peptone + yeast extract. The pairwise comparison of the treatments was performed using a parametric t-test. ns= non-significant. *= $p<0.05$. **=$p<0.005$. ***=$p<0.0005$.

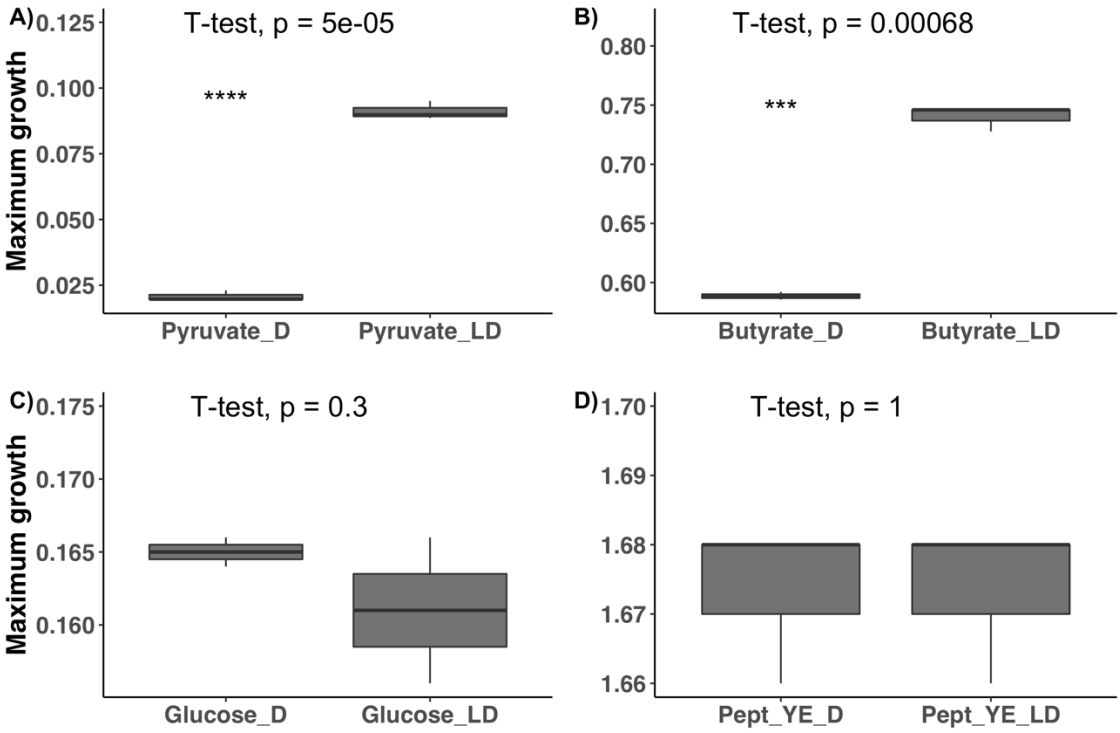

Figure S2.3. The effect of light on maximum OD for *E. longus* grown on different carbon substrates. A) ASW + Pyruvate. B) ASW + Butyrate. C) ASW + Glucose. D) ASW + Peptones + yeast extract. LD= 14h:10h light: dark cycles. D= 24h dark. Pept_YE= Peptone + yeast extract. The pairwise comparison of the treatments was performed using a parametric t-test. ns= non-significant. *= $p<0.05$. **=$p<0.005$. ***=$p<0.0005$. ****=$p<0.00005$.

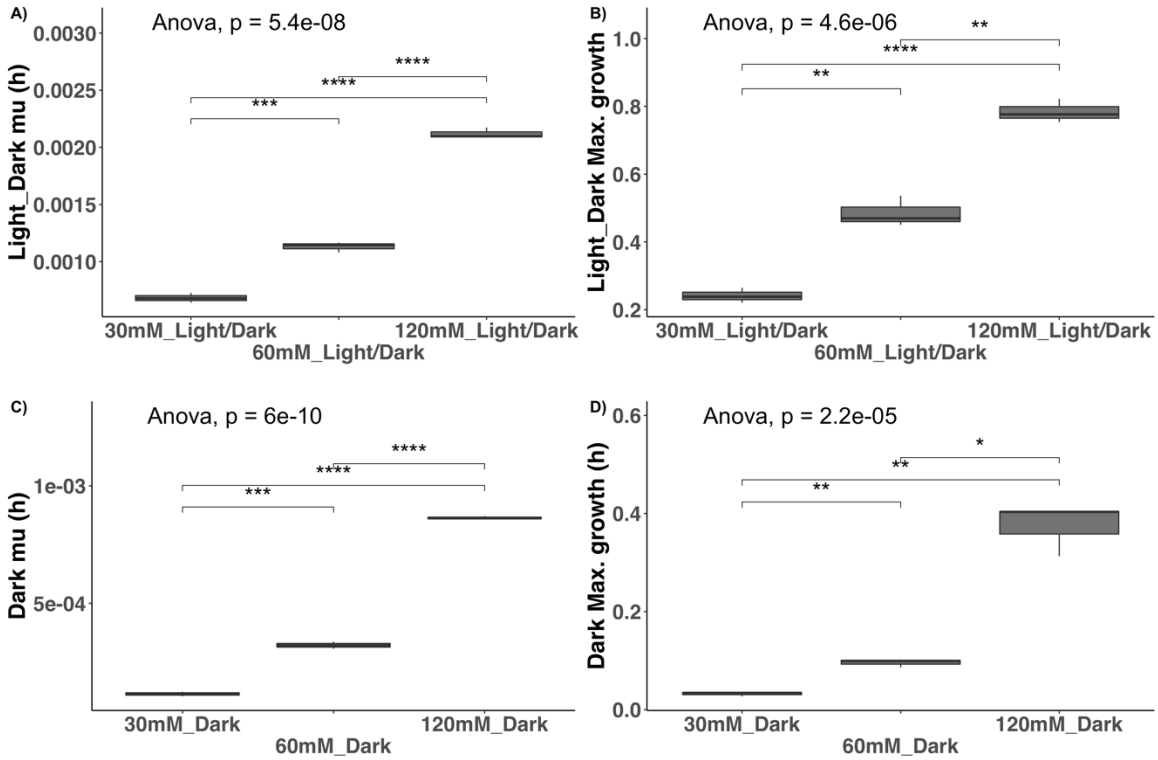

Figure S2.4. Comparison of the growth rate (A and C) and maximum growth (B and D) of *E. longus* wild type cultures growing on ASW + Pyruvate at 30mM, 60mM and 120mM. The cultures were incubated under different light regimes: 14h:10h light: dark (Light/Dark) vs 24h dark (Dark). Global p value calculated using anova, the pairwise comparison of the treatments was performed using a t-test. ns= non-significant. *= $p<0.05$. **=$p<0.005$. ***=$p<0.0005$.

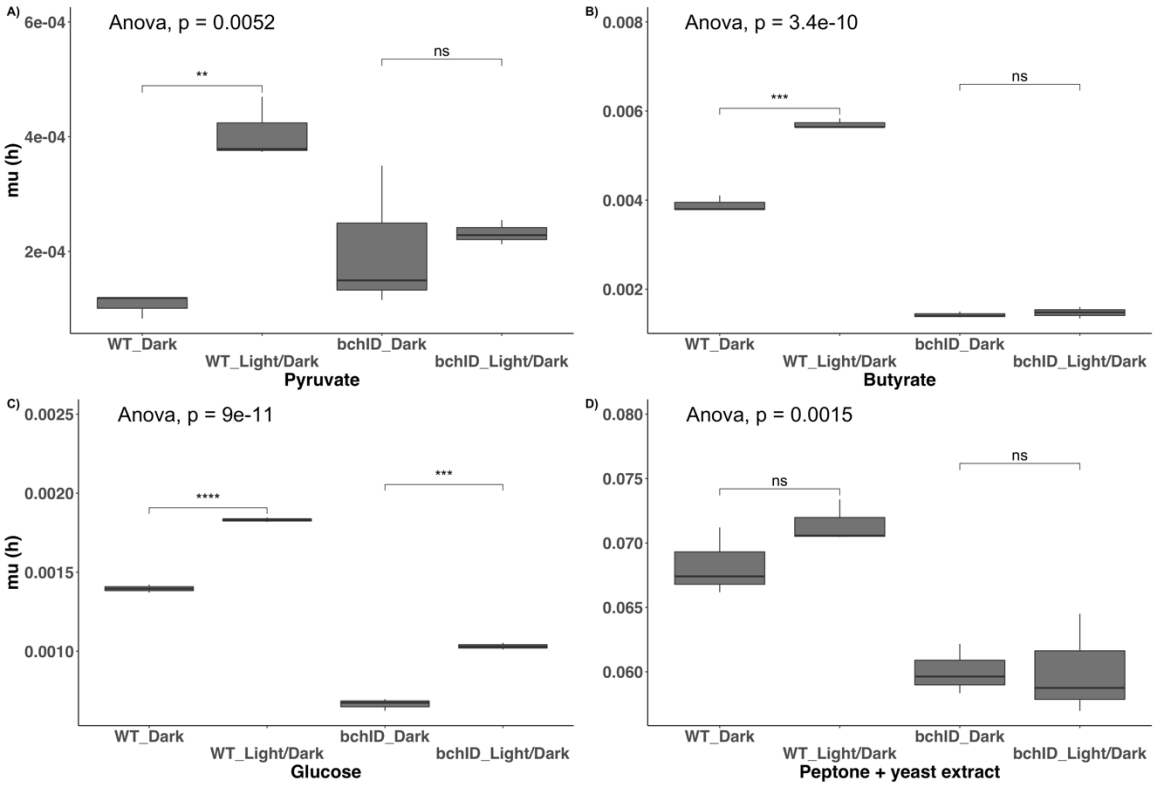

Figure S2.5. Growth rates comparison of *E. longus* wild type versus Δ*bchID* growing in 14h:10h light: dark cycles (Light/Dark) vs 24h dark (Dark) on carbon substrates. A- ASW + Pyruvate. B- ASW + Butyrate. C- ASW + Glucose. D- ASW + Peptones + yeast extract. The pairwise comparison of the light treatments within the strains was performed using a parametric t-test. ns= non significant. *= $p<0.05$. **=$p<0.005$. ***=$p<0.0005$. ****=$p<0.00005$.

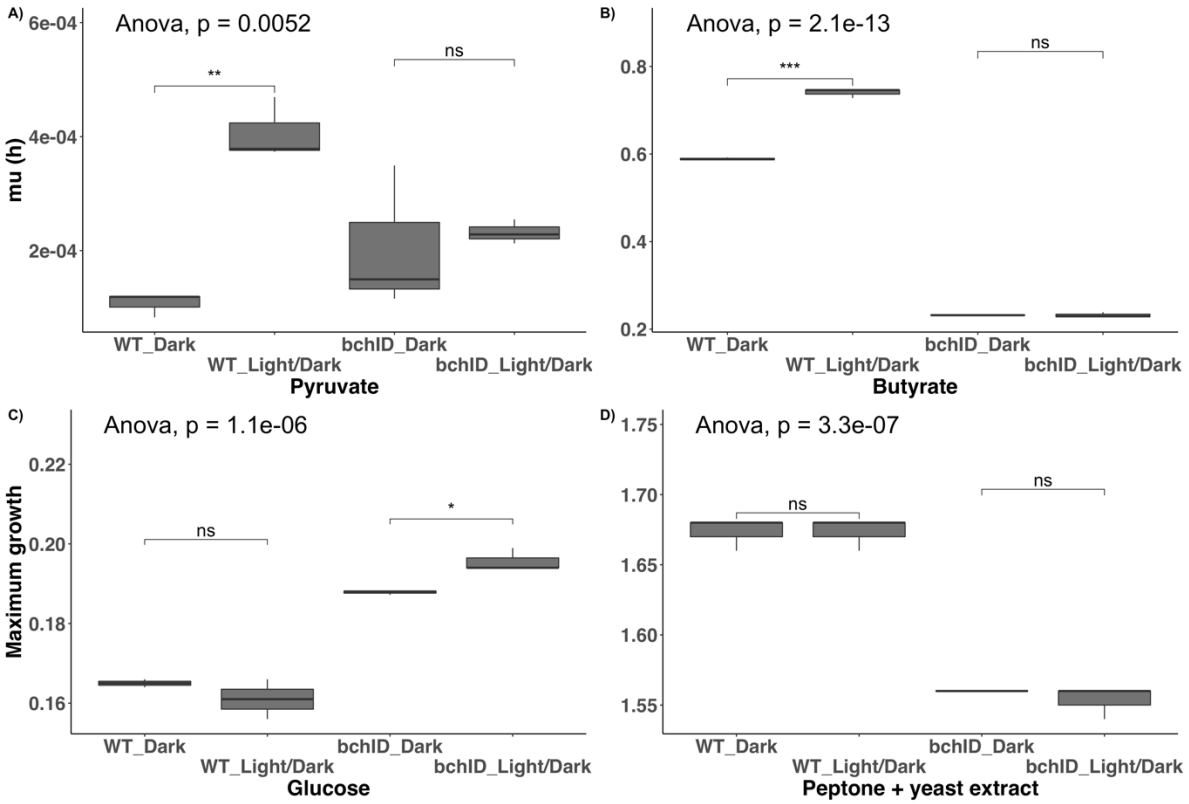

Figure S2.6. Maximum growth comparison of *E. longus* wild type versus Δ*bchID* growing in 14h:10h light: dark cycles (Light/Dark) vs 24h dark (Dark) on carbon substrates. A- ASW + Pyruvate. B- ASW + Butyrate. C- ASW + Glucose. D- ASW + Peptones + yeast extract. The pairwise comparison of the light treatments within the strains was performed using a parametric t-test. ns= non-significant. *= $p<0.05$. **=$p<0.005$. ***=$p<0.0005$. ****=$p<0.00005$.

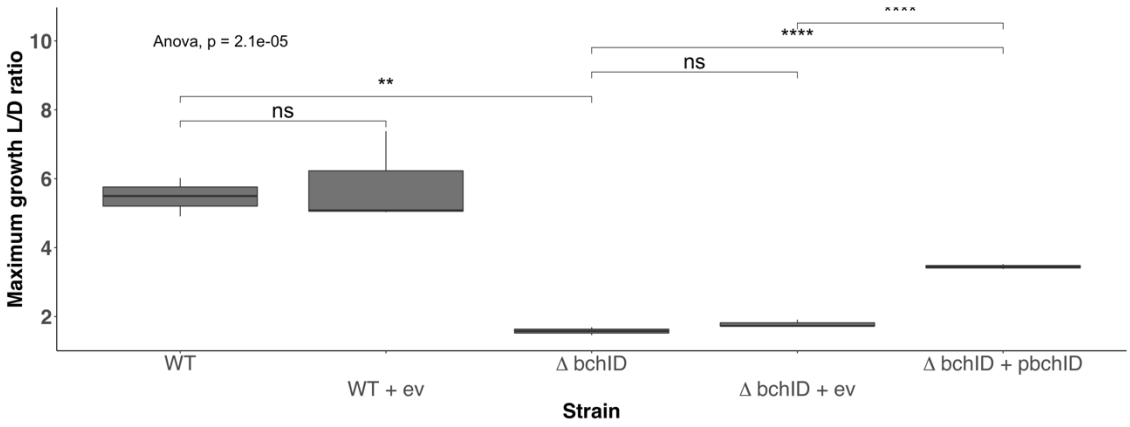

Figure S2.7. Maximum growth Light: dark / Dark ratio comparison of *E. longus* wild type, Δ*bchID* and Δ*bchID* + *pbchID* on ASW + 30mM pyruvate. Ratios were calculated as: 14h:10h light: dark / 24h dark. WT= wild type. WT + ev= wild type carrying empty vector. Δ*bchID*= mutant strain lacking *bchID* genes. Δ*bchID* + ev= mutant strain lacking *bchID* genes carrying empty vector. Δ*bchID* + *pbchID*= mutant strain lacking *bchID* genes complemented with wild type copies of *bchID* genes.

CHAPTER 3

Global fitness profiling reveals interactions between light and carbon metabolism in the aerobic anoxygenic phototroph *Porphyrobacter* sp.

3.1. Abstract

Aerobic anoxygenic phototrophy is a widespread bacterial metabolism that uses bacteriochlorophyll-a to harness sunlight under oxic conditions. This pathway is thought to supplement the energy needs of heterotrophic bacteria, but its molecular details and ecological relevance are poorly understood. Here we examined the genetic factors influencing growth in the light in phototrophic strain *Porphyrobacter* sp. LM6, isolated from Lake Michigan. Light enhanced growth of LM6 with glucose or pyruvate as sole carbon source, but not with butyrate or peptone. Using a barcoded mutant library, we found that mutations in genes involved in phototrophy drove dramatic reductions in fitness in light conditions with glucose as the carbon source, but these mutations did not affect fitness in butyrate-grown cultures. Genes involved in anaplerotic carbon fixation were important for fitness in both glucose and butyrate. PEP carboxylase mutants showed fitness values within the range of the essential genes for glucose light cultures demonstrating that anaplerotic reactions are vital for the phototrophic growth of this strain. Genes involved in detoxification of reactive oxygen species were important for fitness, especially in the light. Our results support *ppsR* as the main regulator of phototrophy, and mutations in *ppsR* cause strong fitness effects. The glyoxylate shunt appears to be essential for growth on butyrate. Our results indicate that phototrophy and carbon metabolism are intertwined, and show that detoxification of reactive oxygen species is key for the survival of these organisms. This study provides new insights into the environmental drivers and molecular mechanisms used by AAP.

3.2. Introduction

Aerobic anoxygenic phototrophic bacteria (AAPB) are widespread in aquatic systems and may play an important role in the global carbon cycle (Cepáková et al., 2016; Koblížek, 2015; Z S Kolber et al., 2000; Zbigniew S Kolber et al., 1999, 2001; Sieracki et al., 2006; Soora & Cypionka, 2013; V. Yurkov & Csotonyi, 2009). These heterotrophic alpha, beta and gamma proteobacteria are capable of supplementing their metabolism with energy harvested from sunlight, an advantageous trait under nutrient starvation (Koblížek, 2015; Tsuneo Shiba, 1984; Sieracki et al., 2006). They are characterized by their aerobic metabolism, their ability to produce bacteriochlorophyll-*a* (Bchl*a*) in the presence of oxygen, and their lack of the enzyme RubisCO (Koblížek, 2015; V. Yurkov & Csotonyi, 2009; V. Yurkov & Hughes, 2013; V. V. Yurkov & Beatty, 1998a). The genomes of AAPB encode an array of adjacent operons called the Photosynthetic Gene Cluster (PGC), which contains the genes for bacteriochlorophyll-*a* and carotenoid biosynthesis, as well as the type II photosystem and regulatory functions (Liotenberg et al., 2008; Zheng et al., 2011; Zsebo & Hearst, 1984). The photosynthetic gene cluster in AAPB resembles that in the closely related purple non-sulfur bacteria, but the expression of these operons in AAPB is not repressed in the presence of oxygen, as it is in classic anoxygenic phototrophs (Bauer et al., 2003; Rathgeber et al., 2004; Tsuneo Shiba, 1984; Swem et al., 2001; Yin et al., 2012). The phototrophic capacity of AAPB, including measurements of the photochemical efficacy of the photosystem, has been demonstrated (Rathgeber et al., 2012; Kai Tang et al., 2010), as well as their capacity to switch electron transfer from the respiratory chain to photophosphorylation under phototrophic conditions (Bill et al., 2017; Hauruseu & Koblížek, 2012). However, many questions remain unanswered, including which environmental signals and molecular cascades control phototrophy, which pathways are involved in light-enhanced growth,

and what fitness tradeoffs govern the distribution of bacteriochlorophyll-based phototrophy across lineages and habitats.

Light produces different effects in the growth and physiology of AAPB. Previous studies of AAPB have shown that the transition from dark to light induces elevated protein synthesis (V. V. Yurkov & van Gemerden, 1993), upregulation of transcriptional and translational machinery (Tomasch et al., 2011), and enhanced biomass production and bacterial growth efficiency (Biebl & Wagner-Dobler, 2006; Cepáková et al., 2016; Hauruseu & Koblížek, 2012; Piwosz et al., 2018). Additionally, light exposure has been shown to increase growth rates of natural populations of AAPB in the Mediterranean Sea and freshwater lakes in Europe (Cepáková et al., 2016; Ferrera et al., 2017), and increased survival under starvation (Tsuneo Shiba, 1984; Soora & Cypionka, 2013) or stationary phase cultures (Giebel et al., 2019). This light-enhanced growth has been attributed in part to a more efficient carbon uptake through the incorporation of inorganic carbon, via anaplerotic reactions such as pyruvate carboxylase, PEP carboxylase, PEP carboxykinase and malic enzyme (Hauruseu & Koblížek, 2012; Koblížek et al., 2003; Kuo-hsiang Tang et al., 2009, 2011). For instance, anaplerotic carbon fixation ranges between 4-11% in *Erythrobacter* NAP1 (Sphingomonadaceae) pyruvate cultures grown in the light (Hauruseu & Koblížek, 2012). In addition, gene expression data from *Dinoroseobacter shibae,* a Rhodobacteraceae AAPB, showed that this strain can use the ethylmalonyl CoA pathway (EMC) (Bill et al., 2017; Tomasch et al., 2011) for inorganic carbon fixation. However, these pathways are not uniformly distributed in AAPB genomes. (Vargas and Coleman *In Prep*).

Here we leverage recently developed transposon mutagenesis methods (Wetmore et al., 2015) to generate a genome-wide mutant library in *Porphyrobacter* LM6, an AAPB strain isolated from Lake Michigan (Sphingomonadaceae). The mutant library was grown with different carbon

sources under light:dark cycles or in continuous darkness to explore the relationships between phototrophy and central metabolism. *Porphyrobacter* LM6 wild-type strain exhibited light-enhanced growth in glucose, but not butyrate. By contrast, strains with transposon insertions in photosynthetic gene cluster genes, anaplerotic reactions, oxidative stress detoxification genes, and others; exhibited reduced fitness in conditions that facilitated light-enhanced growth by the wild-type strain.

3.3. Results

3.3.1. Light enhances growth in a carbon-dependent manner

Porphyrobacter LM6 exhibited enhanced growth in glucose or pyruvate with cycles of 14h:10h light:dark as compared to continuous dark (Fig. 3.1). By contrast, light did not have a significant growth effect for cultures grown on butyrate, maltose, or in complex media containing peptone and yeast extract (Fig. 3.1). Glucose and pyruvate supported lower optical densities (OD660) at the end of exponential phase compared with butyrate and maltose at equimolar concentrations of carbon, suggesting that the former two substrates are less efficiently utilized by this strain.

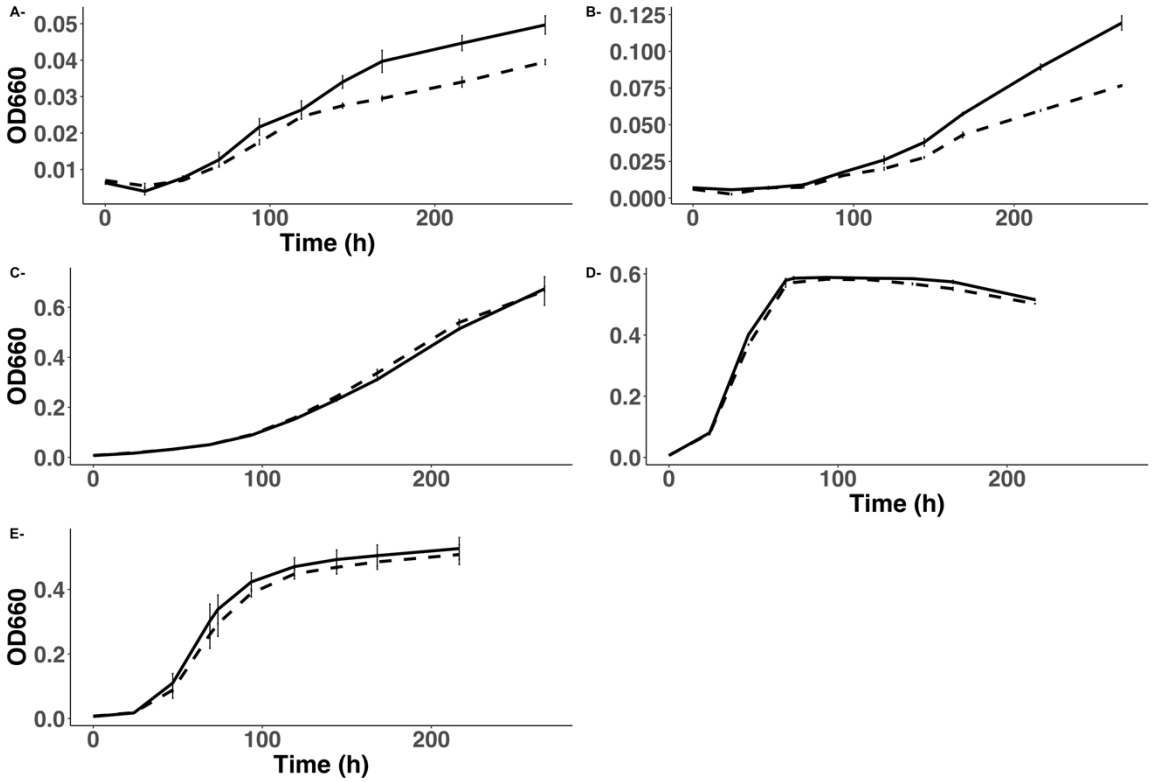

Figure 3.1. Growth curves of Porphyrobacter LM6 in supplemented freshwater MOPs media. A- glucose, B- pyruvate, C- Butyrate, D- Maltose, E- Peptone and yeast extract as sole carbon source. Solid line= 14h light/10h dark cycles. Dashed lines= 24h dark. Error bars= standard deviation.

3.3.2. TnSeq approach identifies genes essential for growth on rich media

To identify genes underlying the observed substrate-specific and light-specific growth phenotypes, we quantified fitness effects using a library of barcoded transposon mutants (Wetmore et al., 2015). Genome mapping of the transposon insertions revealed 457,022 distinct barcodes distributed in 96,060 insertion sites. A total of 2256 genes contained central insertions for a median of 23.6 mutant strains per gene (Table 3.1). The set of genes for which we did not obtain insertions in complex media (PYE media), consisted of 450 genes (15.5% of genes in the genome) (Table S3.1). The essentiality of genes was statistically determined using hidden Markov models and the Gumbel tool, 279 genes were defined essential in the dataset (Table S3.2). The essential genes include core cellular functions such as nucleic acid biosynthesis, ribosomal proteins and others.

Of the genes with no transposon insertions, 20% (89 genes) are hypothetical proteins with unknown function. A gene containing a PAS domain and a histidine kinase domain was also essential in PYE. The domains in this gene have the capacity to sense light, redox state and other environmental factors that can be ecologically important for AAP (Henry & Crosson, 2011). Other essential genes are involved in iron and phosphorus metabolism, including the genes that encode the cytochrome c and cytochrome cbb3. Genes in the photosynthetic gene cluster are not essential for growth in PYE.

Table 3.1. RB-TnSeq library statistics.

	Porphyrobacter LM6
Total no. protein coding genes	2899
Genes with central insertions	2256
Reads	12 489 811
Distinct barcodes	457 022
Usable (%)	166 223 (0.9726)
Insertions	96 060
Median no. strains per gene	23.6
Coverage (naive-expected=1.0)	0.919

3.3.3. Distinct pathways are necessary for growth on glucose and butyrate

A genome wide fitness screen revealed genes involved in carbon metabolism in *Porphyrobacter* LM6. We grew the pool of mutants in equimolar carbon in the form of glucose or butyrate, and under two light regimes, 14h:10h light:dark or continuous darkness (Figure S3.1).

Most insertions showed little or no effect on fitness (average fitness= -0.231, standard deviation= 0.866; Table S3.3, Figure S3.2). The distribution of fitness effects was similar across all experimental treatments (Table S4, Figure S3). Carbon substrate was the primary contributor to variation in mutant fitness. The light was the second contributor to the variation, and its effect was stronger in glucose (Figure S3.4).

Several processes were differentially affected in glucose and butyrate cultures including the ones involved in central carbon metabolism. As a validation of the experimental approach, mutations in genes involved in amino acid metabolism caused some of the lowest gene fitness on both carbon sources (Figure 3.2). A total of 149 genes showed strong phenotypes (|fitness| > 2 and |t-statistic| > 5), these include genes involved in energy metabolism, amino acid and nucleotide metabolisms, among other functions. The strong phenotype genes were grouped in three clusters based on the fitness of their mutants (Figure S3.5). The first cluster consisted of genes which mutations produced detrimental effects regardless of the experimental conditions. The mutants in the second cluster showed low fitness in the butyrate conditions and neutral fitness in glucose, and the third cluster contains mutants with the opposite pattern of fitness presenting lower values in glucose (see details in Table S3.5).

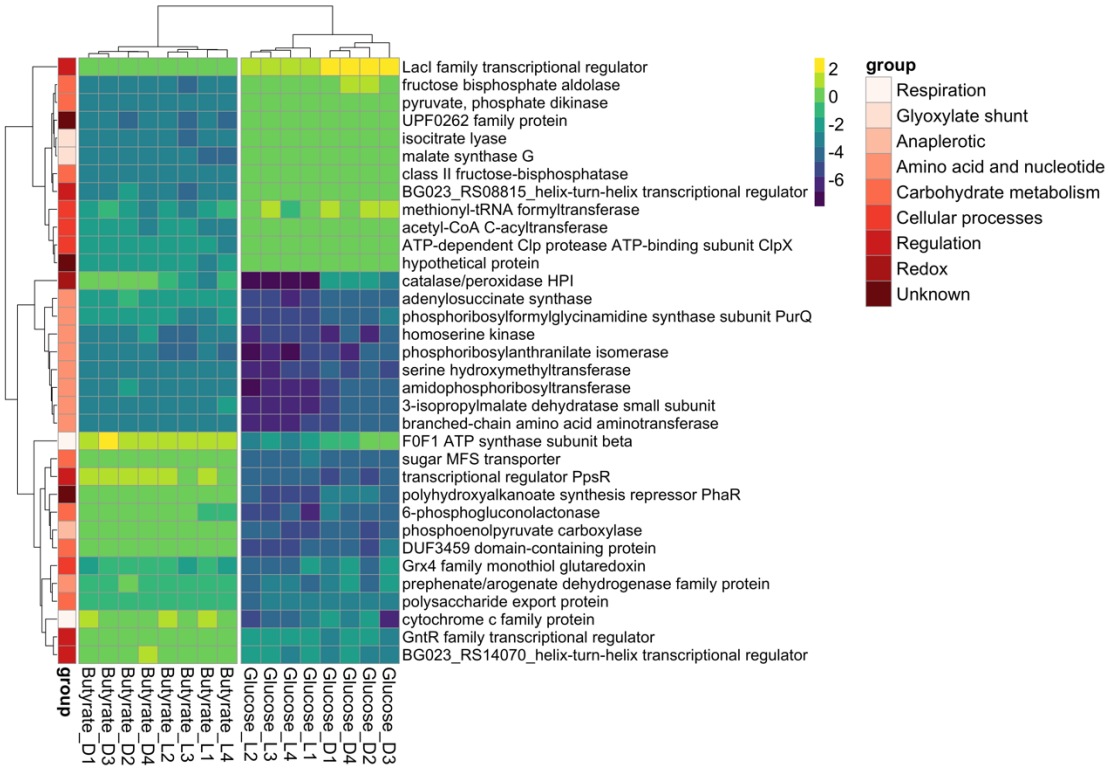

Figure 3.2. Effect of carbon substrate on the fitness of gene mutants. Heatmap of Log2 average fitness values of the mutant that presented an average fitness difference greater than |2Log2| values between glucose and butyrate treatments. Genes are grouped by its functional category based on COG annotations.

In order to separate the effects of carbon substrate from the effects of light, we focused on mutants that had Log2 >= 2 of difference in average fitness between glucose and butyrate cultures regardless of light regime (Figure 3.2, Table S3.6). This approach grouped the gene mutants into two major clusters: one containing mutants of genes with reduced fitness in butyrate and the second containing mutants of genes that showed a reduced fitness in glucose cultures. Within the butyrate reduced fitness cluster is a LacI transcriptional repressor (BG023_RS11560), a gene that has been shown to be a major regulator of carbon metabolism in *C. crescentus* (Ravcheev et al., 2014). This is the only mutation that showed such a contrasting effect on fitness being as it was beneficial in glucose dark cultures. Two genes in the glyoxylate shunt pathway, isocitrate lyase

(BG023_RS08810) and malate synthase (BG023_RS12060), are also included in this cluster, demonstrating the importance of these genes in the metabolisms of carbon molecules that enter the TCA cycle as acetyl CoA. Mutants of acetyl-CoA C-acyltransferase (BG023_RS10040) which is a member of several pathways of fatty acid degradation and amino acid metabolism, also showed lower fitness in butyrate.

Among the mutants in the cluster of mutations with reduced fitness in glucose are several genes involved in anaplerotic carbon fixation and ROS detoxification. This cluster includes mutants of the anaplerotic function phosphoenolpyruvate carboxylase (BG023_RS06680), this enzyme uses HCO3- to produce oxaloacetate from phosphoenolpyruvate. Another gene that stands out from the second cluster is the catalase/peroxidase gene. Mutations in this gene were detrimental in all conditions but this mutation produced the lowest fitness in glucose light/dark. There are four transcriptional regulators mutants in this cluster including the photosynthesis repressor *ppsR* and a homolog of *phaR,* a repressor of polyhydroxyalkanoates biosynthesis (Cai et al., 2015). Mutants of a transcriptional regulator of the GntR family (BG023_RS01800) and a regulator of unknown function (BG023_RS14070) are also linked to glucose metabolism, and showed neutral fitness in butyrate.

3.3.4. Oxidative stress mitigation is vital for growth in light

In contrast to the closely related anoxygenic phototrophs, phototrophy is regulated by light rather than oxygen (V. V. Yurkov & Beatty, 1998b; V. V. Yurkov & van Gemerden, 1993). In order to understand the molecular networks related to light harvesting and photosystems, we identified genes in which insertions altered fitness in light:dark cycles compared to complete darkness. To isolate the effect of light, we averaged the fitness of mutants in glucose and butyrate

cultures, and filtered the list to find mutants with average fitness differences of at least 4-fold (2 log2) between the two light conditions (Figure 3.3, Table S3.7), regardless of carbon source. The largest fitness defects in the light were found for insertions in the hydrogen peroxide inducible gene activator *oxyR* (BG023_RS07970) which belongs to the LysR family of transcriptional regulators. Orthologs of this gene have been shown to be involved in oxidative stress response in *Caulobacter crescentus* (Silva et al., 2019). Strains with insertions in catalase/peroxidase (BG023_RS03885) also had lower fitness in cultures grown in the light (Figure 3.3a). Three other genes involved in carotenoid biosynthesis were also important for fitness: lycopene beta cyclase *crtY* (BG023_RS04590), phytoene/squalene synthase (BG023_RS04570) and phytoene desaturase (BG023_RS04585). AAPB produce soluble carotenoids that quench oxidative damage by reactive oxygen species (ROS), formed from the combination of light and Bchl*a*. Additionally, two other genes contributed to fitness in the light, though they did not pass our initial filtering criteria (Log2 >= 2 of difference in average fitness). One is the transcriptional regulator *dksA* (BG023_RS00810), homologs of which have been demonstrated to be involved in stress response and starvation in other bacteria including *C. crescentus* (England et al., 2010). Insertions in a gene that encodes for a polyprenyl synthetase family protein involved in carotenoid biosynthesis also affected fitness in the light (Figure 3.3b).

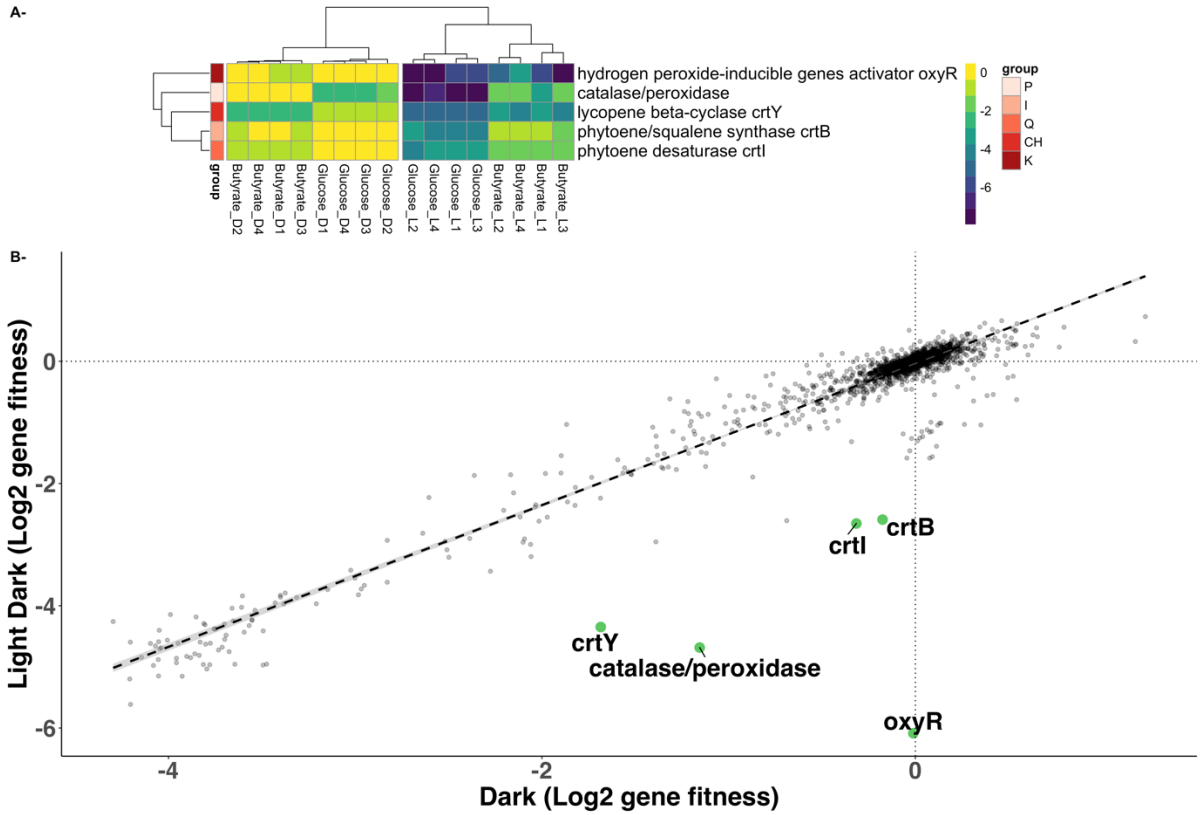

Figure 3.3. Effect of light to the fitness of gene mutants. The genes were filtered by average fitness values greater than 2 Log2 values between Light/dark and Dark treatments. A- Heatmap of genes that passed the filtering criteria. B- Light/dark= 14h light/10h dark cycles, and Dark= 24h dark.

3.3.5. The fitness effect of photosynthesis genes depends on both light and carbon

The genes required for phototrophy in AAPB encompass biosynthesis of Bchl*a* for light harvesting, the structural proteins of the photosystem, regulatory genes, photoprotective carotenoids and some hypothetical genes with unknown function. These adjacent operons are confined to a ~40Kb genomic region known as the photosynthetic gene cluster (PGC). While mutations in these genes produced different fitness profiles across treatments, the most striking effect is the low gene fitness observed for these mutants when growing in glucose in light/dark, a condition in which we observed light-enhanced growth (Figure 3.4). In glucose light/dark, genes encoding the structural components of the photosystem, biosynthesis of Bchl*a* and biosynthesis of

photoprotective carotenoids showed gene fitness values ranging between -2 to -4. The mutant with the lowest fitness in glucose light/dark is the transcriptional repressor *ppsR,* which is known for acting as the oxygen dependent repressor of the photosynthetic operons in anoxygenic phototrophs (Elsen et al., 2005; Yin et al., 2012). However, *ppsR* mutants presented positive fitness suggesting that phototrophy is downregulated in butyrate by an alternative regulatory mechanism. Other mutants with strong negative fitness values include a gene encoding a Major Facilitator Superfamily (MFS) transporter (BG023_RS13245) showed average gene fitness of -2 in glucose light/dark but its mutation was neutral in the other three conditions. Similar cases include a ph domain containing protein (BG023_RS13255) and the Domain of unknown function (BG023_RS13275) for which mutants had average fitness values of -2.35 and -2.08, respectively. The other hypothetical function genes in the PGC had neutral fitness in all the conditions. The mutant fitness profiles observed in glucose are consistent with a model in which *ppsR* acts as a repressor of the phototrophy operons and that mutations in the majority of these genes have detrimental effects for the growth of LM6 in glucose when light is available. When grown in continuous dark, mutations in these genes are largely neutral with the exception of *ppsR* and *mtbc1*. The gene *mtbc1* has been shown to be involved in the regulation of AAP as an anti-repressor of *ppsR* in anoxygenic phototrophs (Vermeulen & Bauer, 2015). These results indicate that the synthesis of pigments is energetically unfavorable for *Porphyrobacter* growing on glucose in the absence of light energy. By contrast, the PGC mutants presented neutral fitness in butyrate regardless of the light regime suggesting that phototrophy is not used, and likely repressed when growing in butyrate as sole carbon source with a mechanism that is independent of light.

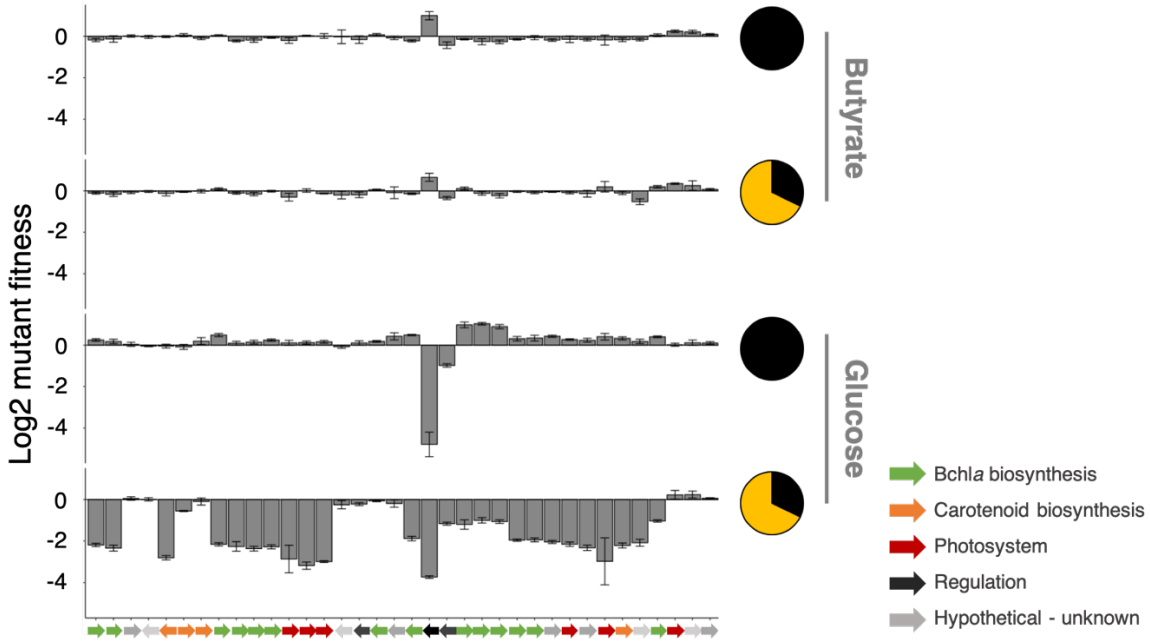

Figure 3.4. Average fitness of the mutants of the photosynthetic gene cluster. Genes are color coded by their function. Yellow/black circles= 14h:10h light:dark cycles. Black circles= 24h dark.

3.3.6. Regulation of phototrophy by *ppsR* is vital for AAPB fitness

The lowest fitness among the PGC mutants in glucose was observed in the transcriptional repressor *ppsR*. The deleterious impact of the loss of regulation by *ppsR* over the PGC operons was confirmed in a mutant strain with a targeted deletion of the *ppsR* gene. *Porphyrobacter* LM6 Δ*ppsR* showed lower growth rate and maximum OD compared to wild type in cultures grown in glucose, pyruvate, maltose and peptone/yeast extract (Figure 3.5). The most severe effects of the absence of *ppsR* were observed in glucose and pyruvate cultures, the carbon substrates that favor light-enhanced growth in this strain. The detrimental effect of the deletion of *ppsR* was larger in the dark cultures, with the exception of the maltose and and butyrate that did not show difference in the light:dark and dark cultures. There was no difference between wild type and Δ*ppsR* cultures on butyrate in any of the light treatments, suggesting that phototrophy is downregulated with a mechanism independent of *ppsR* and light.

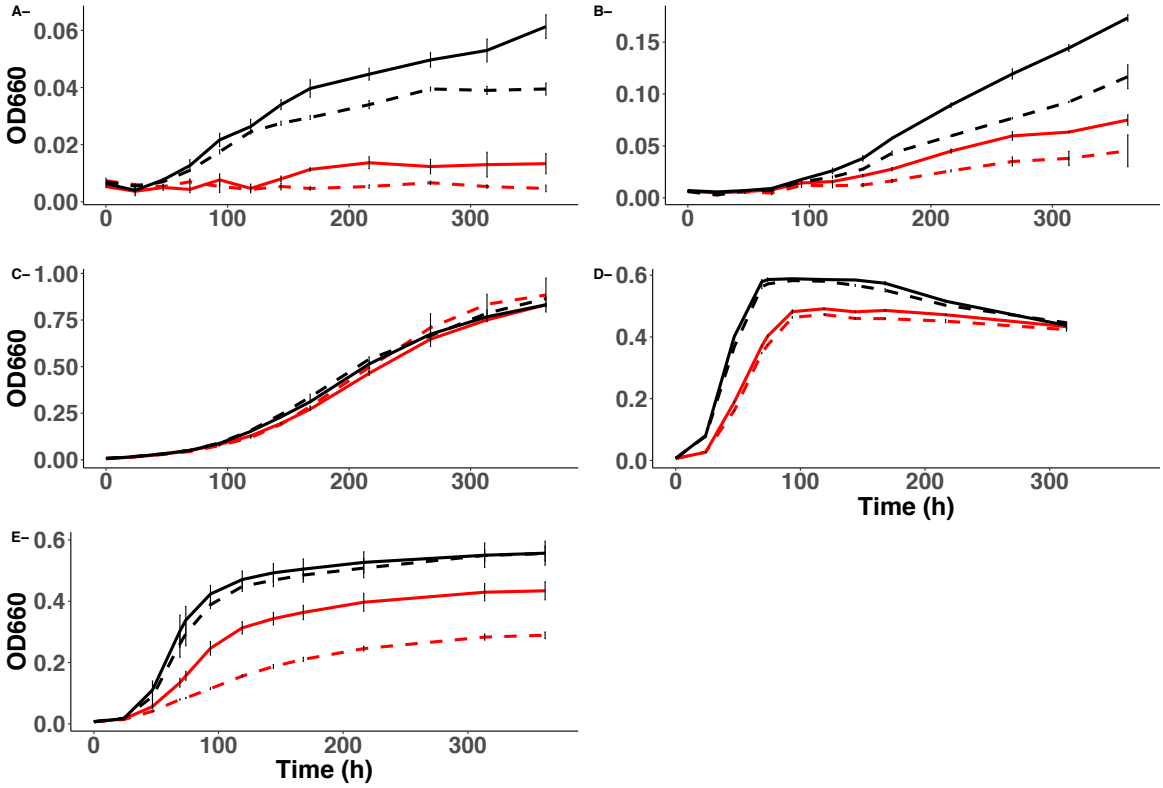

Figure 3.5. Growth curves of *Porphyrobacter* LM6 wild type (black) and *ΔppsR* (red) in supplemented freshwater MOPS base media. A- glucose, B- pyruvate, C- Butyrate, D- Maltose, E- Peptone and yeast extract as carbon source. Solid lines= 14h light/10h dark cycles, and dashed lines= 24h dark.

3.4. Discussion

We grew a barcoded mutant library on two different carbon substrates under light:dark or complete darkness regimes in order to disentangle the pathways used by the freshwater AAPB strain *Porphyrobacter* LM6 to take advantage of light energy. The majority of the mutants with the lowest fitness in the dataset correspond to genes in amino acid and nucleotide biosynthetic pathways, which validates our experiment since neither of the conditions tested include amino acids in the media. Similar results have been observed in experiments of strains grown on minimal media (Hentchel et al., 2019; Pechter et al., 2016; Price et al., 2018; Rubin et al., 2015; Wetmore et al., 2015). These fitness effects were observed in all four conditions in the experiment.

We conducted our experiment in two different carbon substrates. Light enhances the growth of *Porphyrobacter* LM6 cultures growing on glucose, however, light is not advantageous for growth of butyrate cultures. Glucose is a labile carbon source that can support substantial heterotrophic bacterial growth/production in marine systems (Rich et al., 1996). Despite the fact that glucose is an available and easy to utilize substrate, *Porphyrobacter* LM6 did not produce more biomass or grow faster in glucose compared with equal molar concentrations of butyrate the other substrates. The mutants of a transcriptional regulator from the LacI family presented positive fitness in the glucose treatments, especially in the dark. This result suggests that this regulator could be down regulating glucose metabolism in this strain. Another possible explanation of the low biomass yield observed in glucose and pyruvate is the production of an excess of reducing equivalents during photoheterotrophic growth creating a redox imbalance in the cell (Hädicke et al., 2011). Other phototrophic bacteria depend upon reducing power sink mechanisms to dissipate redox constraints on their metabolism. For example, *R. palustris* releases reducing power producing hydrogen gas (Barbosa et al., 2001; McKinlay & Harwood, 2011; Kuo-hsiang Tang et al., 2011) while *Rb sphaeroides* instead uses reducing equivalents to assimilate acetate using the EMC pathway (Laguna et al., 2011; Kuo-hsiang Tang et al., 2011), and *R. denitrificans* used dissimilatory nitrate reduction to ammonium to remove excess of reducing equivalents (Tsuneo Shiba, 1991; Kuo-hsiang Tang et al., 2009). However, *Porphyrobacter* LM6 lacks these pathways limiting its growth on glucose and pyruvate substrates.

Light availability conferred a growth advantage for *Porphyrobacter* LM6 with regard to growth rate and biomass yield only when glucose or pyruvate were provided as carbon sources. Such light-enhanced growth has been previously observed in other AAP strains growing in pyruvate and glucose including the close relatives *Erythrobacter* NAP1 (Hauruseu & Koblížek,

2012), and *Erythrobacter* longus (Vargas & Coleman In prep). In NAP1, higher bacterial growth efficiency values observed in chemostat cultures growing under light/dark cycles were attributed to an increased carboxylation activity (anaplerotic reactions) in pyruvate compared to other substrates such as glutamate. Glutamate enters directly to the TCA cycle as alpha ketoglutarate with no incorporation of inorganic carbon, whereas pyruvate instead enters TCA as acetyl CoA, malate or oxaloacetate, the two latter require the incorporation of inorganic carbon via anaplerotic reactions (Kuo-hsiang Tang et al., 2011). Mutations in two genes that perform anaplerotic reactions, phosphoenolpyruvate (PEP) carboxylase and PEP carboxykinase, had low fitness in glucose demonstrating the importance of inorganic carbon incorporation for this strain under this condition. The contribution of anaplerotic carbon fixation to the growth of AAPB was also observed in *Erythrobacter* NAP1 (Hauruseu & Koblížek, 2012). PEP carboxylase catalyzes the reaction of PEP and bicarbonate to produce oxaloacetate. The inability of performing this reaction in glucose produced fitness values lower than -4. In the context of our study, genes in which mutations produced fitness values lower of -4 can be considered essential to that condition (Hentchel et al., 2019; Wetmore et al., 2015), demonstrating that *Porphyrobacter* LM6 depends on inorganic carbon fixation to grow on glucose in the light. Our data suggest that anaplerotic reactions can be boosted by the excess of ATP produced from phototrophy and help this strain to more efficiently uptake carbon under growth on glucose and other non-optimal carbohydrates (Figure 3.6).

Phototrophy was not advantageous for growth of *Porphyrobacter* in butyrate (Figure 3.1c). Moreover, mutations in pigment biosynthesis and photosystem genes showed neutral fitness effects in butyrate regardless of the light regime, further demonstrating that phototrophy is not used in this condition. Butyrate is commonly considered a source of carbon used by

microorganisms living in anoxic sediments that metabolize it syntrophically with methanogens (Kendall et al., 2006). However, it has been proposed that particle associated chitin metabolizers can also produce organic acids for secondary consumers in the community (Datta et al., 2016; Enke et al., 2019). To be able to grow on butyrate, *Porphyrobacter* LM6 needs the glyoxylate shunt to obtain a net carbon gain from acetate, butyrate and lipids. This acetate assimilation pathway skips the two CO2 expiration steps in the TCA cycle allowing for carbon conservation. Mutations in the genes of the glyoxylate shunt were detrimental for growth in butyrate but neutral in glucose. One explanation for the neutral fitness of the glyoxylate shunt mutants is that this pathway can be subject to catabolite repression. Additionally, glucose inhibits the inactivation of the competing enzyme isocitrate dehydrogenase as observed in *E. coli* growing on glucose (Sauer & Eikmanns, 2005) underscoring the importance of PEP carboxylase to generate TCA intermediaries for *Porphyrobacter* LM6 growing on glucose. Light had no effect on the fitness of the mutants of the glyoxylate shunt genes confirming again that light does not play a role in butyrate assimilation.

Phototrophic organisms use different pathways for acetate assimilation. The glyoxylate shunt was essential for growth of *R. palustris* on acetate, but the mutation of isocitrate lyase did not affect its growth in complex media (McKinlay et al., 2014; McKinlay & Harwood, 2010; Pechter et al., 2016). The majority of genomes of AAP bacteria from the family Rhodobacteraceae encode the ethylmalonyl CoA pathway. In the strain *Dinoroseobacter shibae* this pathway is upregulated in light exposed cultures (Bill et al., 2017). However, the ethylmalonyl CoA pathway is not present in AAP bacteria from the family Sphingomonadaceae, and instead they require the glyoxylate shunt as they lack of other pathways for acetate assimilation (Kuo-hsiang Tang et al., 2011). Additional evidence of the importance of the shunt for this group of AAPB is that isocitrate

lyase mutants in *Erythrobacter longus* were unable to grow in minimal media supplemented with acetate or butyrate as sole carbon substrate (Vargas & Coleman, In prep). In addition to the glyoxylate shunt, the mutants of the genes pyruvate phosphate dikinase and malic enzyme also showed low fitness in butyrate, these enzymes catalyze the ATP dependent reversible conversion of PEP to pyruvate, and the anaplerotic reaction of pyruvate and bicarbonate to produce malate, respectively. These two enzymes act together to convert C4-intermediaries from the TCA cycle to produce PEP, a precursor for other biosynthetic pathways. The reversible nature of the reactions performed by these enzymes allow them to rapidly respond to the metabolic needs of the cell (Sauer & Eikmanns, 2005). The low fitness observed in the mutants for these genes suggest that *Porphyrobacter* LM6 could potentially benefit from the conversion of TCA intermediaries into pyruvate or PEP via pyruvate phosphate dikinase or other mechanisms, coupled to inorganic carbon fixation via malic enzyme (Figure 3.6).

Light is a major ecological driver of AAPB activity. Phototrophy comes with a price, namely, the production of toxic ROS produced in the presence of oxygen, light, and the light harvesting pigment Bchl*a* (Nishimura et al., 1996). Previous studies have been demonstrated that phototrophy is regulated by light in several AAP bacteria and that Bchl*a* biosynthesis occurs mostly during dark periods and it is rapidly downregulated by light (Hauruseu & Koblížek, 2012; Koblížek, 2015; T. Shiba, 1987; Spring et al., 2009; Tomasch et al., 2011); (V. Yurkov & Csotonyi, 2009; V. V. Yurkov & Beatty, 1998b; V. V. Yurkov & van Gemerden, 1993). *Porphyrobacter* LM6 also produces Bchl*a* in the presence of oxygen and its biosynthesis depends on light and carbon source (data not shown). Seven gene mutants showed differential fitness in response to light regardless of the carbon substrate in our experiment. These include two transcriptional regulators: one annotated as hydrogen peroxide inducible gene or *oxyR*, and the other a homolog

of the regulator *dska*. These regulators have been previously linked to oxidative stress, starvation and other stress conditions. The gene *oxyR* belongs to the LysR family of transcriptional regulators and acts as an oxidative stress response regulator in many bacterial strains (Chiang & Schellhorn, 2012; Culligan et al., 2014). A deletion mutant of *oxyR* in *E. coli* produced hypersensibility of the mutant strain to singlet oxygen damage and photo oxidative damage possibly due an impared expression of antioxidant mechanisms like catalase/peroxidase and carotenoids (Kim et al., 2002; Ziegelhoffer & Donohue, 2009). Gene orthologs of *oxyR* in other alphaproteobacteria such as *Zymomonas mobilis* and *C. crescentus* have also been tied to oxidative stress response (Deutschbauer et al., 2014; Silva et al., 2019). Our data indicates that *oxyR* is essential for *Porphyrobacter* survival specifically under light conditions, as the mutation of this gene in the dark cultures shows neutral fitness. The mechanism used by *oxyR* to respond is possibly controlling the expression of catalase/peroxidase similarly to what it has been previously shown in *C. crescentus* (Italiani et al., 2011), and the expression of photoprotective carotenoids. The regulator *dska* is involved in astringent response, and it has been shown to respond to carbon starvation, redox and other stresses in several Proteobacteria strains (Chou & Brynildsen, 2019; England et al., 2010; Ross et al., 2016). Contrary to *oxyR* mutants that only showed fitness defects in the light, mutations in *dksA* were detrimental in the four conditions of the experiment. However, the average fitness of *dksA* mutants is lower by more than two-fold in the light/dark compared to the dark cultures, and almost three-fold in glucose compared to butyrate. This indicates that *dksA* is an important regulator in *Porphyrobacter* LM6 that reacts towards stress produced by light and carbon. The mutants of the catalase/peroxidase, a gene that detoxifies H2O2 in order to prevent oxidative damage to biomolecules, had four-fold lower fitness in the light/dark cultures than in the dark. Additionally, these mutants had almost five-fold lower fitness in glucose compared to

butyrate. This result demonstrates that oxidative stress in *Porphyrobacter* LM6 is largely produced by the combination of Light, Bchl*a* and oxygen; and that catalase/peroxidase and *oxyR* are essential for photoheterotrophic growth in this strain. The rest of the gene mutants that were differentially affected by light correspond to genes involved in carotenoid biosynthesis.

Mutants in carotenoids biosynthesis genes showed lower fitness in light:dark treatments than in continuous dark. Other researchers have hypothesized that the main function of carotenoids in AAP is photoprotection by acting as antioxidants quenching the effect of ROS over other cell components (Koblížek, 2015). AAPB carotenoids are polar and soluble in the cytoplasm of AAP rather than bound to protein complexes of the photosynthetic apparatus (V. Yurkov et al., 1993; V. Yurkov & Csotonyi, 2009) suggesting their involvement in ROS quenching. The mutants of the genes *ispA, crtI* and *crtB* had lower fitness in the light/dark cultures confirming the importance of carotenoids for photoprotection. The mutants of *crtY,* the gene that encodes for the enzyme that catalyzes the conversion of lycopene to beta carotene, showed one of the lowest fitness was observed in glucose light/dark (almost five-fold lower than glucose dark), with values that can be considered essential in this experiment. These mutants also had low fitness in butyrate cultures suggesting that there is oxidative stress in these conditions produced by light even under minimal concentrations of Bchl*a*.

The fitness profiles of the mutants in the PGC genes were influenced by light and carbon. These mutations were neutral in butyrate regardless of the light condition. Contrary, the mutants of these genes were affected by light showing the lowest fitness in glucose light/dark, confirming that photoheterophy is beneficial for *Porphyrobacter* LM6 to grow on glucose. The gene with the strongest phenotype in the PGC was the transcriptional regulator *ppsR*. One of the most important findings obtained in our study is the low fitness (values considered as essential for this condition)

of *ppsR* in glucose dark cultures. We confirmed these results by generating a strain with a deletion of *ppsR*. The Δ*ppsR* mutant was unable to grow in glucose cultures incubated in the dark. Furthermore, we found that Δ*ppsR* presents important growth defects in all the carbon substrates except for butyrate cultures in accordance with what we observed in the RB-TnSeq experiment. The gene *ppsR* has been traditionally described as the oxygen dependent repressor of photosynthesis in anoxygenic phototrophs, but recently it has been shown that *ppsR* can also act as an activator in response to light and redox condition of the cell (Bauer et al., 2003; Elsen et al., 2005; Steunou et al., 2004; Yin et al., 2012). The results obtained for *ppsR* mutants in our strain indicates that this gene acts as a repressor of phototrophy. Additionally, the low fitness values observed for the mutants of the gene *mtbc1* suggest that this is also involved in regulation of phototrophy. This vitamin B12 dependent gene has been shown to act as an anti-repressor of *ppsR* by interacting with *ppsR* in response to light, redox state and starvation (Fang & Bauer, 2017; Soora et al., 2015). The detrimental effects of the inability to regulate the expression of phototrophy in light cultures lays on the increase of ROS product of high concentrations of Bchl*a* in the cell. The growth defect observed in dark cultures can be explained by the energetic cost of producing pigments and the structural proteins of the photosystem without obtaining any energy from light.

In this study we found that phototrophy is not always used by AAP and its benefits largely depend on the carbon substrate available, and the pathway trajectory that the substrate takes to enter the TCA cycle. Also, we found evidence of anaplerotic reactions accounting for the light enhanced growth in glucose and pyruvate. We demonstrated that light regulation of AAP is vital for the growth of this strain, and that it is tightly regulated first by *ppsR* and possibly its anti-repressor *mtbc1*. Furthermore, our data suggest the existence of other mechanisms independent of

light and *ppsR* that regulate the expression of AAP. Oxidative stress seems to impose the largest physiological constraint of AAP expression. Finally, we found several transcriptional regulators of unknown function that seem to be linked to AAP and the differences observed between carbon substrates. To our knowledge we are the first to use a whole genome forward genetics screen to study aerobic anoxygenic phototrophy. The results obtained in this study contribute to a better understanding of the molecular mechanisms that act in response to the major ecological drivers of AAP, and its consequences for their physiology.

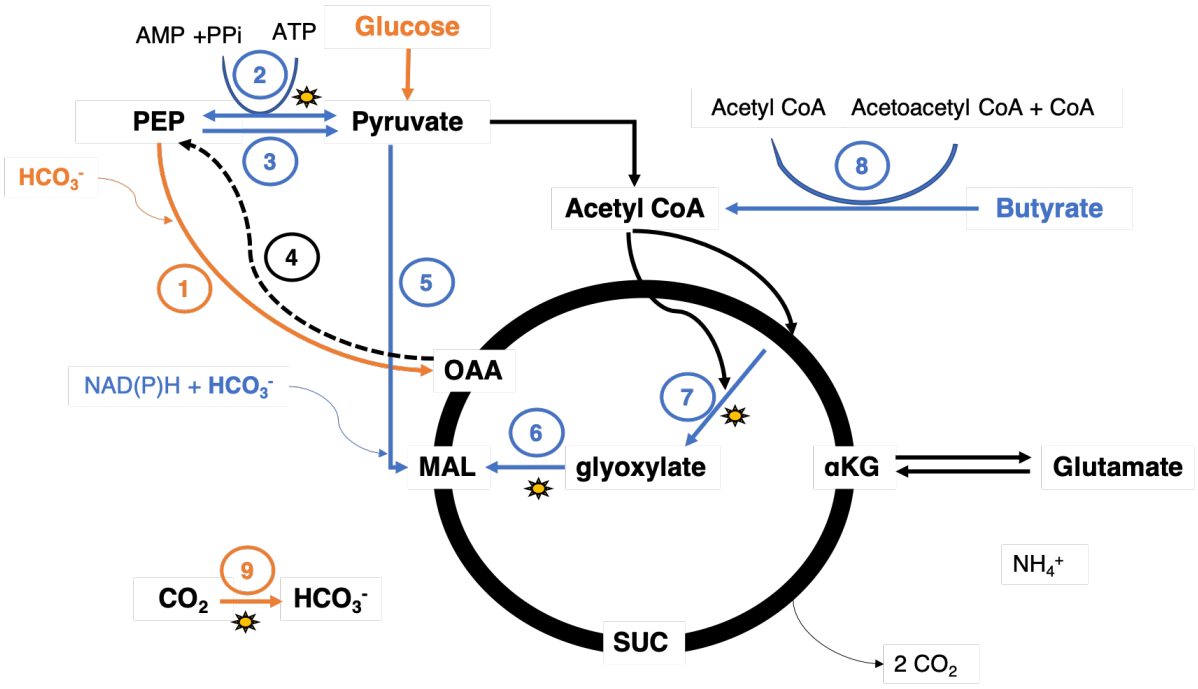

Figure 3.6. Proposed model of metabolism in *Porphyrobacter* LM6 growing in glucose (orange) vs butyrate (blue) as only carbon substrate. Black arrows designate pathways used in both conditions. Key enzymes based on fitness of mutants are numbered as follows: 1- phosphoenolpyruvate carboxylase, 2- pyruvate phosphate dikinase, 3- pyruvate kinase, 4- phosphoenolpyruvate carboxykinase, 5- malic enzyme, 6- malate synthase, 7- isocitrate lyase, 8- acetyl-CoA acyltransferase, 9- carbonic anhydrase. Orange lines= mutants with low fitness in glucose. Blue lines= mutants with low fitness in butyrate. Dashed lines= neutral fitness. Sun= differential fitness in the light:dark vs dark conditions.

3.5. Methods

3.5.1. Bacterial strains

Porphyrobacter LM6 was isolated from Lake Michigan water on peptone and yeast extract (PYE) plates. The genome was sequenced and closed in one chromosome with a length of 2 979 257bp, containing a total of 2895 genes including the ones in the photosynthetic gene cluster typically found on AAPs (accession number: NZ_CP017113). The *E. coli* strains were maintained and propagated in Luria Broth (LB). Antibiotics kanamycin and chloramphenicol were added as needed. The summary of the strains used and generated in this study is in the Table S3.1.

3.5.2. Growth media

Porphyrobacter LM6 was grown and maintained in PYE medium [0.2% peptone (Fisher Scientific), 0.1% yeast extract (Fisher Scientific), 0.5 mM MgSO4, 0.5 mM CaCl2]. Growth curve experiments were performed in using Freshwater MOPS minimal medium (Ehrenreich & Widdel, 1994), ph=7 (see detailed recipe in Supplementary material) supplemented with 30mM dextrose (Fisher Scientific), 30mM sodium butyrate (Alpha Aesar), 30mM sodium pyruvate (Fisher Scientific), 30mM maltose (Fisher Scientific), or 0.2% peptone (Fisher Scientific), 0.1% yeast extract (Fisher Scientific). Solid growth media included 1.5% agar. Antibiotics kanamycin and chloramphenicol were added to maintain plasmids.

3.5.3. Growth curve experiments

Media: The experiments for the growth curves were performed in Freshwater MOPS minimal medium supplemented with 30mM dextrose (Fisher Scientific), 30mM sodium butyrate

(Fisher Scientific), 30 mM sodium pyruvate (Fisher Scientific), 30mM maltose (Fisher Scientific), or 0.2% peptone (Fisher Scientific), 0.1% yeast extract (Fisher Scientific).

Growth curves: Single colonies of wild type and Δ*ppsR* strains were inoculated in liquid PYE and incubated shaking at 250rpm in the dark at 25°C. These starting cultures were washed twice and resuspended in an equal volume of Freshwater MOPS minimal medium (no carbon added). Triplicate 15ml tubes containing 8mL Freshwater MOPS minimal medium supplemented with single carbon substrates were inoculated with the cell suspension. All tubes were incubated on a Percival incubator with fluorescent light at 180uE, over 14h light/ 10h dark cycles or 24h cycles at 24°C and shaking at 250rpm. The 24h dark cycle was achieved by covering the tubes with aluminum foil. The optical density of the cultures was directly measured on a Spec 20 spectrophotometer at 660nm. The growth curves were fitted using the grofit v.1.1.1 (Kahm et al., 2010). The fit of each curve was examined independently.

3.5.4. Construction of RB-TnSeq mutant library

Media: The library was plated on PYE containing 25ug/ml of kanamycin and 1.5% agar. The BarSeq experiments were performed using Freshwater MOPS minimal medium supplemented with 30mM dextrose (Fisher Scientific), 30mM sodium butyrate (Fisher Scientific), or 0.2% peptone (Fisher Scientific), 0.1% yeast extract (Fisher Scientific). The *Escherichia coli* strains were grown in Lysogeny broth (LB) (1% peptone, 0.5% yeast extract, 0.5% NaCl).

Library construction: This RB-TnSeq experiment was conducted as previously described (Hentchel et al., 2019; Wetmore et al., 2015). *Porphyrobacter* LM6 strain was grown until late exponential phase in PYE at 28°C with shaking at 200 rpm. The plasmid donor *E. coli* strain APA752 (Deutschbauer Lab, University of California-Berkeley, USA), carrying the plasmid

pKMW3 (kanamycin resistant) Himar transposon vector library, was inoculated into 20 mL of LB containing kanamycin (30 μg/mL) and 300 μM diaminopimelate (DAP auxotroph) and grown overnight at 37 °C with shaking at 200 rpm. The conjugation of the barcoded transposon pool into *Porphyrobacter* LM6 was performed by mixing the recipient strain and donor strains. In order to do this, both cultures were centrifuged at 8000 × g for 2 minutes and resuspended in a total volume of 500 μL of PYE medium. The cultures were combined at a 10:1 ratio of recipient to donor and mixed by gentle pipetting. The mixed culture was centrifuged again at 8000 × g, and the supernatant decanted. The cells were resuspended in 30 μL of PYE, spotted onto a PYE agar plate containing 300 μM diaminopimelate, and incubated overnight at 30 °C. After growth, the mating spot was scraped from the plate and resuspended in 6.5mL of PYE. This suspension was spread evenly (500μL per plate) over 14 large (150 × 15 mm) PYE agar plates containing 25 μg/mL kanamycin and incubated for approximately 3 days at 28°C. Cells were harvested from all the plates and inoculated into 400 mL of PYE containing 5 μg/mL kanamycin. This cell mixture was grown at 30°C with shaking at 200rpm for three doublings. Cells were centrifuged at 8000 × g, resuspended in 70 mL of PYE containing 15% glycerol, and stored as 1 mL aliquots at −80 °C.

3.5.5. Mapping of the sites of Tn-Himar insertion in the BarSeq library

Genomic DNA was extracted using guanidium thiocyanate as previously described (Pitcher et al., 1989). The DNA was sheared (~300 bp fragments), cleaned with a standard bead protocol, end-repaired and A-tailed, and a custom double-stranded Y adapter was ligated. The custom adapter was prepared by annealing Mod2_TS_Univ and Mod2_TruSeq (Table S3.1) as described (Wetmore et al., 2015). The sheared fragments containing transposons were enriched by PCR using the primers Nspacer_BarSeq_pHIMAR and P7_MOD_TS_index1 (Table S3.1) using

GoTaq® Green Master Mix according to the manufacturer's protocol in 100µL reaction with the following cycling conditions: 94 °C for 2 minutes, 25 cycles at 94 °C for 30 s, 65 ° C for 20 s, and 72 °C for 30 s, followed by a final extension at 72 °C for 10 minutes. After a second bead cleanup, the library was sequenced using a standard Illumina sequencing primer on an Illumina HiSeq2500 at the University of Chicago Genomics Facility with a 150-bp single-end read. The genomic locations of the transposon insertions were mapped using the custom Perl script MapTnSeq.pl. Unique barcodes were assigned to a single genomic location using the Perl script DesignRandomPool.pl. These scripts have been described by Wetmore and colleagues (Wetmore et al., 2015), and are available at https:// bitbucket.org/berkeleylab/feba. The reads were mapped to the *Porphyrobacter* LM6 genome (accession NZ_CP017113).

3.5.6. BarSeq experiment

A 1mL aliquot of the library was thawed in ice and transferred to a 250ml flask containing 24ml of PYE. This culture was incubated in the dark, at 28°C and shaking at 250 rpm until OD_{600}= 0.9. A 10 mL aliquot of this culture was washed twice using Freshwater MOPS minimal medium (FWM) and resuspended in an equal volume of FWM. Four 1 mL samples of the resuspended cells were collected and stored at -80°C for DNA extraction, these correspond to the t=0h samples. The rest of the library suspension was used to inoculate 125ul into each of 8 flasks containing 50mL of either FWM supplemented with 30mM of glucose or FWM supplemented with 30mM of butyrate. All flasks were incubated in a Percival incubator at 28°C and 270rpm over 14h light/ 10h dark cycles. The 24h flasks were covered in aluminum foil and sampled in the dark. The schematic of the experimental design can be found in Figure S3.1. The library growth was monitored by optical density at OD_{660nm} in a Tecan M200 plate reader. The cells were harvested after

approximate 6 generations (OD_{660}=0.2) by filtration using Millipore express plus 0.2um filters. The filters were stored in cryovials at -80°C until DNA extraction. The gDNA extractions were performed using the DNA spin columns of the Qiagen All Prep DNA/RNA/Protein kit following the manufacturer's instructions. The gDNA concentrations of the samples were measured using the Qubit DNA Broad range kit. The quality of the gDNA was assessed by measuring A260/A280, A260/A230 using the Tecan M200 plate reader nanoquant plate. PCR amplifications were performed as previously described (Wetmore et al., 2015) using Q5 DNA polymerase with GC enhancer (New England BioLabs) with the primers BarSeq_P1 and 1 of 28 forward primers (BarSeq_P2_IT021 to BarSeq_P2_IT048; Table S3.1) containing unique 6-bp TruSeq indexes that were sequenced using a separate index primer. The PCR reaction cycle was as follows: 98 °C for 4 minutes followed by 25 cycles of 30 s at 98 °C, 30 s at 55 °C, and 30 s at 72 °C, followed by a final extension at 72 °C for 5 minutes. 10ul of each PCR product were pooled and purified using the Wizard SV gel and PCR clean-up system (Promega). The purified samples were run on a 2.5% agarose gel to confirm correct product size (~200 bp). The pooled PCR samples were assessed for quality, and quantified using a Bioanalyzer. The pool was sequenced on an Illumina HiSeq4000 at the University of Chicago Genomics Facility, multiplexing all 48 samples in one lane with 50-bp single-end reads. All sequence data have been deposited in the NCBI Sequence Read Archive.

3.5.7. Data analysis of mutant fitness

To calculate the fitness of the mutant library in the four experimental conditions we followed the protocols of Wetmore and colleagues (Wetmore et al., 2015) using the scripts available at https:// bitbucket.org/berkeleylab/feba. The abundance of each barcode in the samples and the fitness of each mutant strain are calculated using the scripts: MutiCodes.pl and FEBA.R.

Insertions in the first 10% or last 10% of a gene were not considered in gene fitness calculations with the intention of minimizing polar effects. The fitness of each strain is calculated as the normalized Log2 ratio of the abundance at the end of the experiment compared to its T=0h abundance. The fitness of genes was calculated as the weighted average of strain fitness values. Gene fitness calculations required at least 3 reads per strain and 30 reads for each of the samples to be included in the final analysis. The essentiality analysis was performed on Transit v3.1.0 (DeJesus et al., 2015) using hidden Markov models and Gumbel models.

To assess the mutations with treatment-dependent effects over the four conditions we calculated the Log2 average fitness change between any two conditions, and considered the ones with average fitness ΔLog2 > |2|. We also considered the strong phenotype list of genes determined from the FEBA.R script which includes mutants with Log2 > |2|, and t statistics > |5|. Other calculations and plotting were done in R v3.5.3. The heatmaps were constructed using the R packages pheatmap (available at: https://cran.r-project.org/web/packages/pheatmap/index.html), dendextend (available at: https://cran.r-project.org/web/packages/dendextend/index.html) and dendsort (available at: https://cran.r-project.org/web/packages/dendsort/index.html).

3.5.8. Deletion of *ppsR*

The deletion of the gene *ppsR* was performed by double recombination as previously described (Hmelo et al., 2015). Briefly, 500bp from the upstream and downstream regions of the target gene were PCR amplified using the primers in Table S3.1. These regions were fused using SOE PCR using the same amplification cycles but adding the primers after 20 cycles to allow self-amplification. The resulting product was digested and ligated into the plasmid pNPTS-cat carrying a chloramphenicol resistance marker gene and the gene *sacB* (Table S3.1). The plasmid carrying

the recombinant region was then chemically transformed into *E. coli* TOP10 cells. The new plasmid construct was conjugated into *Porphyrobacter* LM6 by mixing exponentially grown cells of the strain with the *E. coli* TOP10 containing the plasmid construct, and an *E. coli* FC3 helper strain, the conjugation mix was incubated overnight at room temperature in the dark over a 0.2um Poretics filter (GVS Life Sciences). After the incubation the mixture was plated in PYE plates with 4ug/ml of chloramphenicol, chloramphenicol resistant colonies were then streaked in PYE + 5% of sucrose for *sacB* second selection. The candidate colonies were screened by PCR using Promega GoTaq® 2X mix and confirmed by sequencing using primers that anneal outside the recombinant regions (Table S3.1). Three single mutant colonies carrying the right deletion were stored in glycerol at -80°C. We extracted genomic DNA of two of the mutant colonies using the DNA spin columns of the Qiagen All Prep DNA/RNA/Protein kit following the manufacturer's instructions. The genotype of the mutants was confirmed by full genome sequencing using Illumina at Microbial Genomes Sequencing Center MIGs (Pittsburgh PA, USA). The mutant genomes were assembled in SPADES (Bankevich et al., 2012) using the wild type genome as reference.

3.6. References

Bankevich, A., Nurk, S., Antipov, D., Gurevich, A. A., Dvorkin, M., Kulikov, A. S., Lesin, V. M., Nikolenko, S. I., Pham, S., Prjibelski, A. D., Pyshkin, A. V., Sirotkin, A. V., Vyahhi, N., Tesler, G., Alekseyev, M. A., & Pevzner, P. A. (2012). SPAdes: A New Genome Assembly Algorithm and Its Applications to Single-Cell Sequencing. *Journal of Computational Biology*, *19*(5), 455–477.

Barbosa, M. J., Rocha, J. M. S., Tramper, J., & Wijffels, R. H. (2001). Acetate as a carbon source for hydrogen production by photosynthetic bacteria. *Journal of Biotechnology*, *85*(1), 25–33.

Bauer, C., Elsen, S., Swem, L. R., Swem, D. L., & Masuda, S. (2003). Redox and light regulation of gene expression in photosynthetic prokaryotes. *Phil. Trans. R. Soc. Lond.*, 147–154.

Biebl, H., & Wagner-Dobler, I. (2006). Growth and bacteriochlorophyll a formation in

taxonomically diverse aerobic anoxygenic phototrophic bacteria in chemostat culture: Influence of light regimen and starvation. *Process Biochemistry*. *41*, 2153–2159.

Bill, N., Tomasch, J., Riemer, A., Muller, K., Kleist, S., Schmidt-Hohagen, K., Wagner-Döbler, I., & Schomburg, D. (2017). Fixation of CO2 using the ethylmalonyl-CoA pathway in the photoheterotrophic marine bacterium *Dinoroseobacter shibae*. *Environmental Microbiology*, 2645–2669.

Cai, S., Cai, L., Zhao, D., Liu, G., Han, J., Zhou, J., & Xiang, H. (2015). A Novel DNA-Binding Protein, PhaR, Plays a Central Role in the Regulation of Polyhydroxyalkanoate Accumulation and Granule Formation in the Haloarchaeon Haloferax mediterranei. *Applied and Environmental Microbiology*, *81*(1), 373–385.

Cepáková, Z., Hrouzek, P., Žišková, E., Nuyanzina-Boldareva, E., Šorf, M., Kozlíková-Zapomělová, E., Salka, I., Grossart, H.-P., & Koblížek, M. (2016). High turnover rates of aerobic anoxygenic phototrophs in European freshwater lakes. *Environmental Microbiology*, *18*(12), 5063–5071.

Chiang, S. M., & Schellhorn, H. E. (2012). Regulators of oxidative stress response genes in *Escherichia coli* and their functional conservation in bacteria. *Archives of Biochemistry and Biophysics*, *525*(2), 161–169.

Chou, W. K., & Brynildsen, M. P. (2019). Loss of DksA leads to multi-faceted impairment of nitric oxide detoxification by *Escherichia coli*. *Free Radical Biology and Medicine*, *130*, 288–296.

Culligan, E. P., Sleator, R. D., Marchesi, J. R., & Hill, C. (2014). Metagenomic Identification of a Novel Salt Tolerance Gene from the Human Gut Microbiome Which Encodes a Membrane Protein with Homology to a brp/blh-Family β-Carotene 15,15′-Monooxygenase. *PLOS ONE*, *9*(7), e103318.

Datta, M. S., Sliwerska, E., Gore, J., Polz, M. F., & Cordero, O. X. (2016). Microbial interactions lead to rapid micro-scale successions on model marine particles. *Nature Communications*, *7*(1), 1–7.

DeJesus, M. A., Ambadipudi, C., Baker, R., Sassetti, C., & Ioerger, T. R. (2015). TRANSIT--A Software Tool for Himar1 TnSeq Analysis. *PLoS Computational Biology*, *11*(10), e1004401.

Deutschbauer, A., Price, M. N., Wetmore, K. M., Tarjan, D. R., Xu, Z., Shao, W., Leon, D., Arkin, A. P., & Skerker, J. M. (2014). Towards an Informative Mutant Phenotype for Every Bacterial Gene. *Journal of Bacteriology*, *196*(20), 3643–3655.

Ehrenreich, A., & Widdel, F. (1994). Anaerobic oxidation of ferrous iron by purple bacteria, a new type of phototrophic metabolism. *Applied and Environmental Microbiology*, *60*(12), 4517–4526.

Elsen, S., Jaubert, M., Pignol, D., & Giraud, E. (2005). PpsR: A multifaceted regulator of photosynthesis gene expression in purple bacteria. *Molecular Microbiology*, *57*(1), 17–26.

England, J. C., Perchuk, B. S., Laub, M. T., & Gober, J. W. (2010). Global Regulation of Gene Expression and Cell Differentiation in Caulobacter crescentus in Response to Nutrient Availability. *Journal of Bacteriology*, *192*(3), 819–833.

Enke, T. N., Datta, M. S., Schwartzman, J., Cermak, N., Schmitz, D., Barrere, J., Pascual-García, A., & Cordero, O. X. (2019). Modular Assembly of Polysaccharide-Degrading Marine Microbial Communities. *Current Biology*, *29*(9), 1528-1535.e6.

Fang, M., & Bauer, C. E. (2017). The Vitamin B 12 -Dependent Photoreceptor AerR Relieves Photosystem Gene Repression by Extending the Interaction of CrtJ with Photosystem Promoters. *MBio*, 1–14.

Ferrera, I., Sánchez, O., Kolárova, E., Koblízek, M., & Gasol, J. M. (2017). Light enhances the growth rates of natural populations of aerobic anoxygenic phototrophic bacteria. *Isme J*, 2391–2393.

Giebel, H., Wolterink, M., Brinkhoff, T., & Simon, M. (2019). Complementary energy acquisition via aerobic anoxygenic photosynthesis and carbon monoxide oxidation by Planktomarina temperata of the Roseobacter group. *FEMS Microbiology Ecology*. *November 2018*, 1–9.

Hädicke, O., Grammel, H., & Klamt, S. (2011). Metabolic network modeling of redox balancing and biohydrogen production in purple nonsulfur bacteria. *BMC Systems Biology*, *5*, 150.

Hauruseu, D., & Koblížek, M. (2012). Influence of Light on Carbon Utilization in Aerobic Anoxygenic Phototrophs. *Applied and Environmental Microbiology*, *78*(20), 7414–7419.

Henry, J. T., & Crosson, S. (2011). Ligand binding PAS domains in a genomic, cellular, and structural context. *Annual Review of Microbiology*, *65*, 261–286.

Hentchel, K. L., Reyes, L. M., D Curtis, P., Fiebig, A., Coleman, M., & Crosson, S. (2019). Genome-scale fitness profi le of Caulobacter crescentus grown in natural freshwater. *The ISME Journal*, 523–536.

Hmelo, L. R., Borlee, B. R., Almblad, H., Love, M. E., Randall, T. E., Tseng, B. S., Lin, C., Irie, Y., Storek, K. M., Yang, J. J., Siehnel, R. J., Howell, P. L., Singh, P. K., Tolker-nielsen, T., Parsek, M. R., Schweizer, H. P., & Harrison, J. J. (2015). Precision-engineering the *Pseudomonas aeruginosa* genome with two-step allelic exchange. *Nature Protocols*, *10*(11), 1820–1841.

Italiani, V. C. S., Neto, J. F. da S., Braz, V. S., & Marques, M. V. (2011). Regulation of Catalase-Peroxidase KatG Is OxyR Dependent and Fur Independent in *Caulobacter crescentus*. *Journal of Bacteriology*, *193*(7), 1734–1744.

Kahm, M., Hasenbrink, G., Lichtenberg-Fraté, H., Ludwig, J., & Kschiho, M. (2010). grofit: Fitting Biological Growth Curves with R. *Journal of Statistical Software*, *33*(7).

Kendall, M. M., Liu, Y., & Boone, D. R. (2006). Butyrate- and propionate-degrading syntrophs from permanently cold marine sediments in Skan Bay, Alaska, and description of Algorimarina butyrica gen. Novet al, sp. Nov. *FEMS Microbiology Letters*, *262*(1), 107–114.

Kim, S. Y., Kim, E. J., & Park, J.-W. (2002). Control of singlet oxygen-induced oxidative damage in *Escherichia coli*. *Journal of Biochemistry and Molecular Biology*, *35*(4), 353–357.

Koblížek, M. (2015). Ecology of aerobic anoxygenic phototrophs in aquatic environments. *FEMS Microbiology Reviews*, *39*(6), 854–870.

Koblížek, M., Béjà, O., Bidigare, R. R., Christensen, S., Benitez-Nelson, B., Vetriani, C., Kolber, M. K., Falkowski, P. G., & Kolber, Z. S. (2003). Isolation and characterization of *Erythrobacter* sp. Strains from the upper ocean. *Archives of Microbiology*, *180*(5), 327–338.

Kolber, Z S, Van Dover, C. L., Niederman, R. a, & Falkowski, P. G. (2000). Bacterial photosynthesis in surface waters of the open ocean. *Nature*, *407*(1993), 177–179.

Kolber, Zbigniew S, Plumley, F. G., Lang, A. S., Beatty, J. T., Blankenship, R. E., Vandover, C. L., Vetriani, C., Koblizek, M., Rathgeber, C., & Falkowski, P. G. (2001). Contribution of Aerobic Photoheterotrophic Bacteria to the Carbon Cycle in the Ocean. *Science*, *292*, 2492–2495.

Laguna, R., Tabita, F. R., & Alber, B. E. (2011). Acetate-dependent photoheterotrophic growth and the differential requirement for the Calvin–Benson–Bassham reductive pentose phosphate cycle in *Rhodobacter sphaeroides* and *Rhodopseudomonas palustris*. *Archives of Microbiology*, *193*(2), 151–154.

Liotenberg, S., Steunou, A.-S., Picaud, M., Reiss-Husson, F., Astier, C., & Ouchane, S. (2008). Organization and expression of photosynthesis genes and operons in anoxygenic photosynthetic proteobacteria. *Environmental Microbiology*, *10*(9), 2267–2276.

McKinlay, J. B., & Harwood, C. S. (2010). Carbon dioxide fixation as a central redox cofactor recycling mechanism in bacteria. *Proceedings of the National Academy of Sciences*, *107*(26), 11669–11675.

McKinlay, J. B., & Harwood, C. S. (2011). Calvin Cycle Flux, Pathway Constraints, and Substrate Oxidation State Together Determine the H2 Biofuel Yield in Photoheterotrophic Bacteria. *MBio*, *2*(2).

McKinlay, J. B., Oda, Y., Rühl, M., Posto, A. L., Sauer, U., & Harwood, C. S. (2014). Non-

growing *Rhodopseudomonas palustris* Increases the Hydrogen Gas Yield from Acetate by Shifting from the Glyoxylate Shunt to the Tricarboxylic Acid Cycle. *Journal of Biological Chemistry*, *289*(4), 1960–1970.

Nishimura, K., Shimada, H., Ohta, H., Masuda, T., Shioi, Y., & Takamiya, K. (1996). Expression of the puf Operon in an Aerobic Photosynthetic Bacterium, *Roseobacter denitrificans*. *Plant Cell Physiology*, *37*(2), 153–159.

Pechter, K. B., Gallagher, L., Pyles, H., Manoil, C. S., & Harwood, C. S. (2016). Essential Genome of the Metabolically Versatile Alphaproteobacterium *Rhodopseudomonas palustris*. *Journal of Bacteriology*, *198*(5), 867–876.

Pitcher, D. G., Saunders, N. A., & Owen, R. J. (1989). Rapid extraction of bacterial genomic DNA with guanidium thiocyanate. *Letters in Applied Microbiology*, *8*(4), 151–156.

Piwosz, K., Kaftan, D., Dean, J., Šetlík, J., & Koblížek, M. (2018). Nonlinear effect of irradiance on photoheterotrophic activity and growth of the aerobic anoxygenic phototrophic bacterium *Dinoroseobacter shibae*. *Environmental Microbiology*, *20*(2), 724–733.

Price, M. N., Wetmore, K. M., Waters, R. J., Callaghan, M., Ray, J., Liu, H., Kuehl, J. V., Melnyk, R. A., Lamson, J. S., Suh, Y., Carlson, H. K., Esquivel, Z., Sadeeshkumar, H., Chakraborty, R., Zane, G. M., Rubin, B. E., Wall, J. D., Visel, A., Bristow, J., … Deutschbauer, A. M. (2018). Mutant phenotypes for thousands of bacterial genes of unknown function. *Nature*, *557*(7706), 503–509.

Rathgeber, C., Alric, J., Andre, E. H., & Yurkov, V. (2012). The photosynthetic apparatus and photoinduced electron transfer in the aerobic phototrophic bacteria *Roseicyclus mahoneyensis* and *Porphyrobacter meromictius*. *Photosynthesis Research*, *110*, 193–203.

Rathgeber, C., Beatty, J. T., & Yurkov, V. (2004). Aerobic phototrophic bacteria: New evidence for the diversity, ecological importance and applied potential of this previously overlooked group. *Photosynthesis Research*, 113–128.

Ravcheev, D. A., Khoroshkin, M. S., Laikova, O. N., Tsoy, O. V., Sernova, N. V., Petrova, S. A., Rakhmaninova, A. B., Novichkov, P. S., Gelfand, M. S., & Rodionov, D. A. (2014). Comparative genomics and evolution of regulons of the LacI-family transcription factors. *Frontiers in Microbiology*, *5*.

Rich, J. H., Ducklow, H. W., & Kirchman, D. L. (1996). Concentrations and uptake of neutral monosaccharides along 140°W in the equatorial Pacific: Contribution of glucose to heterotrophic bacterial activity and the DOM flux. *Limnology and Oceanography*, *41*(4), 595–604.

Ross, W., Sanchez-Vazquez, P., Chen, A. Y., Lee, J.-H., Burgos, H. L., & Gourse, R. L. (2016). PpGpp binding to a site at the RNAP-DksA interface accounts for its dramatic effects on transcription initiation during the stringent response. *Molecular Cell*, *62*(6), 811–823.

Rubin, B. E., Wetmore, K. M., Price, M. N., Diamond, S., Shultzaberger, R. K., Lowe, L. C., Curtin, G., Arkin, A. P., Deutschbauer, A., & Golden, S. S. (2015). The essential gene set of a photosynthetic organism. *Proceedings of the National Academy of Sciences of the United States of America*, *112*(48), E6634-43.

Sauer, U., & Eikmanns, B. J. (2005). The PEP—pyruvate—oxaloacetate node as the switch point for carbon flux distribution in bacteria: We dedicate this paper to Rudolf K. Thauer, Director of the Max-Planck-Institute for Terrestrial Microbiology in Marburg, Germany, on the occasion of his 65th birthday. *FEMS Microbiology Reviews*, *29*(4), 765–794.

Shiba, T. (1987). O2 regulation of bacteriochlorophyll synthesis in the aerobic bacterium *Erythrobacter*. *Plant Cell Physiol.*, *28*(7), 1313–1320.

Shiba, Tsuneo. (1984). Utilization of Light Energy By the Strictly Aerobic Bacterium *Erythrobacter* sp. OCH 114. *J. Gen. Appl. Microbiol*, *30*, 239–244.

Shiba, Tsuneo. (1991). *Roseobacter litoralis* gen. Nov., sp. Nov., and *Roseobacter denitrificans* sp. Nov., Aerobic Pink-Pigmented Bacteria which Contain Bacteriochlorophyll a. *Systematic and Applied Microbiology*, *14*(2), 140–145.

Sieracki, M. E., Gilg, I. C., Thier, E. C., Poulton, N. J., & Goericke, R. (2006). Distribution of planktonic aerobic anoxygenic photoheterotrophic bacteria in the northwest Atlantic. *Limnology and Oceanography*, *51*(1), 38–46.

Silva, L. G., Lorenzetti, A. P. R., Ribeiro, R. A., Alves, I. R., Leaden, L., Galhardo, R. S., Koide, T., & Marques, M. V. (2019). OxyR and the hydrogen peroxide stress response in *Caulobacter crescentus*. *Gene*, *700*, 70–84.

Soora, M., & Cypionka, H. (2013). Light Enhances Survival of Dinoroseobacter shibae during Long-Term Starvation. *PLoS ONE*, *8*.

Soora, M., Tomasch, J., Wang, H., Michael, V., Petersen, J., Engelen, B., Wagner-Döbler, I., & Cypionka, H. (2015). Oxidative stress and starvation in *Dinoroseobacter shibae*: The role of extrachromosomal elements. *Frontiers in Microbiology*, *6*(March), 1–12.

Spring, S., Lunsdorf, H., Fuchs, B. M., & Tindall, B. J. (2009). The Photosynthetic Apparatus and Its Regulation in the Aerobic Gammaproteobacterium *Congregibacter litoralis* gen. Nov ., sp. Nov . *PLoS ONE*, *4*(3).

Steunou, A.-S., Astier, C., & Ouchane, S. (2004). Regulation of Photosynthesis Genes in Rubrivivax gelatinosus: Transcription Factor PpsR Is Involved in both Negative and Positive Control. *Journal of Bacteriology*, *186*(10), 3133–3142.

Swem, L. R., Elsen, S., Bird, T. H., Swem, D. L., Koch, H.-G., Myllykallio, H., Daldal, F., & Bauer, C. E. (2001). The RegB/RegA two-component regulatory system controls synthesis

of photosynthesis and respiratory electron transfer components in *Rhodobacter capsulatus*. *Journal of Molecular Biology*, *309*(1), 121–138.

Tang, Kai, Zong, R., & Zhang, F. (2010). Characterization of the Photosynthetic Apparatus and Proteome of *Roseobacter denitrificans*. *Current Microbiology*, *60*, 124–133.

Tang, Kuo-hsiang, Feng, X., Tang, Y. J., & Blankenship, R. E. (2009). Carbohydrate Metabolism and Carbon Fixation in *Roseobacter denitrificans* OCh114. *PLoS ONE*, *4*(10).

Tang, Kuo-hsiang, Tang, Y. J., & Blankenship, R. E. (2011). Carbon metabolic pathways in phototrophic bacteria and their broader evolutionary implications. *Frontiers in Microbiology*, *2*(August), 1–23.

Tomasch, J., Gohl, R., Bunk, B., Diez, M. S., & Wagner Dobler, I. (2011). Transcriptional response of the photoheterotrophic marine bacterium *Dinoroseobacter shibae* to changing light regimes. *Isme J*, 1957–1968.

Vermeulen, A. J., & Bauer, C. E. (2015). Members of the PpaA/AerR Antirepressor Family Bind Cobalamin. *Journal of Bacteriology*, *197*(16), 2694–2703.

Wetmore, K. M., Price, M. N., Waters, R. J., Lamson, J. S., He, J., Hoover, C. A., Blow, M. J., Bristow, J., Butland, G., Arkin, A. P., & Deutschbauer, A. (2015). Rapid Quantification of Mutant Fitness in Diverse Bacteria by Sequencing Randomly Bar-Coded Transposons. *MBio*, *6*(3), 1–15.

Yin, L., Dragnea, V., & Bauer, C. E. (2012). PpsR, a regulator of heme and bacteriochlorophyll biosynthesis, is a heme-sensing protein. *Journal of Biological Chemistry*, *287*(17), 13850–13858.

Yurkov, V., & Csotonyi, J. T. (2009). The Purple Phototrophic Bacteria. Chapter 3. New Light on Aerobic Anoxygenic Phototrophs. *C. Neil Hunter, Fevzi Daldal, Marion C. Thurnauer and J. Thomas Beatty (eds)* (31-55).

Yurkov, V., Gad'on, N., & Drews, G. (1993). The major part of polar carotenoids of the aerobic bacteria *Roseococcus thiosulfatophilus* RB3 and *Erythromicrobium ramosum* E5 is not bound to the bacteriochlorophyll a-complexes of the photosynthetic apparatus. *Archives of Microbiology*, *160*(5), 372–376.

Yurkov, V., & Hughes, E. (2013). Genes Associated with the Peculiar Phenotypes of the Aerobic Anoxygenic Phototrophs. In *Advances in Botanical Research* (Vol. 66, p. 358). Elsevier.

Yurkov, V. V., & Beatty, J. T. (1998). Aerobic Anoxygenic Phototrophic Bacteria. *Microbiology and Molecular Biology Reviews. 62*(3), 695–724.

Yurkov, V. V., & van Gemerden, H. (1993). Impact of light/dark regimen on growth rate, biomass formation and bacteriochlorophyll synthesis in *Erythromicrobium hydrolyticum*. *Archives*

of Microbiology, 84–89.

Zheng, Q., Zhang, R., Koblížek, M., Boldareva, E. N., Yurkov, V., Yan, S., & Jiao, N. (2011). Diverse arrangement of photosynthetic gene clusters in aerobic anoxygenic phototrophic bacteria. *PLoS ONE*, *6*(9), 1–7.

Ziegelhoffer, E. C., & Donohue, T. J. (2009). Bacterial responses to photo-oxidative stress. *Nature Reviews. Microbiology*, *7*(12), 856–863.

Zsebo, K. M., & Hearst, J. E. (1984). Genetic-physical mapping of a photosynthetic gene cluster from R. capsulata. *Cell*, *37*(3), 937–947.

3.7. Supporting Figures

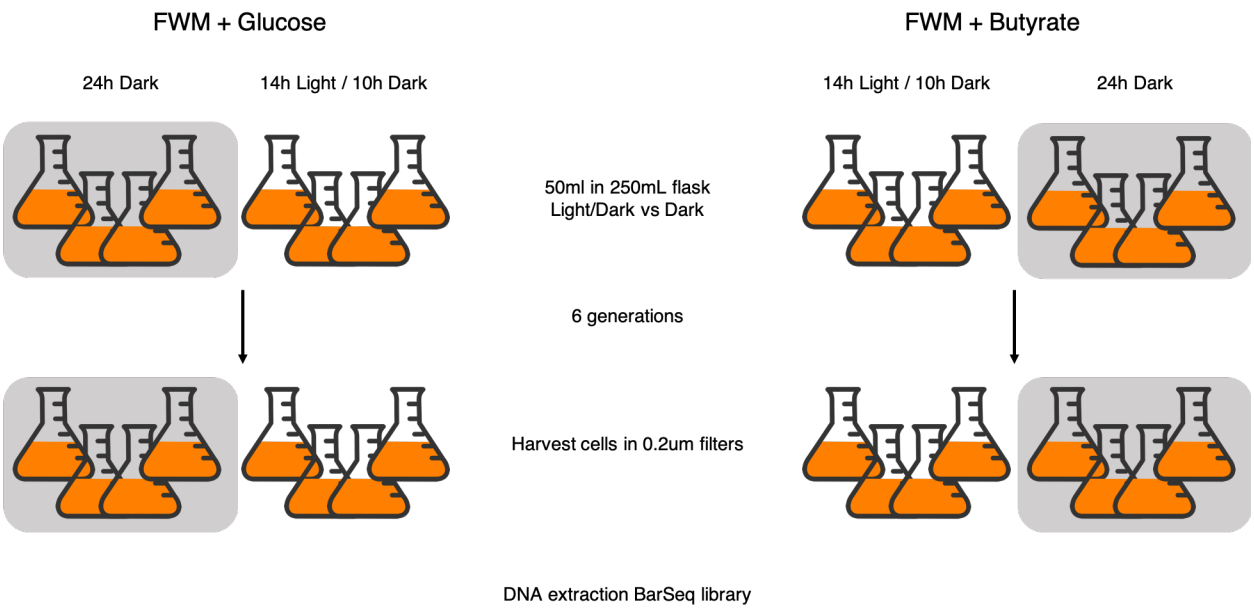

Figure S3.1. Schematic of experimental design.

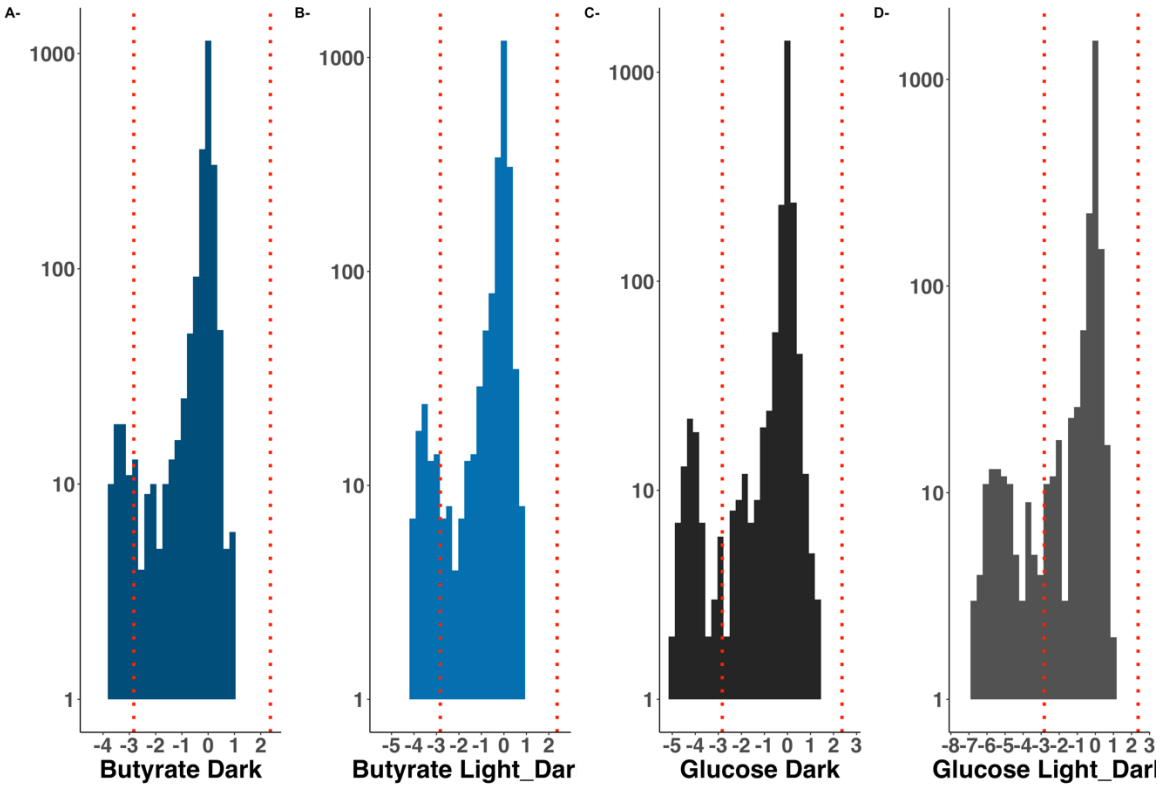

Figure S3.2. Distribution of average gene fitness of the mutant strains in the four experimental conditions.

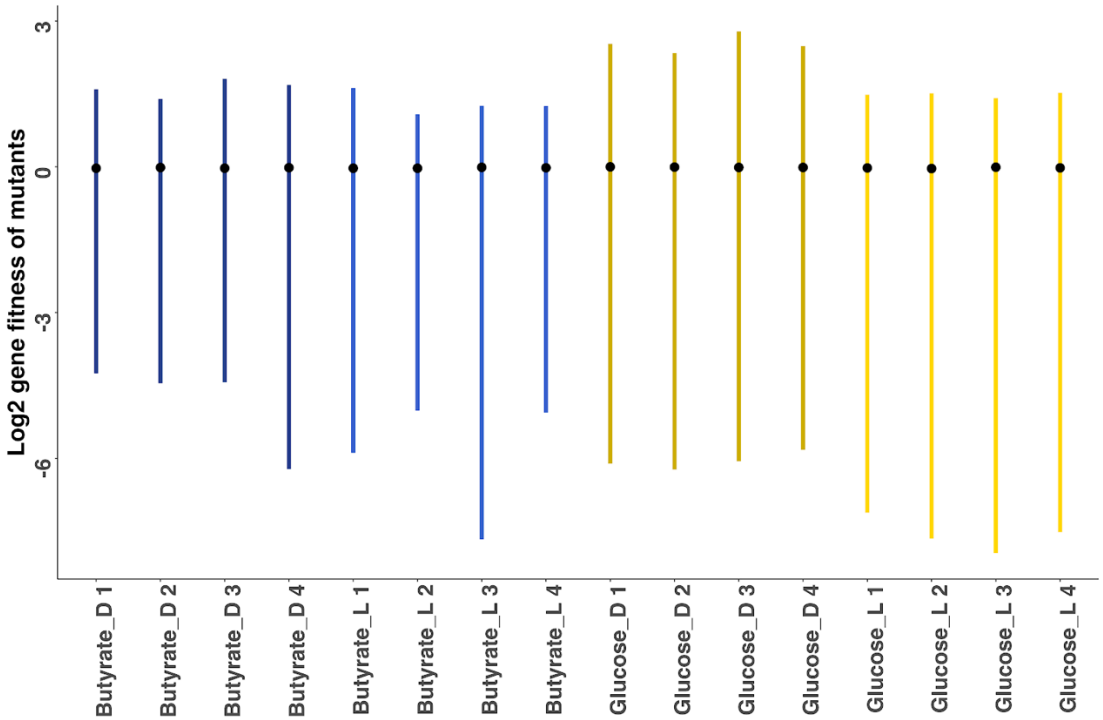

Figure S3.3. Interquartile range of gene fitness values of *Porphyrobacter* LM6 mutants. The black dot represents the mean of the interquartile range.

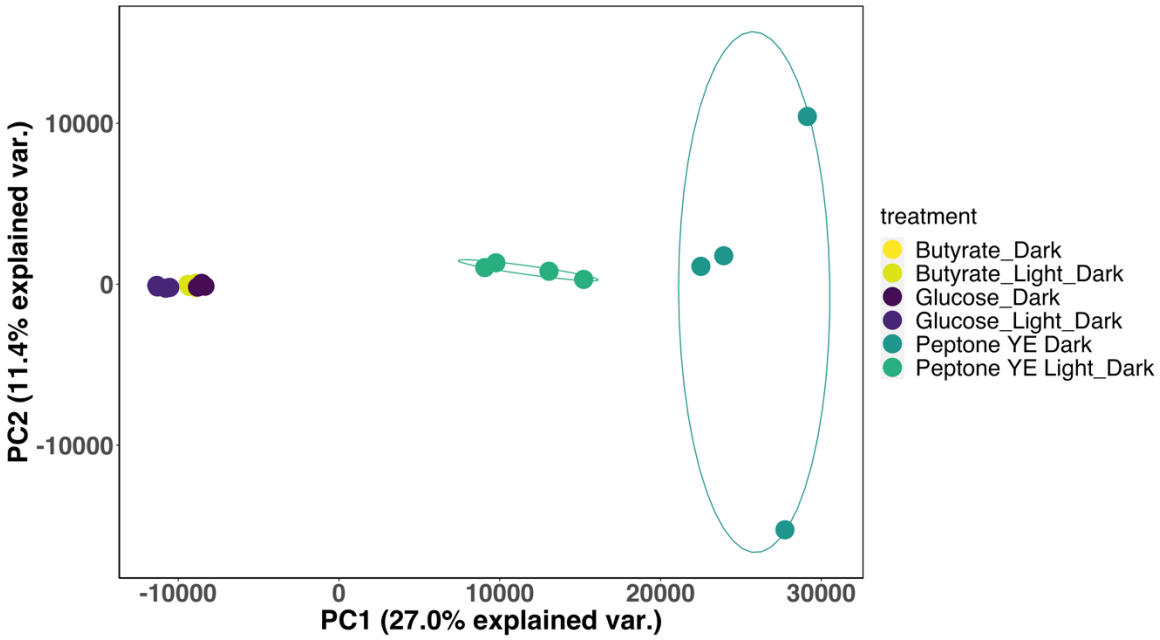

Figure S3.4 . Principal component analysis of variation in fitness of *Porphyrobacter* LM6 mutants. Comparison single carbon substrates glucose and butyrate vs complex media. Substrates: FWM + glucose, FWM + butyrate and FWM + peptone + yeast extract; and two light regimes. Light_Dark= 14h:10h light:dark. Dark: 24h dark.

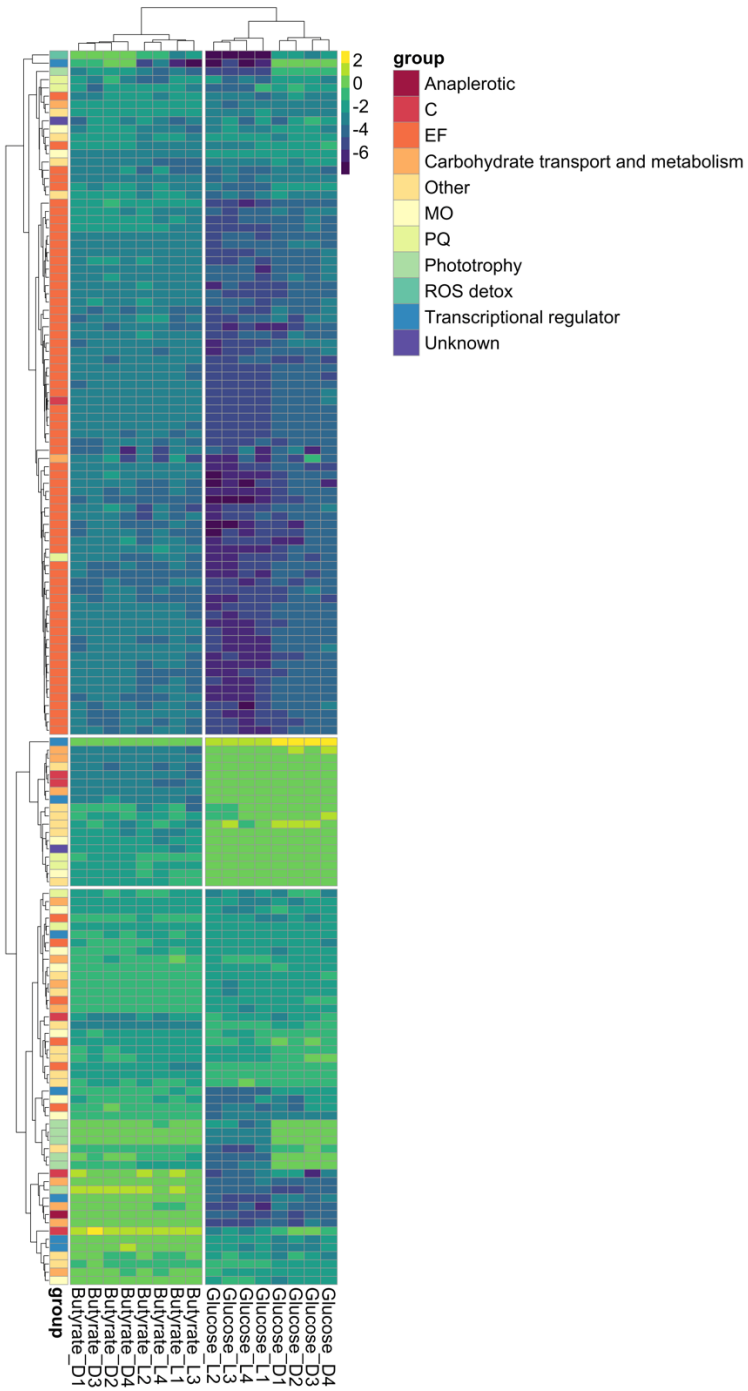

Figure S3.5. Heatmap of mutants with strong phenotypes |fitness| > 2 and |t-statistic| > 5 (defined as in Wetmore et al., 2015). Genes are classified by its functional category based on COG annotations. See details of functional annotations and fitness values in Table S5.

CHAPTER 4

Global fitness profiling in response to light and oxidative stress in the aerobic anoxygenic phototroph *Erythrobacter longus*

4.1. Abstract

The biosynthesis of bacteriochlorophyll-*a* (Bchl*a*) in aerobic conditions increases the generation of reactive oxygen species. To cope with this stress, aerobic anoxygenic phototrophic bacteria (AAPB) have evolved mechanisms to alleviate oxidative stress. To elucidate such mechanisms, we grew a barcoded mutant library of the model organism *Erythrobacter longus* under different light regimes and exogenous hydrogen peroxide additions. As expected, we found that superoxide dismutase and catalase are important enzymes against reactive oxygen species (ROS). Mutants deficient in carotenoid biosynthesis also had low fitness under increased oxidative stress, confirming their photoprotective role in AAPB. Glutathione-based systems for repairing ROS damage are vital for the survival of *E. longus*, as the enzymes glutathione synthase and glutathione peroxidase are required for growth. Mutants of the transcriptional regulator *oxyR* present some of the lowest fitness suggesting its role as major regulator in response to oxidative stress. The mutants of catalase and glutathione reductases showed similar fitness patterns to *oxyR* regulon suggesting that these could be part of its regulon in *E. longus.* Taken together, our results demonstrate that *E. longus,* and likely other AAPB, use a combination of enzymatic mechanisms and photoprotective carotenoids against reactive oxygen species (ROS). We also show that *E. longus* response against ROS and its *oxyR* regulon differ from what has been observed in anoxygenic photosynthetic alphaproteobacteria.

4.2. Introduction

The evolution of oxygenic photosynthesis by cyanobacteria changed the redox landscape affecting every ecosystem on the planet (Hohmann-Marriott & Blankenship, 2011; Schmitt et al., 2014; Ziegelhoffer & Donohue, 2009). Before oxygenic photosynthesis, microorganisms lived under reducing conditions; as oxygen started to accumulate in the atmosphere, they were pressured to evolve mechanisms to alleviate the effects of oxidative stress (Johnson & Hug, 2019). Oxidative stress is produced by an imbalance between oxidants and antioxidants in the cell due to the accumulation of reactive oxygen species (ROS) which result from aerobic metabolism (Sies et al., 2017). Reactive oxygen species are created by electron transfer or energy transfer to oxygen producing superoxide, hydrogen peroxide (H_2O_2) and hydroxyl radicals (Gao et al., 2020; Imlay, 2019; Keyer & Imlay, 1996; Ziegelhoffer & Donohue, 2009). ROS are small reactive molecules that cause a broad spectrum of damage to biological molecules (Imlay, 2008). Some of the harmful effects of ROS include the inactivation of enzymes involved in amino acid synthesis and other carbon metabolism such as the dehydratases fumarase and aconitase (Dixon & Stockwell, 2014; Flint et al., 1993; Imlay, 2008, 2019; Kovács et al., 2005). Superoxide and H_2O_2 also cause the oxidation of other proteins producing protein peroxides (Ziegelhoffer & Donohue, 2009). ROS additionally target lipid membranes and DNA. Hydrogen peroxide causes potentially lethal lesions to DNA by the Fenton reaction (Ziegelhoffer & Donohue, 2009).

Bacteria have evolved several mechanisms to counteract the effects of ROS distributed amongst most phyla (Johnson & Hug, 2019). The bacterial defenses against ROS include non-enzymatic and enzymatic mechanisms of detoxification. The non-enzymatic defense mechanisms include several antioxidants such as NADH, NADPH, ascorbic acid, alpha-tocopherol, glutathione, flavonoids and carotenoids (Hamilton, 2019; Schmitt et al., 2014). The enzymatic

defenses of cells include superoxide dismutase (SOD) superoxide reductase, catalase, glutathione peroxidases, thioredoxins and others. The most studied ROS detoxification enzymes include SOD, catalase and peroxidases. SOD uses metal cofactors for the conversion of superoxide into H_2O_2 and O_2. The H_2O_2 produced by SOD activity, as well as other sources of endogenous and exogenous H_2O_2, is scavenged by catalase and peroxidase enzymes to produce H_2O and O_2 (Johnson & Hug, 2019; McCord & Fridovich, 1969; Sies et al., 2017).

Phototrophic organisms are subject to additional sources of ROS due to the capacity of chlorophyll and bacteriochlorophyll pigments to accept electrons from light, that are subsequently transferred to oxygen (Elsen et al., 2005; Kovács et al., 2005; Schmitt et al., 2014). Anoxygenic phototrophs reduce photo-oxidative stress by downregulating the synthesis of chlorophylls and photoprotective carotenoids in aerobic environments (Ziegelhoffer & Donohue, 2009). However, because aerobic anoxygenic phototrophic bacteria (AAPB) are obligate aerobes, they require mechanisms to deal with light- and oxygen-derived ROS. The photoprotective carotenoids produced by AAPB differ from those in anoxygenic phototrophs. Contrary to photosystem-bound carotenoids that participate in light harvesting, the carotenoids of AAPB are polar and therefore soluble in the cytoplasm (V. Yurkov et al., 1993; V. Yurkov & Csotonyi, 2009). Soluble carotenoids enable phototrophs to combat oxidative stress by quenching excited Bchl*a* and triplet oxygen, and dissipating this energy as heat (Berghoff et al., 2011; Borland et al., 1989; Cogdell & Frank, 1987; Jens Glaeser & Klug, 2005). Cytochromes and other sinks in the electron transport chain also aid phototrophs with ROS quenching (Hamilton, 2019).

Phototrophic bacteria sense and respond to oxidative stress using diverse regulatory mechanisms, some of which are analogous to those in non-phototrophic organisms such as *E. coli.* Known regulatory networks related to oxidative stress include alternative sigma factors *rpoH* and

rpoE, and the regulons controlled by *oxyR* and *soxRS.* The transcriptional regulators *oxyR* and *soxRS* respond to H_2O_2 and superoxide respectively (Ziegelhoffer & Donohue, 2009). OxyR controls the expression of genes including catalase and *ahpCF*, glutathione reductase and glutaredoxins and thioredoxins, among others (Imlay, 2008; Silva et al., 2019; M. Zheng et al., 2001; Ziegelhoffer & Donohue, 2009). SoxRS controls the expression of oxidant-resistant fumarase and aconitase, manganese-containing SOD, genes for DNA repair and others (Pomposiello et al., 2001; Ziegelhoffer & Donohue, 2009). In anoxygenic phototrophic strains of *Rhodobacter, rpoH* and *rpoE* are overexpressed in the light and initiate cellular defenses against oxidative stress (Q. Li et al., 2018). Similar *rpoH* and *rpoE* results were observed in the AAPB strain *Roseobacter denitrificans* but with stronger induction than in *Rhobacter sphaeroides*. Despite the similarities observed for the *rpoH-rpoE* regulons in these two strains, the genes controlled by the regulons were different (Berghoff et al., 2011). In *Erythrobacter litoralis* DSM8509 (also AAPB), *rpoH* and *rpoE*, in combination with histidine kinases, were found to respond to light and initiate general stress response (Fiebig et al., 2019).

Here, we use a barcoded mutant library of the model AAPB *Erythrobacter longus* to assess the genome-wide effects of light-derived and exogenous oxidative stress. Our data show the mechanisms used by this strain to survive oxidative stress, and shed light into the regulatory functions involved in this process.

4.3. Results

4.3.1. The essential genome of *Erythrobacter longus* on complex media

The mutant library generated for *E. longus* was mapped to determine the insertion sites of every barcoded transposon. During TnSeq experiments, there is a set of genes for which no

transposon mutants are recovered in the sequencing run. These genes are defined as essential under the prescribed experimental conditions, and they often include genes encoding for replication, transcription and translation machinery. By this definition (i.e. genes with no insertions detected), *E. longus* has 597 essential genes, 564 of which have homologs in functional databases (Table S4.1). The essential genes are distributed among several COG functional categories (Fig S4.2). The majority of these are involved in translation (96), followed by genes of unknown function (71), coenzyme metabolism (52) and energy production and conversion (49). There were 32 genes that could not be assigned to any category.

The essential genes involved in energy production included TCA cycle enzymes, the proton-pumping NADH:ubiquinone oxidoreductase, the respiratory complex I (*nuo* genes) and the ATP synthase. A total of 99 genes involved in the metabolism of carbohydrates, lipids, amino acids and nucleotides were also essential for *E. longus*. Genes for the biosynthesis of heme, NAD and riboflavin cofactors are also essential for *E. longus*. Similarly, *E. longus* also require DNA polymerase, topoisomerases and other DNA repair enzymes, along with the *mur* system for peptidoglycan biosynthesis and other cell envelope biogenesis genes to grow in this condition. Additionally, ten genes involved in signal transduction were also essential. Notably, the gene that encodes the glutathione peroxidase (GPx), one of the major H_2O_2 scavengers in the cell, and thioredoxin I (*trxA*), which participates in glutathione-dependent redox processes, are also essential for *E. longus*. The *suf* system for FeS cluster assembly was also required for growth of this strain.

The essentiality of the TCA cycle enzymes and the respiratory chain when growing on peptone as the major carbon substrate demonstrates that *E. longus* grows heterotrophically on complex media. Furthermore, the requirement of enzymes involved in ROS detoxification for the

growth of *E. longus* confirms the importance of these processes for AAPB. None of the genes in the photosynthetic gene cluster were essential in this condition.

4.3.2. Light and hydrogen peroxide affect the growth of *E. longus*

To determine the effect of exogenous H_2O_2 on the growth of *E. longus*, we grew wild-type cultures in artificial seawater medium (ASW) amended with peptone, yeast extract and other trace nutrients under varying concentrations of H_2O_2. *E. longus* growth on complex media was negatively affected by the addition of H_2O_2 to the media. The addition of exogenous H_2O_2 in concentrations up to 615µM decreased the growth rate of cultures over 14:10h light:dark cycles, though these cultures eventually reached the same maximum OD660 as cultures with no added H_2O_2. Concentrations of 1.23mM H_2O_2 or higher prevented the growth of *E. longus* (Fig.1a). Based on these results, we selected 100µM H_2O_2 as the concentration for BarSeq experiments, as this concentration imposed a strong pressure but also allowed cells to grow to sufficient OD660.

The mutant library was grown over six different conditions with the goal of disentangling the effects of ROS derived from light and/or exogenous H_2O_2 on the fitness of the mutants (Fig. S4.1). The growth rates obtained for cultures of the mutant library decreased with increasing oxidative stress as a result of both light (intensity and exposure) and the addition of H_2O_2 (Fig 4.1b). Increased light exposure and intensity inhibited growth rates; cultures exposed to continuous dark, low light intensity, and 14:10h light:dark cycles respectively corresponded to the fastest three growth rates. Oxidative stress effects on fitness were more evident in the high light 24h cultures, and then in the cultures with extra H_2O_2. As expected, the condition resulting in slowest growth rates was the high intensity light 24h cultures with 100µM exogenous H_2O_2.

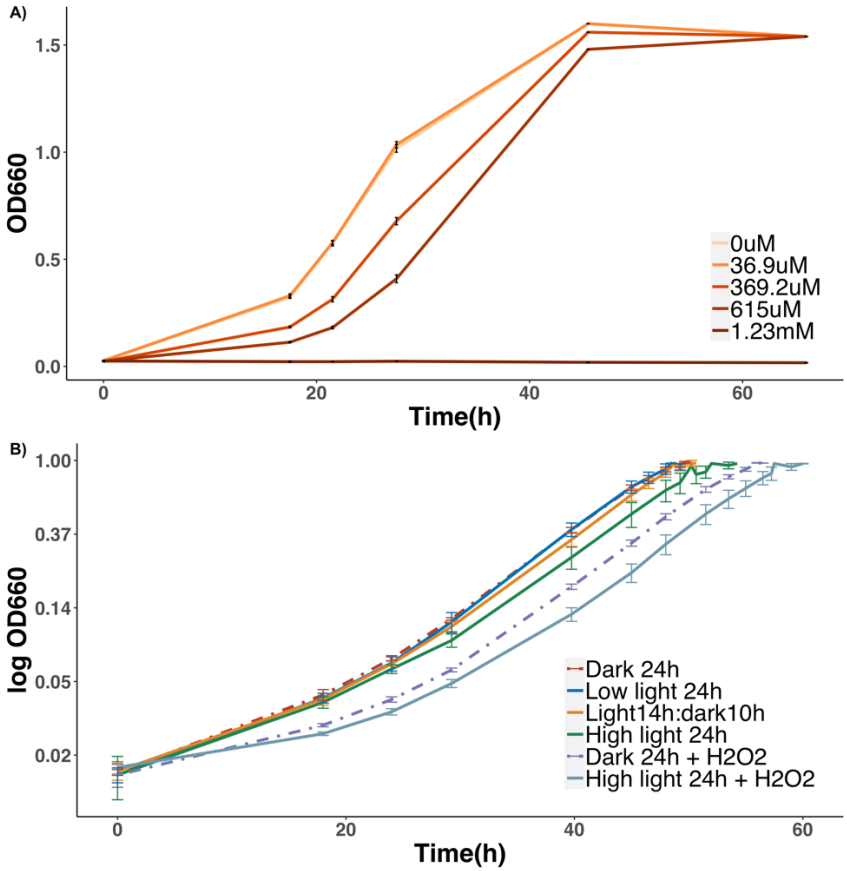

Figure 4.1. Growth of *Erythrobacter longus* with varying light regimes and exogenous hydrogen peroxide. A) Wild-type *E. longus* growth with increasing concentrations of hydrogen peroxide. Cultures were grown in 14:10h light: dark cycles. B) Growth of the pooled transposon mutant library in different oxidative stress conditions. Low_light= 80uE. High light= 240uE. H2O2= 100uM.

4.3.3. Light increases oxidative stress in *E. longus* cultures

The effects of light and exogenous ROS on the fitness of *E. longus* were evaluated by growing a barcoded mutant library under different light regimes and with the addition of H_2O_2. The mean fitness of the 2559 mutants in the library was -0.13 (stdev= 0.65). From those, 72 mutants presented average fitness values > from 3 standard deviations from the mean (Fig S4.3 and Table S4.2).

We identified mutants with fitness effects that were driven by the light regimes in the experiment using pairwise comparisons (average fitness difference > |1.5 Log2|). Only nine mutants passed this filtering criteria, three of which correspond to mutants in genes of unknown function (Fig. 4.2, Table S4.2). The other six mutants include uracil-DNA glycosylase and the exodeoxyribonuclease VII small subunit *xseB,* both involved in DNA repair. Mutants of these genes showed positive or neutral fitness in cultures exposed to continuous dark and 14:10h light:dark treatments, but low fitness in cultures incubated in continuous light. The phage shock protein *pspC,* a gene that has been shown to be involved in nutrient and energy limitation, showed low fitness in continuous high light. The mutants of genes involved in detoxification of ROS also showed differential fitness in response to light. The mutants for heme synthesis *ctaA* and the superoxide dismutase *sodB* are among the mutants with the lowest fitness values in all conditions of the experiments demonstrating that AAPB experience oxidative stress pressure due to their metabolism. Interestingly, these two genes showed opposite patterns of fitness: *ctaA* mutants conferred the lowest fitness in continuous dark but *sodB* mutants were least fit in continuous high light.

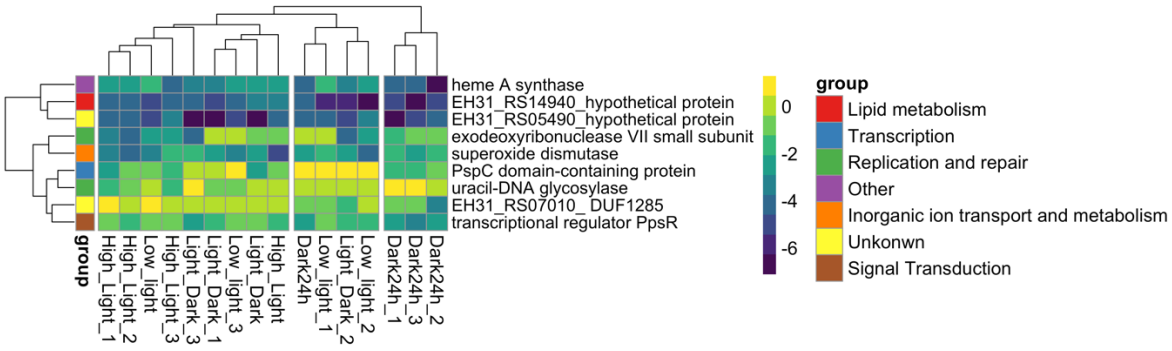

Figure 4.2. Differential light effects on the fitness of *E. longus* mutants. Genes were filtered by having > |1.5 Log2| average fitness between any two light regimes. The functional categories were assigned based on COG annotations.

Finally, the major transcriptional regulator of phototrophy in AAPB, *ppsR,* showed low fitness across all conditions but most significantly in continuous dark (Fig S4.4). This result is similar to what was observed in the freshwater AAPB *Porphyrobacter* LM6 *ppsR* mutants that showed low fitness in the dark (Vargas and Coleman. *In Prep*). Other genes in the photosynthetic gene cluster showed differences in fitness across treatments. Mutations in Bchl*a* biosynthesis genes were neutral or slightly beneficial in all the conditions suggesting that this pigment is being produced but *E. longus* is not growing phototrophically in this condition (Figure S4.5). On the other hand, carotenoid biosynthesis genes mutants showed low fitness in most conditions. The mutants of *ispA, crtL, crtI* and *crtB* presented lowest fitness in the conditions in which cultures were exposed to light (Fig S4.6). These findings demonstrate the importance of carotenoids for photoprotection in *E. longus*.

Together, our results indicate that *E. longus* relies on ROS detoxification enzymes, photoprotective carotenoids, DNA repair machinery, and tight regulation over phototrophy to overcome the oxidative stress generated by AAP metabolism in the light.

4.3.4. Exogenous ROS have harmful effects on *E. longus* growth

AAPB are exposed to H_2O_2 through both the intracellular combination of Bchla, light, and oxygen, as well as exogenous H_2O_2 produced as a metabolic byproduct from other community members. To determine the mechanism that *E. longus* uses for ROS detoxification, we added 100μM exogenous H_2O_2 to cultures growing on continuous light and continuous dark. Pairwise comparisons were made between continuous light with and without addition of H_2O_2, continuous dark with and without addition of H_2O_2, and continuous light and continuous dark both with H_2O_2 (average fitness difference > |1.5 Log2|). There were 37 genes that responded to H_2O_2 distributed

in three main clusters according to their effect on fitness (Fig. 4.3). These 37 mutants include the majority of the mutants shown in Figure 4.2, except for the uracil-DNA glycosylase. This result demonstrates an overlap in the response of *E. longus* against both types of oxidative stress. The first cluster of mutants consist of four genes including heme A synthase and three other genes of unknown function that showed low fitness in all the treatments. The second clusters have mutants that showed neutral or positive fitness in the treatments with no extra H_2O_2, but that had low fitness when H_2O_2 was added regardless of the light regime. Several genes stand out within the second cluster of mutants including catalase. Catalase and glutathione peroxidase are the major scavengers of H_2O_2 and are vital for ROS detoxification. A transcriptional regulator annotated as Rrf2 family regulator is also in this cluster, homologs of this regulator have been shown to be involved in sensing nitric oxide levels in the cell. In addition to several proteins of unknown function, several mutants of genes for DNA repair complete the second cluster. The mutants in the third cluster of Figure 4.3, presented low fitness values in most treatments, but with lowest fitness was observed in the cultures with extra H_2O_2. This cluster contains mutants of two transcriptional regulators: *ppsR* and *oxyR*. The latter is known for controlling a regulon in response to H2O2 induced oxidative stress. Several other mutants of genes for replication and repair are also included in this last cluster.

The addition of exogenous H_2O_2 strongly affected the fitness of mutants with DNA repair and stringent response functions. Mutations of *polA* in H_2O_2 treatment had negative fitness values in the range of the essential genes (average fitness <-4), but this gene was nonessential in treatments without H_2O_2 (Fig S4.7). Similarly, the mutants of *recA* presented almost three times lower fitness in the H_2O_2 conditions. In the case of stringent response, the fitness of the mutants of *spoT* was also the lowest when H_2O_2 was added to the cultures.

This data demonstrates that *E. longus* response mechanisms to light-derived oxidative stress largely overlap with the response to exogenous H_2O_2. Furthermore, both light and H_2O_2 are detrimental to the fitness of this strain which rely on key enzymes such as catalase and superoxide dismutase, along with other stress response and other DNA repair mechanisms to survive increased oxidative stress.

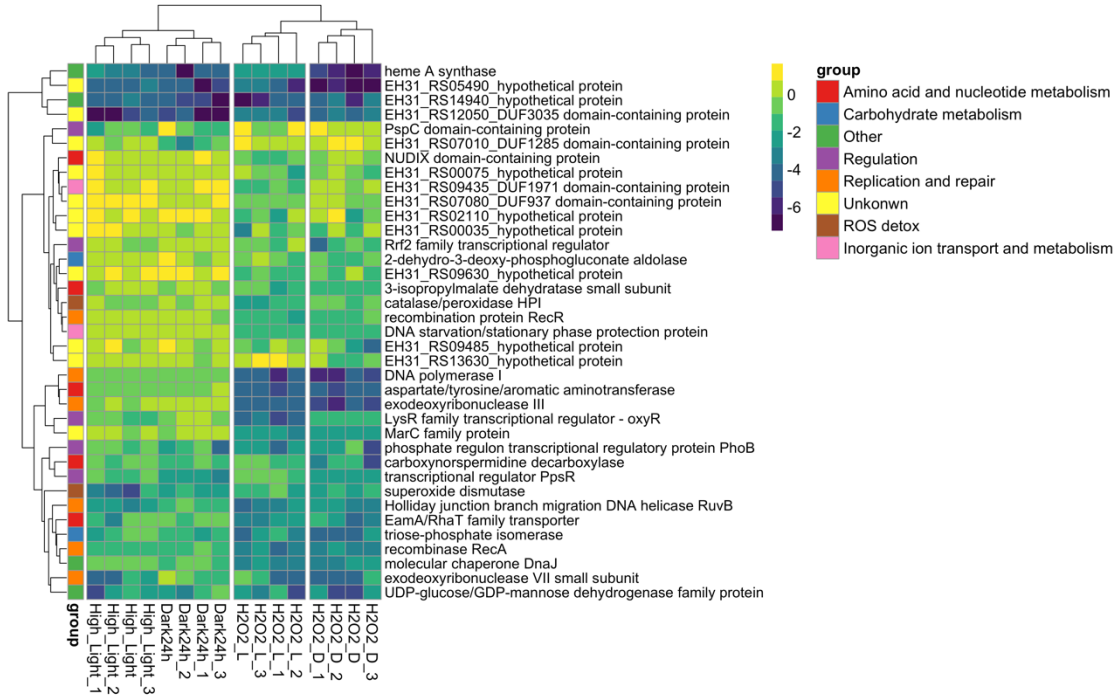

Figure 4.3. Differential effects of exogenous H_2O_2 on the fitness of *E. longus* mutants. Genes were filtered by having > |1.5 Log2| average fitness between any two treatments. The functional categories were assigned based on COG annotations.

4.3.5. ROS detoxification in *E. longus*

Compared to non-phototrophic and anaerobic phototrophic bacteria, AAPB must deal with additional ROS due to the biosynthesis of Bchl*a* under oxic conditions. Photons harvested by Bchl*a* are easily transferred to O_2 generating singlet oxygen which damages biomolecules. The majority of the mutants of genes involved in ROS detoxification in *E. longus* were essential or

presented low fitness under at least one of the experimental conditions (Fig. 4.4). Two genes in the pathway were essential for *E. longus*: glutathione synthase (*gshB*) and the glutathione peroxidase (*gpX*) suggesting that the latter is the main H2O2 scavenger in this strain. Mutants of superoxide dismutase (*sodB*) showed low fitness in all the conditions, however the lowest values were observed in the light. Together with the photoprotective carotenoids, superoxide dismutase is the first line of protection against $^1O_2$. Similarly, the mutants of catalase had low fitness in all the conditions but the fitness was particularly low in the cultures incubated under 24h of continuous high light and extra H_2O_2, the condition designed to have the most oxidative stress. Three mutants of glutathione reductases also showed differential fitness in the treatments: *gsr, gor,* and *grxC*; their fitness however was lower in the cultures with additional H_2O_2 (Fig. S4.8). The genome of *E. longus* encodes for several glutathione transferases (GSTs), most of which showed neutral effects of mutation in the experiment. The mutants of one of such GSTs (locusId= EH31_RS03995), has an interesting pattern of fitness values, presenting higher fitness in the H_2O_2 treatments compared with the ones with no extra peroxide (Fig S9). Mutants of the lycopene cyclase (*crtL*), a key enzyme in the biosynthesis of carotenoids showed low fitness in all the treatments (>3s.d. From mean) demonstrating the important role of carotenoids quenching the toxic effects of $^1O_2$.

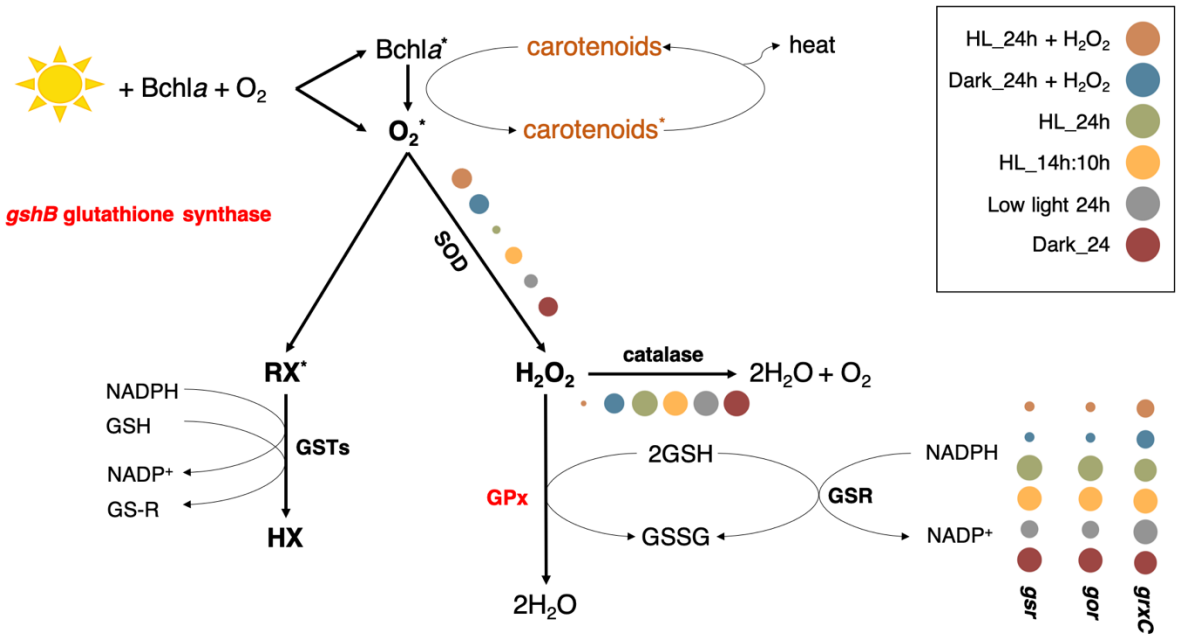

Figure 4.4. Pathways for ROS detoxification in *E. longus* based on genome content. The size of the bubble corresponds to the relative fitness of the gene in each condition. *gshB*, glutathione synthase; GPx, glutathione peroxidase; GSR, glutathione reductases; GSTs, glutathione transferases; SOD, superoxide dismutase. The genes in red are essential for *E. longus*. The size of the bubble is relative to the fitness of the mutant (lowest fitness= smallest bubble).

4.3.6. Light and exogenous H2O2 produced opposing fitness effects in *oxyR* and *soxR*

The regulons operated by the transcriptional regulators *oxyR* and *soxR* have been characterized in several Proteobacteria. *E. longus* contains both oxyR and soxR, neither of which were essential for the strain in complex media. However, their mutants showed different fitness effects over the experimental conditions. The mutation of *oxyR* showed large fitness effects in the conditions with additional H_2O_2; however, the most severe effect was observed on the cultures incubated under continuous high light (Fig. 4.5). The average fitness of *oxyR* in this condition is within the range of essential genes for this experiment, indicating that this gene is vital for the survival of *E. longus* over elevated oxidative stress. The results obtained for *oxyR* are consistent with the fitness effects observed in the H_2O_2 scavenger catalase (showed above). The genes *ahpC*

and *ahpF* have also been involved in H_2O_2 scavenging in other Proteobacteria, however the mutants of these genes had neutral fitness effects in this experiment (Fig S4.10).

The mutants of *soxR* presented less severe fitness effects compared to *oxyR*. The *soxR* mutants showed neutral fitness in the conditions with additional H_2O_2, regardless of the light regime, but they showed negative fitness in the other four conditions. The lowest fitness observed for *soxR* mutants were in the continuous dark treatments. The mutants of genes recognized to be part of the *soxR* regulon also showed neutral fitness over the conditions in this experiment (Fig S4.11). Mutations in the general stress response regulators *ecf* and its anti-anti-sigma factor *phyR* showed neutral fitness under the conditions of this experiment.

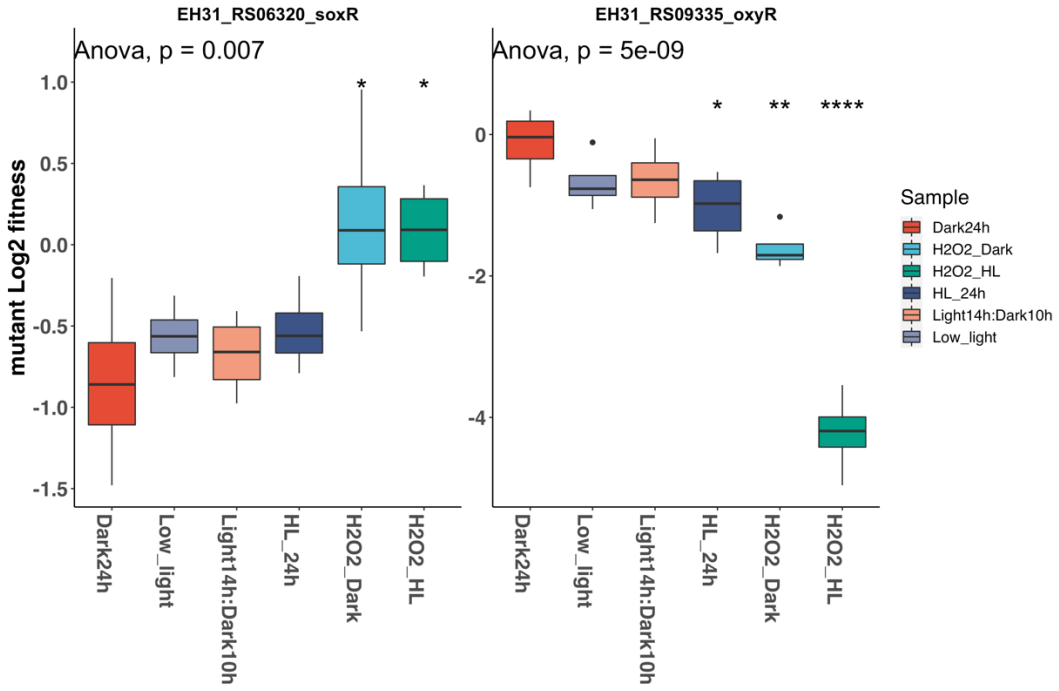

Figure 4.5. Fitness of strains with insertions in the transcriptional regulators *oxyR* and *soxR*. The global p value was calculated by ANOVA. Pairwise treatment comparisons were performed using t-test using Dark24h as reference. * p<0.05; ** p<0.005; *** p<0.0005.

4.4. Discussion

We interrogated the genome of the model AAPB *E. longus* to disentangle the mechanisms used by this strain in response to reactive oxygen species. In order to do that, we challenged a barcoded mutant library of *E. longus* to different light regimes and exogenous ROS, and assessed the fitness effect of the mutation each gene at the end of the experiment. AAPB face a constant pressure imposed by both endogenous and exogenous ROS in the environment. These bacteria adopted surface waters as their niche, and therefore had to evolve mechanisms to survive in this challenging environment where they not only face high concentrations of ROS, but also predation and competition (Berghoff et al., 2011; Ferrera et al., 2017; Garcia-Chaves et al., 2015; Kirchman et al., 2014; Koblížek, 2015; Ruiz-González et al., 2020). AAPB produce endogenous ROS as a result of their aerobic metabolism, however, the intracellular production increases as a result of phototrophy (Jens Glaeser & Klug, 2005). Light harvesting using Bchl*a* under aerobic conditions generates singlet oxygen, a very reactive species that produces damage to biological molecules (Borland et al., 1989; Jens Glaeser & Klug, 2005). The enzymatic detoxification of singlet oxygen produces H_2O_2, another harmful ROS (Berghoff et al., 2011; J. Glaeser et al., 2011; Pérez et al., 2018). Light is also a major contributor to exogenous ROS in the ocean, specifically in the photic zone where ROS concentrates due to photochemical production and rainfall (Zinser, 2018).

One of the first lines of protection that AAPB used against ROS, specifically singlet oxygen, is the biosynthesis of photoprotective carotenoids (J. Glaeser et al., 2011). It has been suggested that the function of AAPB carotenoids is to quench singlet oxygen and triplet Bchl*a* produced by the photosystem (Borland et al., 1989; Cogdell & Frank, 1987). Recently, molecular evidence has emerged in *Porphyrobacter* LM6 supporting the role of its carotenoids to counteract light-derived ROS in AAPB (Vargas and Coleman, In Prep). The quenching effect of carotenoids

has been also observed in *Rhodobacter sphaeroides,* an anoxygenic phototroph which produces small amounts of singlet oxygen when growing in the light. It was shown that *R. sphaeroides* mutants of carotenoids biosynthesis were less tolerant to light and O_2 than the wild type strain (Jens Glaeser & Klug, 2005; Griffiths et al., 1955). Unlike anoxygenic photoautotrophs, the carotenoids of AAPB are not involved in light harvesting, instead they are polar and thought to be soluble in the cytoplasm supporting their role as ROS quenchers (V. Yurkov et al., 1993; V. Yurkov & Csotonyi, 2009; V. Yurkov & Hughes, 2013; V. V. Yurkov & Beatty, 1998; Q. Zheng et al., 2011). Superoxide dismutase (*sodB*) also acts against singlet oxygen, this gene is not essential for *E. longus* but its mutants showed low fitness in all the experimental conditions. The lowest values of fitness of the *sodB* mutants were observed in cultures grown on continuous light. Interestingly, the fitness of *sodB* in the cultures grown in continuous light but with extra H_2O_2 presented fitness values similar to that of the cultures grown in the dark. This data suggests the existence of regulatory mechanisms that sense the type of molecule causing oxidative stress to orchestrate the appropriate response against it, or product inhibition of this enzyme. Glutathione can also cooperate with singlet oxygen toxic effects. Singlet oxygen can transfer electrons to organic groups damaging biomolecules, glutathione transferases (GSTs) can reduce these activated groups with the aid of NADPH (Allocati et al., 2009; Vuilleumier & Pagni, 2002). *E. longus* genome encodes for several GSTs, yet any of their mutants presented dramatic fitness effects suggesting that *sodB* and carotenoids are the major players against singlet oxygen and superoxide.

The dismutation of singlet oxygen by *sodB* produces endogenous H_2O_2, another harmful ROS (ref). H2O2 has also the highest concentration of all ROS in the ocean, (about 1000 times higher than superoxide), and longer lifetimes in water. (Miller & Kester, 1994; Zinser, 2018). Consequently, AAPB has to battle endogenous and exogenous H_2O_2 in the environment. Catalase

and glutathione peroxidase are the most important enzymes that act against H_2O_2 in the cell. Glutathione peroxidase (GPx) was essential for *E. longus* confirming its importance for the survival of this strain. The glutathione reductases that aid GPx H_2O_2 clearing had lower fitness in the cultures with additional H_2O_2. The non essential classification of the glutathione reductases can be explained by the existence of several enzymes with this function in the genome of *E. longus.* Catalase mutants on the other hand showed fitness values close to neutral in the conditions in which no exogenous H_2O_2 was added, but low fitness in the cultures with extra 100uM of H_2O_2. The detrimental effect of the mutation in catalase doubled in the continuous light, suggesting that light has an additive effect on the acculturation of H_2O_2 in the cell. Our experiment also demonstrated that glutathione peroxidase is the most important enzyme that *E. longus* uses to detoxify H2O2. Mutants of the H_2O_2 scavengers *ahpCF* had neutral fitness confirming the importance of GPx and catalase in *E. longus.*

Bacteria have evolved a myriad of regulatory mechanisms against oxidative stress. However, little is known about the mechanisms used by AAPB, one of the bacterial groups that are more exposed to oxidative stress in the environment. The genome of *E. longus* encodes for several known regulatory functions that have been described in other bacteria. One of these mechanisms is the use of extracytoplasmic function sigma factors (ECF), and anti-sigma factors in response to stress (Staroń & Mascher, 2010). Alphaproteobacteria uses ecf sigma factors and the anti-anti-sigma factor *phyR* for general stress response (Fiebig et al., 2015; Francez-Charlot et al., 2015; Gourion et al., 2009; Staroń & Mascher, 2010). It has been shown that light activates this system in some phototrophic strains of alphaproteobacteria including *Rhodobacter sphaeroides*, *Roseobacter denitrificans* (Berghoff et al., 2011; Nuss et al., 2009) and *Erythrobacter litoralis* (Fiebig et al., 2019). The mutants of homologs of ECF subfamily sigma factors and *phyR*

showed neutral fitness effects in all the conditions of our experiments demonstrating that *E. longus* doesn't use this mechanism to respond to oxidative stress. Instead, the regulons controlled by *oxyR* and *soxR,* two master regulators of response against oxidative stress, seem to be the main regulatory functions used by *E. longus* (Imlay, 2008, 2013). The mutation of *oxyR* had strong detrimental effects in fitness, specifically in continuous light and additional H2O2, a condition for which this gene was essential. The mutants of *oxyR* had neutral fitness in the cultures under continuous dark but low fitness in continuous dark with H_2O_2. The genes for catalase *katG*, and the glutathione reductases *gor, gsr* and *grxC* seems to be part of the *oxyR* regulon in *E. longus.* This result differs from the anoxygenic phototroph *Rhodobacter capsulatus* in which the glutathione reductases are not part of the *oxyR* regulon (K. Li et al., 2004). The mutants of *soxR* showed the opposite fitness profile, presenting the lowest fitness in cultures under continuous dark. The fitness of *soxR* mutants was neutral in the cultures with H_2O_2 confirming the capacity of *oxyR* to respond to H_2O_2. These results demonstrate that *oxyR* is the main regulator responding to light-derive and exogenous oxidative stress in *E. longus* and possibly most AAPB strains since recent findings in *Porphyrobacter* LM6 showed that these genes was required for the survival of this strain in the light (Vargas and Coleman, In Prep).

Our data reveal that ROS detoxification and the regulatory response to ROS are vital for AAPB survival. *E. longus* defense mechanisms against light-derived and exogenous ROS consist of a combinatory effect of photoprotective carotenoids, superoxide dismutase, catalase and the glutathione dependent reduction system. We demonstrated that *oxyR* is the major regulator for oxidative stress response in *E. longus*, and that its regulatory response towards ROS differs from what has been observed in anoxygenic photosynthetic alphaproteobacteria.

4.5. Methods

4.5.1. Bacterial strains

These experiments were conducted with *Erythrobacter longus* DSM6997^T (GenBank assembly accession: GCA_000715015.1) (Wang et al., 2014). The *E. coli* strains used for the genetics experiments were maintained and propagated in Luria Broth (LB). The antibiotic kanamycin was added as needed. The summary of strains used and generated in this study can be found in Table S4.5.

4.5.2. Growth media

Erythrobacter longus was maintained and propagated in 0.5X Marine Broth Difco 2216 BD (MBh= 0.5X Marine Broth liquid cultures, MAh= 0.5X Marine agar plates) at 28°C, and preserved in 10% glycerol stocks. Solid media was achieved by the addition of 15g/L of agar (Fisher Scientific).

The H2O2 tolerance growth curves were performed in modified Artificial Seawater (ASW) base media (Wyman et al., 1985), supplemented with 2mM of NH_4Cl (Fisher Scientific), 0.13mM of K_2HPO_4 * $3H_2O$ (Fisher Scientific), trace metal mix (Waterbury & Willey, 1988), and vitamin mix (Guillard & Ryther, 1962). The ASW base media was also amended with carbon in the form of 5g/L of peptone (Difco) and 1g/L of yeast extract (Difco). H2O2 was diluted in H2O and added to the desired concentration.

4.5.3. Growth curve experiments

The starting cultures for this experiment were initiated by picking a single colony of the wild type strain into MBh, and incubated shaking at 280rpm in the dark at 25°C. The starting culture was

washed twice and resuspended in an equal volume of ASW base media (no carbon added). Triplicate 15ml tubes containing 8mL ASW + peptone + yeast extract, and serial dilutions of H2O2, were inoculated with the starting culture cell suspension. All tubes were incubated on a Percival incubator under fluorescent light at 240uE, over 14h:10h light:dark cycles at 24°C and shaking at 280rpm. The optical density of the cultures was directly measured on a Spec 20 spectrophotometer (Thermo) at 660nm.

4.5.4. Construction of RB-TnSeq mutant library

Media. The library was plated on MAh containing 25ug/ml of kanamycin and 1.5% agar. The BarSeq experiments were performed using ASW + peptone and yeast extract. The *Escherichia coli* strains were grown in Lysogeny broth (LB) (1% peptone, 0.5% yeast extract, 0.5% NaCl). Kanamycin 50ug/mL and DAP 300μM were added to grow *E. coli*.

Library construction. The RB-TnSeq experiment was conducted as previously described (Hentchel et al., 2019; Wetmore et al., 2015). A culture of wild type *E. longus* was grown until late exponential phase in MBh at 28°C with shaking at 280 rpm. The plasmid donor *E. coli* strain APA752 (Deutschbauer Lab, University of California-Berkeley, USA), carrying the plasmid pKMW3 (kanamycin resistant) which contains the Himar transposon vector library, was inoculated into 20 mL of LB containing kanamycin (50 μg/mL) and 300 μM diaminopimelate (DAP auxotroph), and grown overnight at 37 °C with shaking at 280 rpm. The conjugation of the barcoded transposon pool into *E. longus* was performed by mixing the recipient strain and donor strains. In order to do this, both cultures were centrifuged at 8000 × g for 2 minutes and resuspended in a total volume of 500 μL of MBh + 10% LB DAP. The cultures were combined at

a 10:1 ratio of recipient to donor and mixed by gentle pipetting. The mixed culture was centrifuged again at 8000 × g, and the supernatant decanted. The cells were resuspended in 100 μL and spotted on a 0.22um Poretic filter (GVS Life Sciences) previously placed on top of a MAh plate, and incubated for at room temperature in the dark. The mating spots were scraped from the plate and resuspended in 6.5mL of MBh. This suspension was spread evenly (500μL per plate) over 70 large (150 × 15 mm) MAh agar plates containing 25 μg/mL kanamycin and incubated for approximately 6 days at 28°C. Cells were harvested from all the plates and inoculated into 400 mL of MBh containing 25 μg/mL kanamycin. This cell mixture was grown at 30°C with shaking at 280rpm for three doublings. Cells were centrifuged at 8000 × g, resuspended in 100 mL of MBh containing 15% glycerol, and stored as 1 mL aliquots at −80 °C.

4.5.5. Mapping of the sites of Tn-Himar insertion in the BarSeq library

The genomic DNA of a library aliquot was extracted using DNA easy Blood and Tissue (Qiagen) following the protocol of the manufacturer. The DNA was sheared (~300 bp fragments), cleaned with a standard bead protocol, end-repaired and A-tailed, and a custom double-stranded Y adapter was ligated. The custom adapter was prepared by annealing Mod2_TS_Univ and Mod2_TruSeq (Table S4.5) as described (Wetmore et al., 2015). The sheared fragments containing transposons were enriched by PCR using the primers Nspacer_BarSeq_pHIMAR and P7_MOD_TS_index1 (Table S4.5) using GoTaq® Green Master Mix according to the manufacturer's protocol in 100μL reaction with the following cycling conditions: 94 °C for 2 minutes, 25 cycles at 94 °C for 30 s, 65 ° C for 20 s, and 72 °C for 30 s, followed by a final extension at 72 °C for 10 minutes. After a second bead cleanup, the library was sequenced using a standard Illumina sequencing primer on an Illumina HiSeq2500 at the University of Chicago

Genomics Facility with a 150-bp single-end read. The genomic locations of the transposon insertions were mapped using the custom Perl script MapTnSeq.pl. Unique barcodes were assigned to a single genomic location using the Perl script DesignRandomPool.pl. These scripts have been described by Wetmore and colleagues (Wetmore et al., 2015), and are available at https://bitbucket.org/berkeleylab/feba. The reads were mapped to the *E. longus* genome (GenBank assembly accession: GCA_000715015.1).

4.5.6. BarSeq experiment

A 1mL aliquot of the library was thawed in ice and transferred to a 250ml flask containing 24ml of MBh. This culture was incubated in the dark, at 28°C and shaking at 280 rpm for 2h. A 10 mL aliquot of this culture was washed twice using ASW base medium and resuspended in an equal volume of the same medium. Four 1 mL samples of the resuspended cells were collected and stored at -80°C for DNA extraction, these correspond to the t=0h samples. The rest of the library suspension was used to inoculate 60ul into each of the 15mL tubes containing 8mL of either ASW + peptone + yeast extract, and amended with 100uM of H2O2 to the corresponding replicate tubes. All tubes were incubated in a Percival incubator at 28°C and 280rpm over 14h:10h light:dark cycles. The continuous dark tubes were covered in aluminum foil and sampled in the dark, the low light tubes were covered with two layers of protective screen to reduce the light to ⅓ of the high light condition. The schematic of the experimental design can be found in Figure S1. The library growth was monitored by optical density at OD_{660} in a Tecan M200 plate reader. The cells were harvested after approximately 6 generations (OD_{660}=1) by centrifugation and stored in cryovials at -80°C until DNA extraction. The gDNA extractions were performed using the DNA spin columns of the Qiagen All Prep DNA/RNA/Protein kit following the manufacturer's instructions.

The gDNA concentrations of the samples were measured using the Qubit DNA Broad range kit. The quality of the gDNA was assessed by measuring A260/A280, A260/A230 using the Tecan M200 plate reader nanoquant plate. PCR amplifications were performed as previously described (Wetmore et al., 2015) using Q5 DNA polymerase with GC enhancer (New England BioLabs) with the primers BarSeq_P1 and 1 of 28 forward primers (BarSeq_P2_IT021 to BarSeq_P2_IT048; Table S5) containing unique 6-bp TruSeq indexes that were sequenced using a separate index primer. The PCR reaction cycle was as follows: 98 °C for 4 minutes followed by 25 cycles of 30 s at 98 °C, 30 s at 55 °C, and 30 s at 72 °C, followed by a final extension at 72 °C for 5 minutes. 10ul of each PCR product were pooled and purified using the Wizard SV gel and PCR clean-up system (Promega). The purified samples were run on a 2.5% agarose gel to confirm correct product size (~200 bp). The pooled PCR samples were assessed for quality, and quantified using a Bioanalyzer. The pool was sequenced on an Illumina HiSeq4000 at the University of Chicago Genomics Facility, multiplexing all 48 samples in one lane with 50-bp single-end reads. All sequence data have been deposited in the NCBI Sequence Read Archive.

4.5.7. Data analysis of mutant fitness

To calculate the fitness of the mutant library over the conditions we followed the protocols of Wetmore and colleagues (Wetmore et al., 2015) using the scripts available at: https:// bitbucket.org/berkeleylab/feba. The abundance of each barcode in the samples and the fitness of each mutant strain are calculated using the scripts: MutiCodes.pl and FEBA.R. Insertions in the first 10% or last 10% of a gene were not considered in gene fitness calculations with the intention of minimizing polar effects. The fitness of each strain is calculated as the normalized Log2 ratio of the abundance at the end of the experiment compared to its T=0h abundance. The fitness of

genes was calculated as the weighted average of strain fitness values. Gene fitness calculations required at least 3 reads per strain and 30 reads for each of the samples to be included in the final analysis.

To assess the mutations with treatment-dependent effects over the six conditions we calculated the Log2 average fitness change between two conditions, and considered the ones with average fitness difference > |1.5 Log2|. We also considered the mutants that presented average fitness > 3 standard deviations from the global mean. Other calculations and plotting were done in R v3.5.3. The heatmaps were constructed using the R packages pheatmap (available at: https://cran.r-project.org/web/packages/pheatmap/index.html), dendextend (available at: https://cran.r-project.org/web/packages/dendextend/index.html) and dendsort (available at: https://cran.r-project.org/web/packages/dendsort/index.html). All statistical analysis and plotting was done in Rv3.5.3 using the packages ggpubr (https://cran.r-project.org/web/packages/ggpubr/index.html) and ggplot2 (https://cloud.r-project.org/web/packages/ggplot2/index.html). The statistical comparison of treatment effects on multiple groups was performed using an ANOVA test. The pairwise comparisons between groups were calculated using a parametric t-test and the all vs all method. Both analyses were done using the package ggpubr.

4.6. References

Allocati, N., Federici, L., Masulli, M., & Ilio, C. D. (2009). Glutathione transferases in bacteria. *The FEBS Journal*, *276*(1), 58–75.

Berghoff, B. A., Glaeser, J., Nuss, A. M., Zobawa, M., Lottspeich, F., & Klug, G. (2011). Anoxygenic photosynthesis and photooxidative stress: A particular challenge for Roseobacter. *Environmental Microbiology*. *13*, 775–791.

Borland, C. F., Cogdell, R. J., Land, E. J., & Truscott, T. G. (1989). Bacteriochlorophyll a triplet

state and its interactions with bacterial carotenoids and oxygen. *Journal of Photochemistry and Photobiology B: Biology*, *3*(2), 237–245.

Cogdell, R. J., & Frank, H. A. (1987). How carotenoids function in photosynthetic bacteria. *Biochimica et Biophysica Acta*, *895*(1987), 63–79.

Dixon, S. J., & Stockwell, B. R. (2014). The role of iron and reactive oxygen species in cell death. *Nature Chemical Biology*, *10*(1), 9–17.

Ferrera, I., Sánchez, O., Kolářová, E., Koblížek, M., & Gasol, J. M. (2017). Light enhances the growth rates of natural populations of aerobic anoxygenic phototrophic bacteria. *The ISME Journal*, *11*(10), 2391–2393.

Fiebig, A., Herrou, J., Willett, J., & Crosson, S. (2015). General Stress Signaling in the Alphaproteobacteria. *Annual Review of Genetics*, *49*, 603–625.

Fiebig, A., Varesio, L. M., Navarreto, X. A., & Crosson, S. (2019). Regulation of the *Erythrobacter litoralis* DSM 8509 general stress response by visible light. *Molecular Microbiology*, *112*(2), 442–460.

Flint, D. H., Tuminello, J. F., & Emptage, M. H. (1993). The inactivation of Fe-S cluster containing hydro-lyases by superoxide. *Journal of Biological Chemistry*, *268*(30), 22369–22376.

Francez-Charlot, A., Kaczmarczyk, A., Fischer, H.-M., & Vorholt, J. A. (2015). The general stress response in Alphaproteobacteria. *Trends in Microbiology*, *23*(3), 164–171.

Gao, L., Zhou, Z., Chen, X., Zhang, W., Lin, M., & Chen, M. (2020). Comparative Proteomics Analysis Reveals New Features of the Oxidative Stress Response in the Polyextremophilic Bacterium *Deinococcus radiodurans*. *Microorganisms*, *8*(3), 451.

Garcia-Chaves, M. C., Cottrell, M. T., Kirchman, D. L., Derry, A. M., Bogard, M. J., & Giorgio, P. A. del. (2015). Major contribution of both zooplankton and protists to the top-down regulation of freshwater aerobic anoxygenic phototrophic bacteria. *Aquatic Microbial Ecology*, *76*(1), 71–83.

Glaeser, J., Nuss, A. M., Berghoff, B. A., & Klug, G. (2011). Chapter 4—Singlet Oxygen Stress in Microorganisms. In R. K. Poole (Ed.), *Advances in Microbial Physiology* (Vol. 58, pp. 141–173). Academic Press.

Glaeser, Jens, & Klug, G. (2005). Photo-oxidative stress in *Rhodobacter sphaeroides*: Protective role of carotenoids and expression of selected genes. *Microbiology, 151*(6), 1927–1938.

Gourion, B., Sulser, S., Frunzke, J., Francez-Charlot, A., Stiefel, P., Pessi, G., Vorholt, J. A., & Fischer, H.-M. (2009). The PhyR-sigma (EcfG) signaling cascade is involved in stress response and symbiotic efficiency in *Bradyrhizobium japonicum*. *Molecular Microbiology*, *73*(2), 291–305.

Griffiths, M., Sistrom, W. R., Cohen-Bazire, G., & Stanier, R. Y. (1955). Function of Carotenoids in Photosynthesis. *Nature*, *176*(4495), 1211–1214.

Guillard, R. R. L., & Ryther, J. H. (1962). Studies of Marine Planktonic Diatoms: I. Cyclotella Nana Hustedt, and Detonula Confervacea (cleve) Gran. *Canadian Journal of Microbiology*, *8*(2), 229–239.

Hamilton, T. L. (2019). The trouble with oxygen: The ecophysiology of extant phototrophs and implications for the evolution of oxygenic photosynthesis. *Free Radical Biology and Medicine*, *140*, 233–249.

Hentchel, K. L., Reyes, L. M., D Curtis, P., Fiebig, A., Maureen, M., & Crosson, S. (2019). Genome-scale fitness profi le of *Caulobacter crescentus* grown in natural freshwater. *The ISME Journal*, 523–536.

Hohmann-Marriott, M. F., & Blankenship, R. E. (2011). Evolution of Photosynthesis. *Annual Review of Plant Biology*, *62*(1), 515–548.

Imlay, J. A. (2008). Cellular Defenses against Superoxide and Hydrogen Peroxide. *Annual Review of Biochemistry*, *77*(1), 755–776.

Imlay, J. A. (2013). The molecular mechanisms and physiological consequences of oxidative stress: Lessons from a model bacterium. *Nature Reviews Microbiology*, *11*(7), 443–454.

Imlay, J. A. (2019). Where in the world do bacteria experience oxidative stress? *Environmental Microbiology*, *21*(2), 521–530.

Johnson, L. A., & Hug, L. A. (2019). Distribution of reactive oxygen species defense mechanisms across domain bacteria. *Free Radical Biology and Medicine*, *140*, 93–102.

Keyer, K., & Imlay, J. A. (1996). Superoxide accelerates DNA damage by elevating free-iron levels. *Proceedings of the National Academy of Sciences*, *93*(24), 13635–13640.

Kirchman, D. L., Stegman, M. R., Nikrad, M. P., & Cottrell, M. T. (2014). Abundance , size , and activity of aerobic anoxygenic phototrophic bacteria in coastal waters of the West Antarctic Peninsula. *Aquatic Microbial Ecology*, *73*, 41–49.

Koblížek, M. (2015). Ecology of aerobic anoxygenic phototrophs in aquatic environments. *FEMS Microbiology Reviews*, *39*(6), 854–870.

Kovács, Á. T., Rákhely, G., & Kovács, K. L. (2005). The PpsR regulator family. *Research in Microbiology*. *156*, 619–625.

Li, K., Hein, S., Zou, W., & Klug, G. (2004). The Glutathione-Glutaredoxin System in *Rhodobacter capsulatus*: Part of a Complex Regulatory Network Controlling Defense

against Oxidative Stress. *Journal of Bacteriology*, *186*(20), 6800–6808.

Li, Q., Peng, T., & Klug, G. (2018). The PhyR homolog RSP_1274 of *Rhodobacter sphaeroides* is involved in defense of membrane stress and has a moderate effect on RpoE (RSP_1092) activity. *BMC Microbiology*, *18*(1), 18.

McCord, J. M., & Fridovich, I. (1969). Superoxide dismutase. An enzymic function for erythrocuprein (hemocuprein). *The Journal of Biological Chemistry*, *244*(22), 6049–6055.

Miller, W. L., & Kester, D. R. (1994). Peroxide variations in the Sargasso Sea. *Marine Chemistry*, *48*(1), 17–29.

Nuss, A. M., Glaeser, J., & Klug, G. (2009). RpoHII Activates Oxidative-Stress Defense Systems and Is Controlled by RpoE in the Singlet Oxygen-Dependent Response in *Rhodobacter sphaeroides*. *Journal of Bacteriology*, *191*(1), 220–230.

Pérez, V., Dorador, C., Molina, V., Yáñez, C., & Hengst, M. (2018). *Rhodobacter* sp. Rb3, an aerobic anoxygenic phototroph which thrives in the polyextreme ecosystem of the Salar de Huasco, in the Chilean Altiplano. *Antonie van Leeuwenhoek*, *111*(8), 1449–1465.

Pomposiello, P. J., Bennik, M. H., & Demple, B. (2001). Genome-wide transcriptional profiling of the *Escherichia coli* responses to superoxide stress and sodium salicylate. *Journal of Bacteriology*, *183*(13), 3890–3902.

Ruiz-González, C., Garcia-Chaves, M. C., Ferrera, I., Niño-García, J. P., & Giorgio, P. A. del. (2020). Taxonomic differences shape the responses of freshwater aerobic anoxygenic phototrophic bacterial communities to light and predation. *Molecular Ecology*, *29*(7), 1267–1283.

Schmitt, F. J., Renger, G., Friedrich, T., Kreslavski, V. D., Zharmukhamedov, S. K., Los, D. A., Kuznetsov, V. V., & Allakhverdiev, S. I. (2014). Reactive oxygen species: Re-evaluation of generation, monitoring and role in stress-signaling in phototrophic organisms. *Biochimica et Biophysica Acta - Bioenergetics*, *1837*(6), 835–848.

Sies, H., Berndt, C., & Jones, D. P. (2017). Oxidative Stress. *Annual Review of Biochemistry*, *86*(1), 715–748.

Silva, L. G., Lorenzetti, A. P. R., Ribeiro, R. A., Alves, I. R., Leaden, L., Galhardo, R. S., Koide, T., & Marques, M. V. (2019). OxyR and the hydrogen peroxide stress response in *Caulobacter crescentus*. *Gene*, *700*, 70–84.

Staroń, A., & Mascher, T. (2010). General stress response in α-proteobacteria: PhyR and beyond. *Molecular Microbiology*, *78*(2), 271–277.

Vuilleumier, S., & Pagni, M. (2002). The elusive roles of bacterial glutathione S-transferases: New lessons from genomes. *Applied Microbiology and Biotechnology*, *58*(2), 138–146.

Waterbury, J. B., & Willey, J. M. (1988). Isolation and growth of marine planktonic cyanobacteria. In *Methods in Enzymology* (Vol. 167, pp. 100–105). Academic Press.

Wetmore, K. M., Price, M. N., Waters, R. J., Lamson, J. S., He, J., Hoover, C. A., Blow, M. J., Bristow, J., Butland, G., Arkin, A. P., & Deutschbauer, A. (2015). Rapid Quantification of Mutant Fitness in Diverse Bacteria by Sequencing Randomly Bar-Coded Transposons. *MBio*, *6*(3), 1–15.

Wyman, M., Gregory, R. P. F., & Carr, N. G. (1985). Novel Role for Phycoerythrin in a Marine Cyanobacterium, *Synechococcus* Strain DC2. *Science*, *230*(4727), 818–820.

Yurkov, V., & Csotonyi, J. T. (2009). The Purple Phototrophic Bacteria. Chapter 3. New Light on Aerobic Anoxygenic Phototrophs. *C. Neil Hunter, Fevzi Daldal, Marion C. Thurnauer and J. Thomas Beatty (eds)* (31-55).

Yurkov, V., Gad'on, N., & Drews, G. (1993). The major part of polar carotenoids of the aerobic bacteria *Roseococcus thiosulfatophilus* RB3 and *Erythromicrobium ramosum* E5 is not bound to the bacteriochlorophyll a-complexes of the photosynthetic apparatus. *Archives of Microbiology*, *160*(5), 372–376.

Yurkov, V., & Hughes, E. (2013). Genes Associated with the Peculiar Phenotypes of the Aerobic Anoxygenic Phototrophs. In *Advances in Botanical Research* (Vol. 66, p. 358). Elsevier.

Yurkov, V. V., & Beatty, J. T. (1998). Aerobic Anoxygenic Phototrophic Bacteria. *Microbiology and Molecular Biology* Reviews. 62(3), 695–724.

Zheng, M., Wang, X., Templeton, L. J., Smulski, D. R., LaRossa, R. A., & Storz, G. (2001). DNA microarray-mediated transcriptional profiling of the Escherichia coli response to hydrogen peroxide. *Journal of Bacteriology*, *183*(15), 4562–4570.

Zheng, Q., Zhang, R., Koblížek, M., Boldareva, E. N., Yurkov, V., Yan, S., & Jiao, N. (2011). Diverse arrangement of photosynthetic gene clusters in aerobic anoxygenic phototrophic bacteria. *PLoS ONE*, *6*(9), 1–7.

Ziegelhoffer, E. C., & Donohue, T. J. (2009). Bacterial responses to photo-oxidative stress. *Nature Reviews. Microbiology*, *7*(12), 856–863.

Zinser, E. R. (2018). The microbial contribution to reactive oxygen species dynamics in marine ecosystems. *Environmental Microbiology Reports*, *10*(4), 412–427.

4.7. Supporting figures

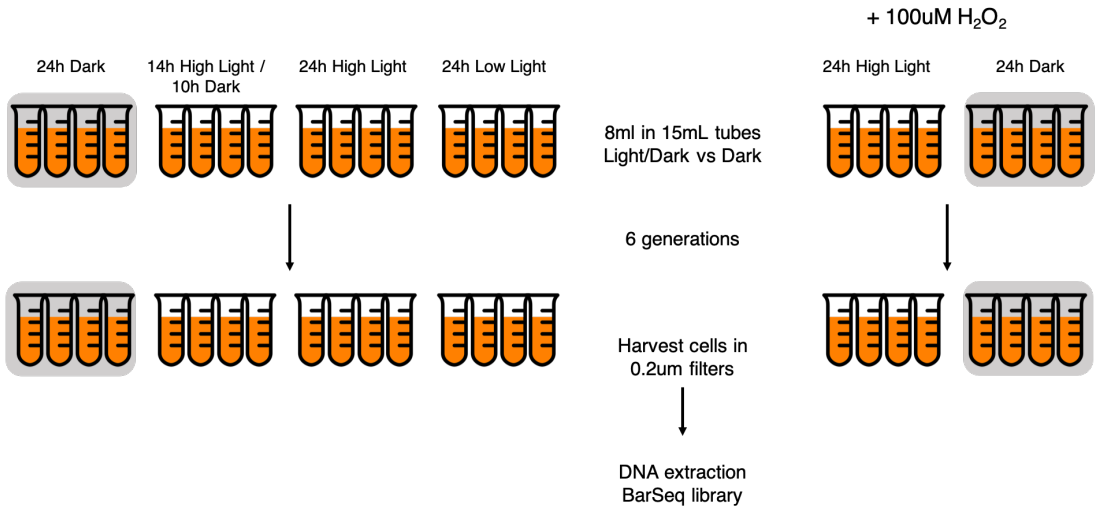

Figure S4.1. Schematic of experimental design.

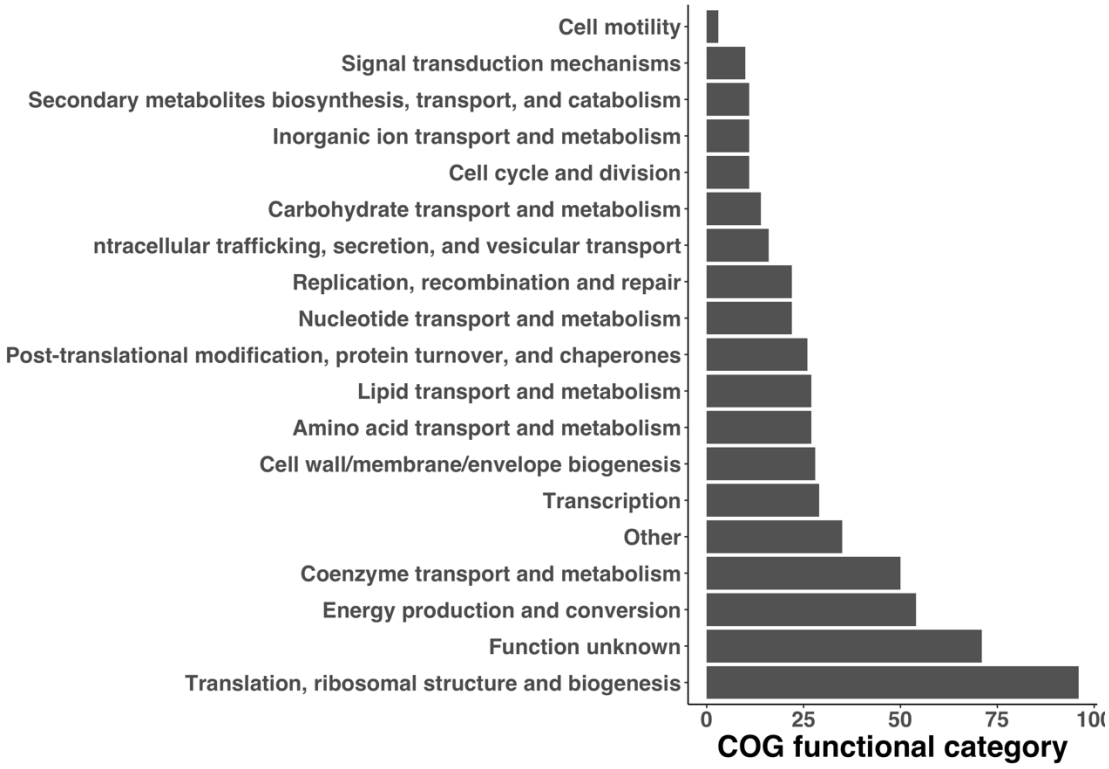

Figure S4.2. COG functional categories of the *E. longus* essential gene set.

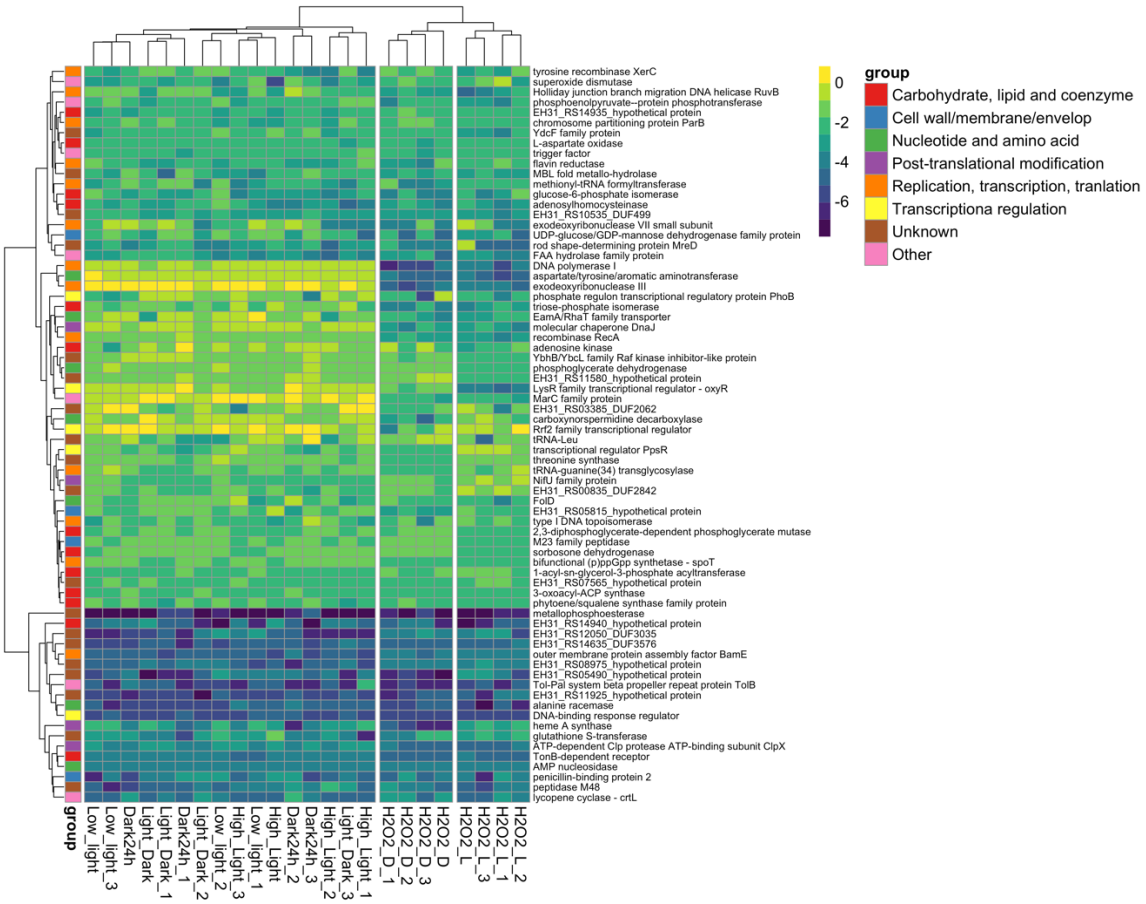

Figure S4.3. Heatmap of mutants with average fitness greater than 3 standard deviations from the global dataset mean. The functional categories were assigned based on COG annotations.

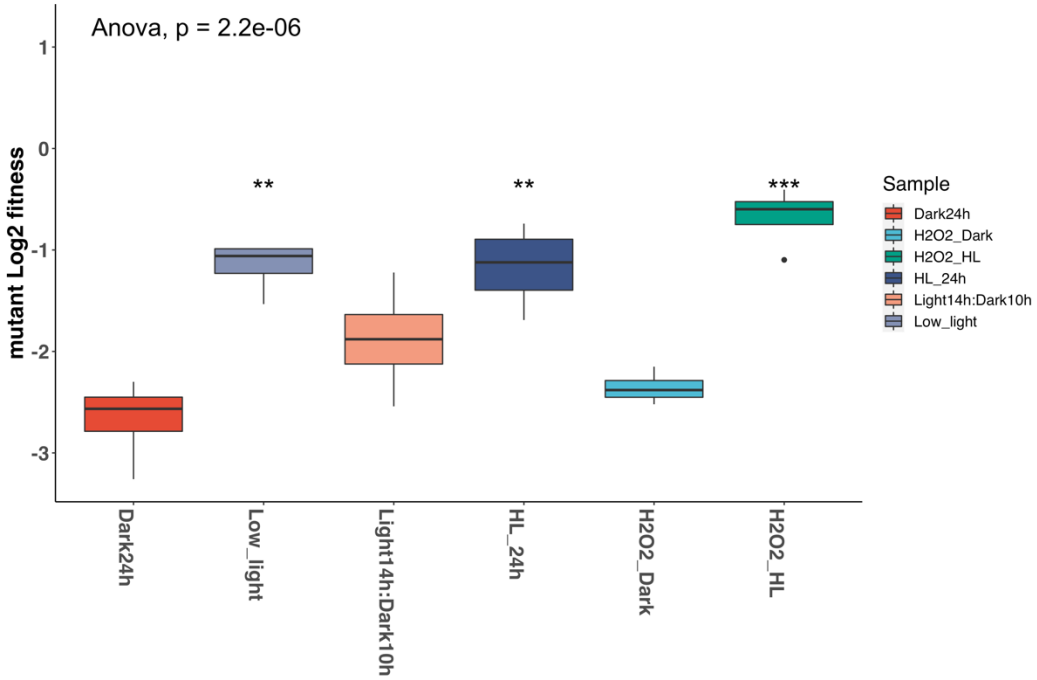

Figure S4.4. Fitness of *E. longus* strains with insertions in the transcriptional regulator *ppsR*. The global p value was calculated by ANOVA; pairwise treatment comparisons were performed using t-test using Dark24h as reference. ns, non-significant; * $p<0.05$; ** $p<0.005$; *** $p<0.0005$.

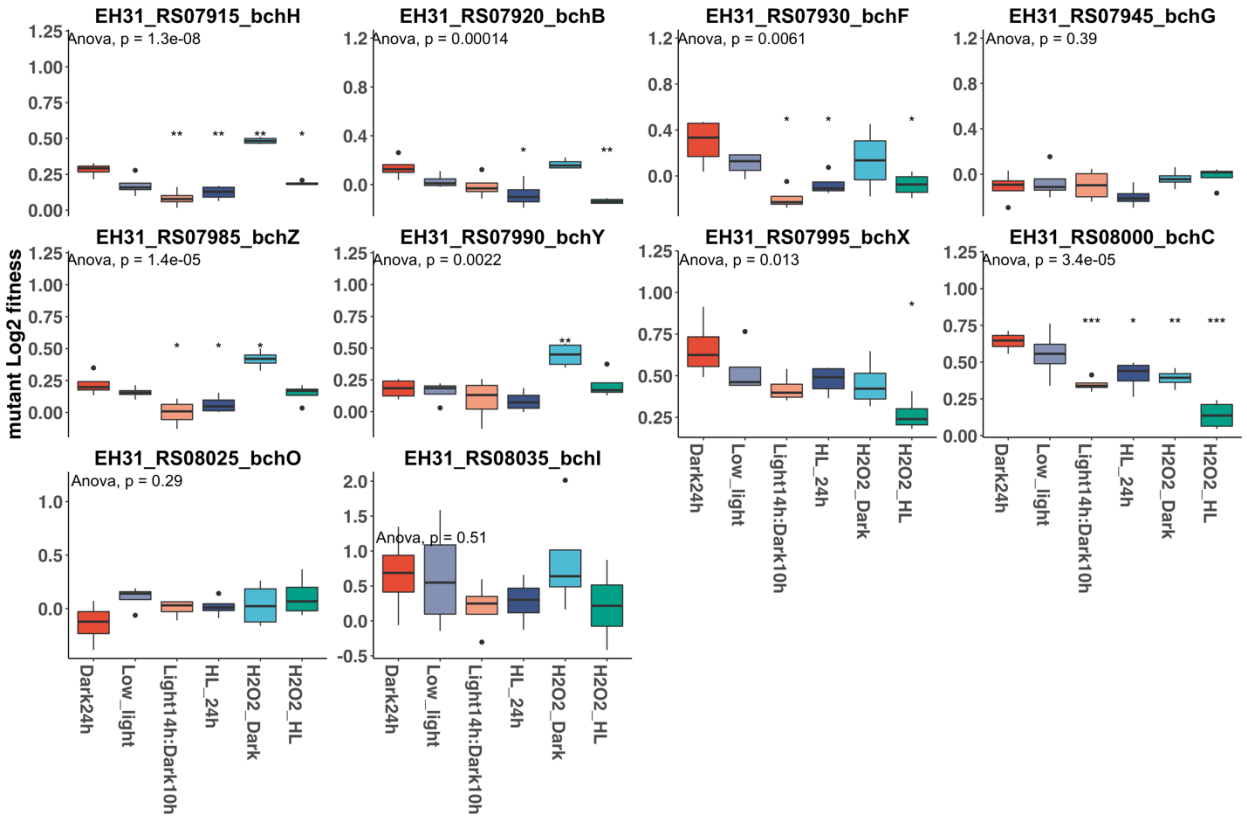

Figure S4.5. Fitness of strains with insertions in genes for Bchl*a* biosynthesis. The global p value was calculated by ANOVA. Pairwise treatment comparisons were performed using t-test using Dark 24h as reference. ns, non-significant; * p<0.05; ** p<0.005; *** p<0.0005.

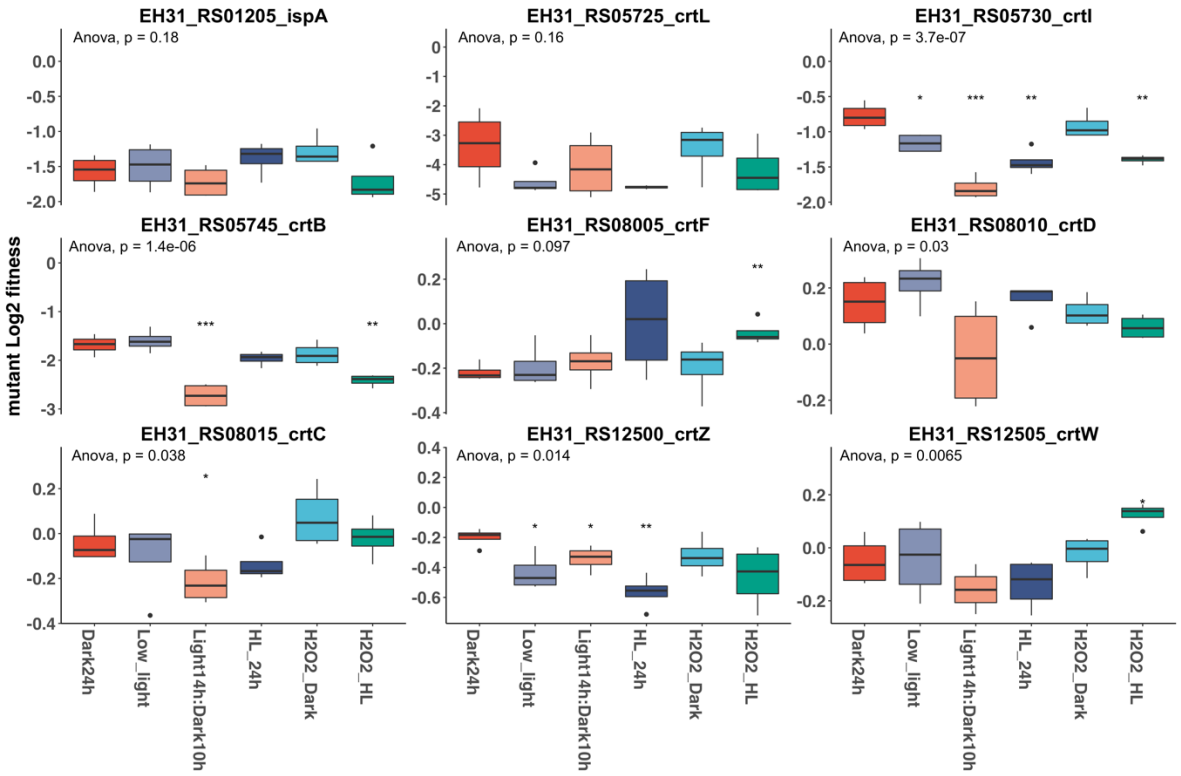

Figure S4.6. Fitness of strains with insertions in carotenoids biosynthesis genes. The global p value was calculated by ANOVA. Pairwise treatment comparisons were performed using t-test using Dark 24h as reference. ns, non-significant; * p<0.05; ** p<0.005; *** p<0.0005.

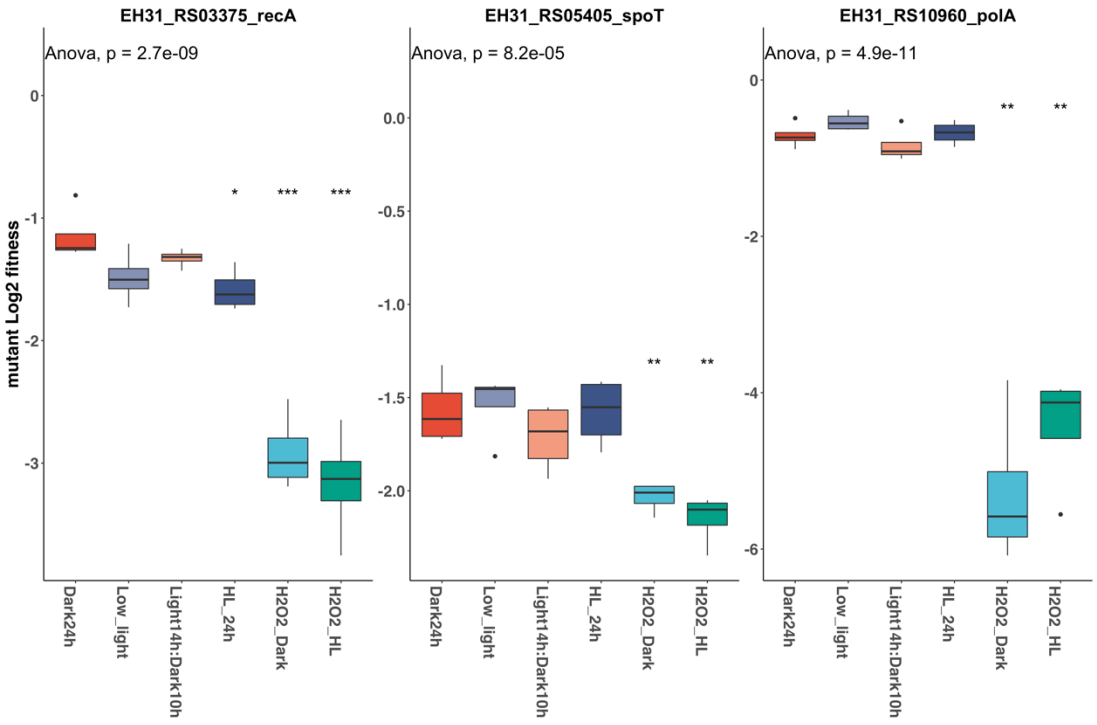

Figure S4.7. Fitness of strains with insertions in genes involved in DNA repair and stringent response. The global p value was calculated by ANOVA. Pairwise treatment comparisons were performed using t-test using Dark 24h as reference. ns, non-significant; * p<0.05; ** p<0.005; *** p<0.0005.

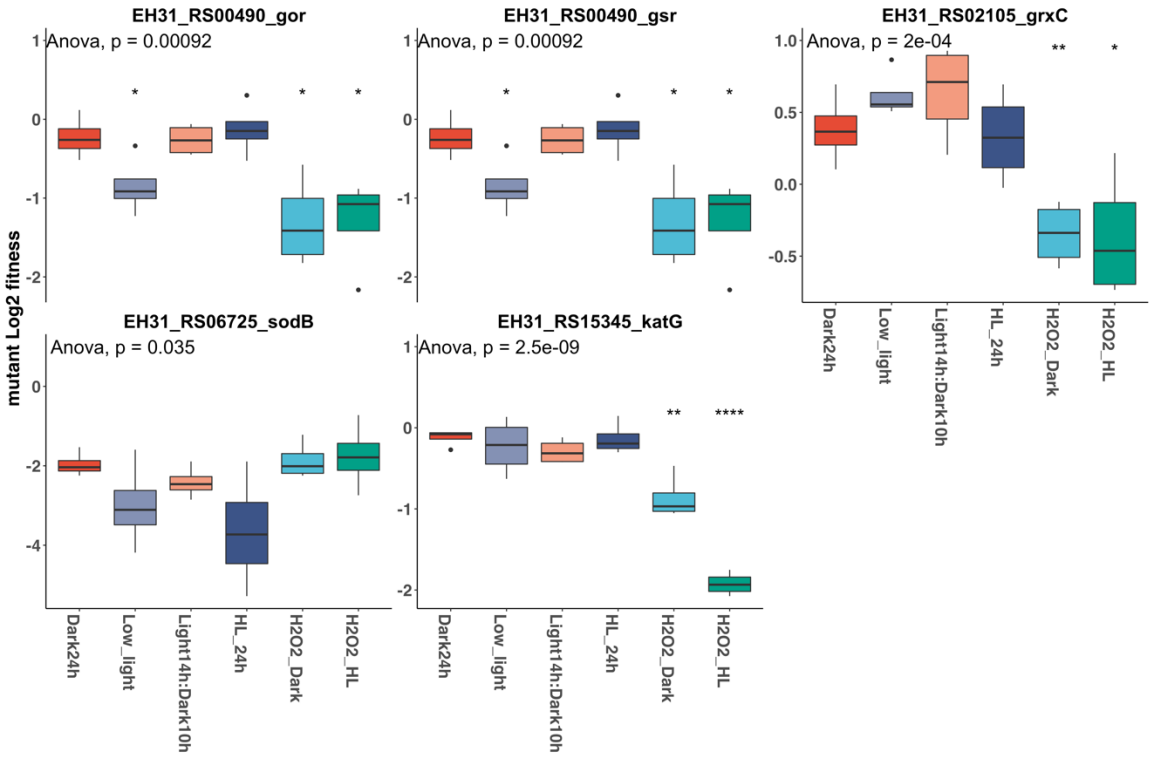

Figure S4.8. Fitness of strains with insertions in genes involved in ROS detoxification. The global p value was calculated by ANOVA. Pairwise treatment comparisons were performed using t-test. ns, non-significant; * p<0.05; ** p<0.005; *** p<0.0005.

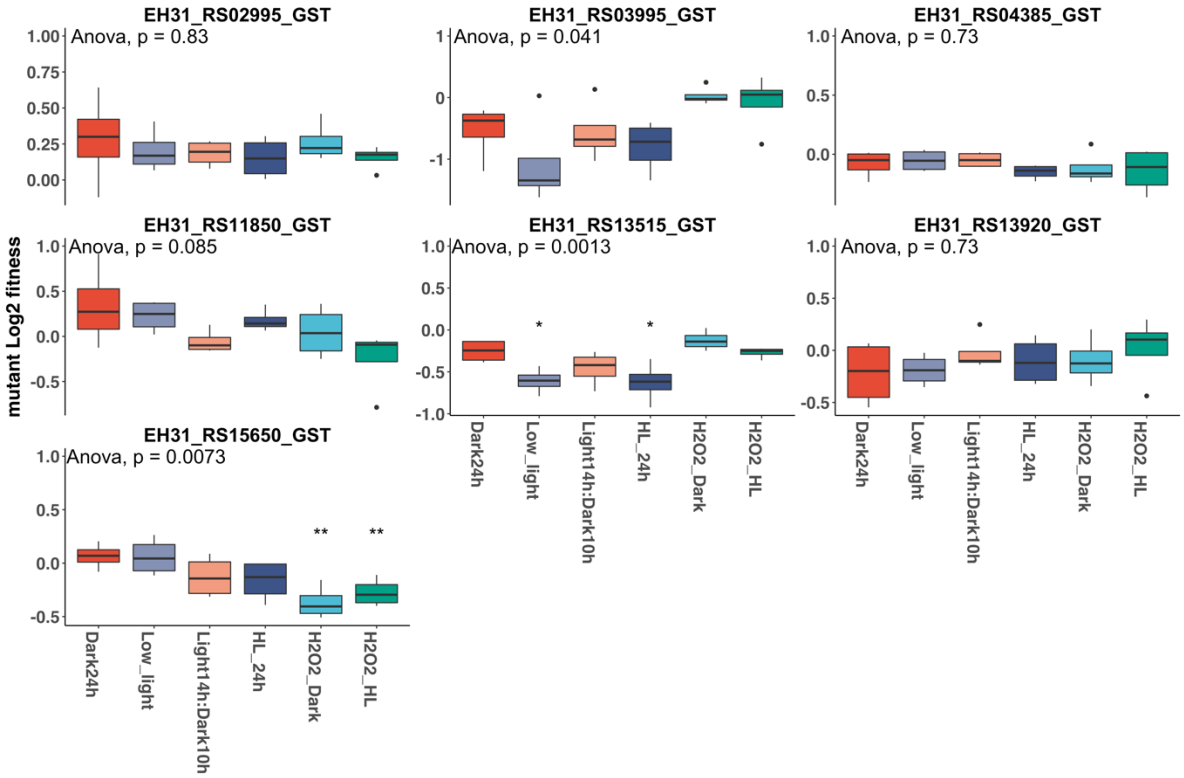

Figure S4.9. Fitness of strains with insertions in glutathione transferase (GST) genes. The global p value was calculated by ANOVA. Pairwise treatment comparisons were performed using t-test. ns, non-significant; * p<0.05; ** p<0.005; *** p<0.0005.

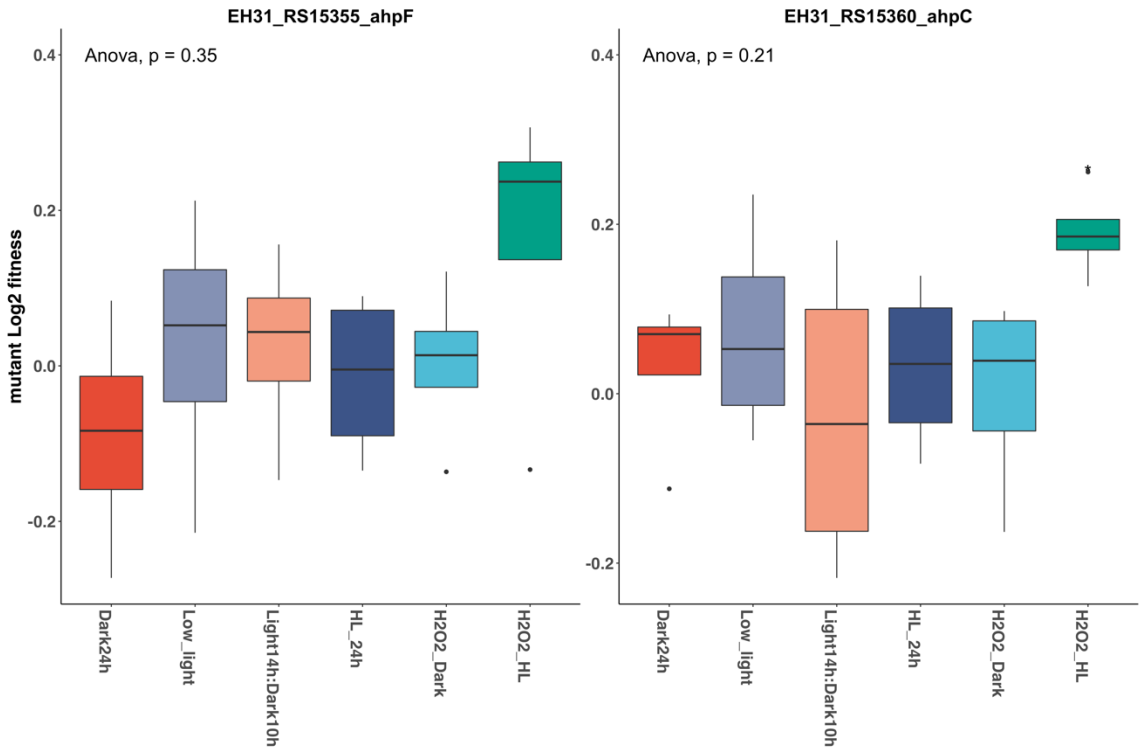

Figure S4.10. Fitness of strains with insertions in genes encoding *ahpC* and *ahpF*. The global p value was calculated by ANOVA. Pairwise treatment comparisons were performed using t-test. ns, non-significant; * $p<0.05$; ** $p<0.005$; *** $p<0.0005$.

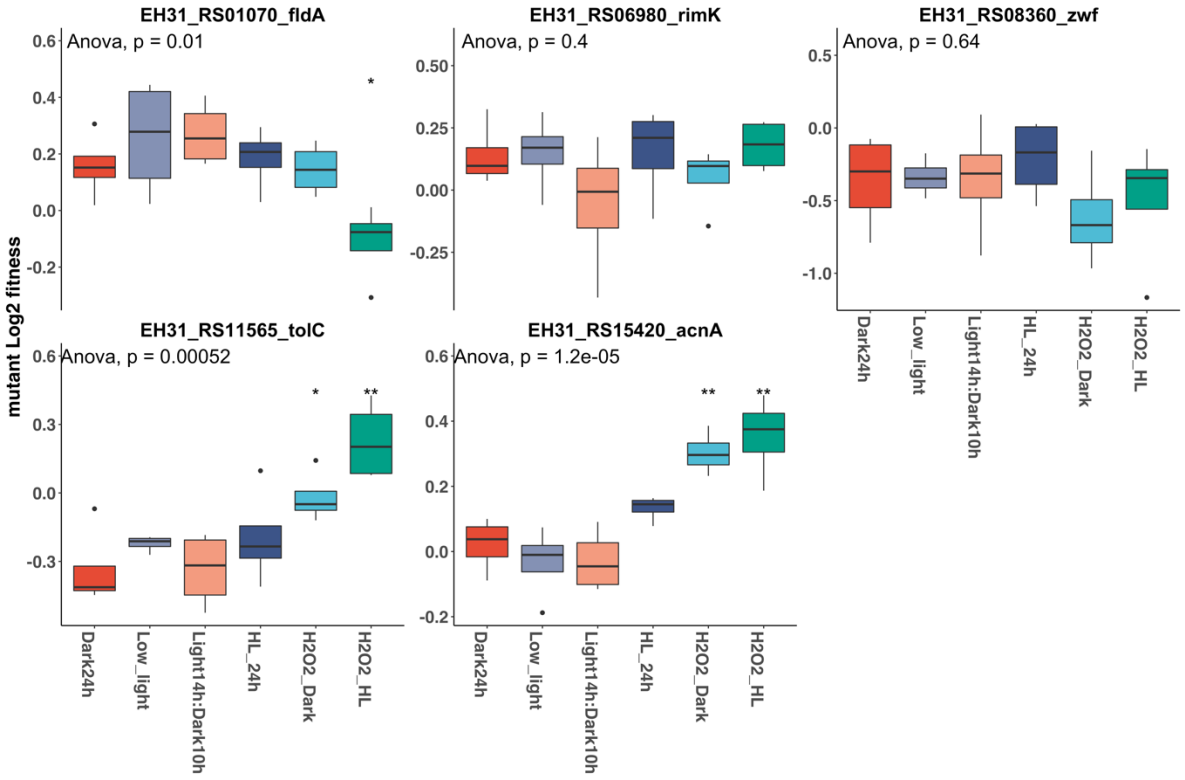

Figure S4.11. Fitness of strains with insertions in genes of the SoxR regulon. The global p value was calculated by ANOVA. Pairwise treatment comparisons were performed using t-test. ns, non-significant; * p<0.05; ** p<0.005; *** p<0.0005.

CHAPTER 5

Summary and future directions

This work contributed to our understanding of the physiology and the molecular mechanisms used by aerobic anoxygenic phototrophic bacteria. We increased the existing knowledge about these bacteria by performing genetics experiments in AAP strains from the order Sphingomonadales. Furthermore, by studying both marine and freshwater strains we were able to find mechanisms shared by these strains indicating the importance of these mechanisms for the physiology of AAP bacteria in the environment. Here we used genetics to address fundamental questions about the physiology of AAP bacteria. The findings generated here will contribute to a better comprehension of the role of AAP bacteria in the carbon cycle.

5.1. Summary

Cultivating *Erythrobacter longus* and *Porphyrobacter* LM6 under different carbon substrates and light regimes showed that light is advantageous to the growth of these strains when growing in single substrates like pyruvate, butyrate and glucose (Chapter 2 and Chapter 3). The light enhanced growth observed was a product of light energy uptake, this was confirmed by comparing the growth of the wild type strain of *E. longus* and a Bchl*a* deficient mutant (Chapter 2). The growth of this mutant under several carbon substrates presented a decrease in light-enhanced growth but also indicated that the Bchl*a* deficient phenotype is linked to carbon metabolism. We identified carbon metabolism pathways in the genomes of AAP bacteria that could benefit from light energy. AAP strains from the order Rhodobacterales use the ethylmalonyl CoA (EMC) pathway to enhance their growth in the light (Bill et al., 2017). We found that the EMC pathway is not prevalent in Sphingomonadales AAP bacteria, and therefore there must be

other pathways that interact with AAP. Using comparative genomics, we identified the glyoxylate shunt as a candidate pathway to aid Sphingomonadales AAP to take advantage of light. Others have previously proposed that the glyoxylate shunt is responsible for light enhanced growth in other photoheterotrophs given that this pathway allows carbon preservation by skipping CO2 lost during respiration (Palovaara et al., 2014). In order to test the role of the shunt, we created a mutant strain lacking the gene isocitrate lyase, the first enzymatic step in this pathway. We demonstrated that the glyoxylate shunt is the only pathway in *E. longus*, and possibly all Sphingomonadales AAP bacteria, for acetate assimilation as this gene is required for growth in acetate and butyrate. The glyoxylate shunt is important for AAP strains lacking similar pathways because it facilitates the use of potentially relevant carbon substrates such as acetate, butyrate and other fatty acids that enter TCA as C2-moleculas (Tang et al., 2011). However, we did not find evidence that the glyoxylate shunt is involved in light enhanced growth under the conditions tested.

The results presented in Chapter 3 provide evidence of the involvement of anaplerotic carbon fixation in the light-enhancement growth observed in AAP. These reactions catalyze the incorporation of inorganic carbon as intermediaries of carbon metabolism pathways (Tang et al., 2011). Hauruseu and Koblížek previously demonstrated that *Erythrobacter* NAP1 increases carboxylation activity in the light, and found a correlation between anaplerotic carbon fixation and increased bacterial growth efficiency (Hauruseu & Koblížek, 2012). Our experimental data supports that observation, and indicates that the enzymes phosphoenolpyruvate carboxylase, and to a second degree phosphoenolpyruvate carboxykinase, performed the anaplerotic reactions that enable light-enhancing growth in *Porphyrobacter* LM6.

This work also revealed the role of transcriptional regulators which function is required for this strain. These include the transcriptional repressor *ppsR* which has been described as the aerobic repressor of photosynthesis in anoxygenic phototrophs (Elsen et al., 2005; Kovács et al., 2005). PpsR also works as a repressor on AAP bacteria, however it does not respond to oxygen but instead it responds to light. Our results show that mutations of *ppsR* are detrimental to *Porphyrobacter* growing on phototrophic conditions. We confirmed this phenotype by creating a deletion mutant of this gene which was incapable of growing on glucose regardless of the light regime. Other genes of the photosynthetic gene cluster showed detrimental effects on the fitness of *Porphyrobacter* growing in light-enhancing conditions. One important finding obtained from this experiment was the strong effect of the mutations in genes that participate in reactive oxygen species detoxification, especially in the transcriptional regulator *oxyR*. The role of this gene in stress response has been demonstrated in other alphaproteobacteria, however, its function has not been reported in AAP bacteria.

In Chapter 4 we studied more in detail the effects of oxidative stress in the physiology of AAP bacteria. We believe that AAP bacteria are subject to increased concentrations of reactive oxygen species produced both endogenously by the action of the photosystem, and exogenously by the respiration of the microbial community in the photic zone. Here, we used a barcoded mutant library in *E. longus* and tested the effects of light derived and exogenous ROS. We confirmed the photoprotective role of carotenoids in AAP. We also tested the participation of several known enzymatic mechanisms of ROS detoxification and found that glutathione metabolism is required for the growth of this strain. The genes glutathione synthase and glutathione peroxidase are essential for *E. longus*. Furthermore, the mutants of several glutathione reductases showed

detrimental fitness effects, especially under increased concentrations of hydrogen peroxide, demonstrating the importance of glutathione in the detoxification of these compounds. Our experiments also showed that the transcription regulator *oxyR* is one of the major regulators of oxidative stress response. The mutants of this gene in both *E. longus* and *Porphyrobacter* LM6 presented low fitness in cultures exposed to light confirming the role of this regulator against light-derived oxidative stress. Interestingly, the system *ecf-phyR* for stress response that was previously reported in the strain *Erythrobacter litoralis* did not show important effects of mutation in *E. longus*. We concluded that oxidative stress produced by the use of phototrophy imposes a strong pressure on AAP bacteria. Therefore, these bacteria had to evolve several mechanisms to survive in the photic zone.

5.2. Future directions

The strategy used was to interrogate the role of the majority of the genes in two strains of AAP bacteria that revealed the participation of several pathways and transcriptional regulators in their physiology. However, as it is usual of forward genetics screens, some of the genes with interesting phenotypes are of unknown functions. Some of the most intriguing phenotypes were found in poorly characterized transcriptional regulators which mutants showed both positive and negative fitness effects in our experiments. One *Porphyrobacter* LM6 gene encoding a LacI family transcriptional regulator represents an example of those rare mutants that had positive fitness. These regulators resemble the LacI repressor of *Escherichia coli* and are associated with the control of catabolic operons in response to carbon availability (Ravcheev et al., 2014). The mutants of this regulator had positive fitness in glucose dark suggesting that its function is to selectively repress the catabolism of glucose and possibly other glucogenic substrates in the absence of light.

This type of regulators that act in a substrate dependent manner could represent the link between carbon metabolism and light. The fitness profiles obtained for other unknown transcription regulators provided hints into their functions that should be further explored.

In this work we showed the impact of oxidative stress on the physiology of AAP bacteria. Similarly to the ones in Chapter 3, the experiments performed in Chapter 4 produced intriguing phenotypes in genes of unknown function that need to be explored in more detail. Some of those include transcriptional regulators and genes containing DNA binding domains. The regulation of the response against oxidative stress is of the most relevance for AAP physiology, as it might be one of the strongest selection pressures that these bacteria face in the environment. Hence, further work needs to be done in order to fully characterize the regulatory network that AAP uses to fight ROS.

One of the most important findings of this thesis is the difference we found between Sphingomonadales and Rhodobacterales AAP. We contributed with evidence of how members of these two groups differ in their utilization of carbon metabolism pathways and regulatory networks. A comprehensive phylogenetic profile including several hundreds of genomes available for AAP in these two orders is necessary in order to better understand their evolution, and ecological roles.

Finally, the knowledge generated here needs to be incorporated in analysis and models of the carbon cycle. By doing this, we will be able to better define the magnitude of the contribution

of AAP bacteria to the carbon cycle, and apply it for a more precise calculation of carbon budgets in aquatic environments.

5.3. References

Bill, N., Tomasch, J., Riemer, A., Muller, K., Kleist, S., Schmidt-Hohagen, K., Wagner-Döbler, I., & Schomburg, D. (2017). Fixation of CO2 using the ethylmalonyl-CoA pathway in the photoheterotrophic marine bacterium *Dinoroseobacter shibae*. *Environmental Microbiology*, 2645–2669.

Elsen, S., Jaubert, M., Pignol, D., & Giraud, E. (2005). PpsR : a multifaceted regulator of photosynthesis gene expression in purple bacteria. *Molecular Microbiology*. *57*, 17–26.

Hauruseu, D., & Koblížek, M. (2012). Influence of Light on Carbon Utilization in Aerobic Anoxygenic Phototrophs. *Applied and Environmental Microbiology*, *78*(20), 7414–7419.

Kovács, Á. T., Rákhely, G., & Kovács, K. L. (2005). The PpsR regulator family. *Research in Microbiology*. 156, 619–625.

Palovaara, J., Akram, N., Baltar, F., Bunse, C., Forsberg, J., & Pedrós-alió, C. (2014). Stimulation of growth by proteorhodopsin phototrophy involves regulation of central metabolic pathways in marine planktonic bacteria. *PNAS*, E3650–E3658.

Ravcheev, D. A., Khoroshkin, M. S., Laikova, O. N., Tsoy, O. V., Sernova, N. V., Petrova, S. A., Rakhmaninova, A. B., Novichkov, P. S., Gelfand, M. S., & Rodionov, D. A. (2014). Comparative genomics and evolution of regulons of the LacI-family transcription factors. *Frontiers in Microbiology*, *5*.

Tang, K., Tang, Y. J., & Blankenship, R. E. (2011). Carbon metabolic pathways in phototrophic bacteria and their broader evolutionary implications. *Frontiers in Microbiology*, *2*(August), 1–23.